IDENTIFICATION AND CHARACTERIZATION OF ZEOLITES IN WESTERN NORTH DAKOTA

A Thesis
Submitted to the Graduate Faculty
of the
North Dakota State University
of Agriculture and Applied Science

By

Jason Wayne Triplett

In Partial Fulfillment of the Requirements
for the Degree of
MASTER OF SCIENCE

Major Program:
Environmental and Conservation Sciences

March 2012

Fargo, North Dakota

North Dakota State University
Graduate School

Title

Identification and Characterization of Fibrous Zeolites in Western North Dakota

By

Jason W. Triplett

The Supervisory Committee certifies that this ***disquisition*** complies with North Dakota State University's regulations and meets the accepted standards for the degree of

MASTER OF SCIENCE

SUPERVISORY COMMITTEE:

Bernhardt Saini-Eidukat
Chair

Kenneth Lepper

Achintya Bezbaruah

Lisa Montplaisir

Approved:

March 7, 2012
Date

Craig Stockwell
Department Chair

ABSTRACT

The fibrous zeolite mineral erionite is a concern due to its potential for causing lung disease in humans. Studies have shown that exposure to altered volcanic bedrock containing erionite may be the explanation for a high lung disease rate throughout regions of the world (Metintas et al., 1999). Erionite was reported by Forsman (1986) as occurring in tuffaceous rock units of the Arikaree Formation in the Killdeer Mountains of western North Dakota. Rock and soil samples were collected where zeolite minerals are known or suspected to be present including North and South Killdeer Mountains in Dunn County and West and East Rainy Buttes and White Butte in Slope County. Analysis and identification was carried out using XRD, SEM, and EMPA. Zeolitic material was confirmed in units for both North and South Killdeer Mountains. The chemical compositions of the fibers resulted in a majority being classified as offretite rather than erionite.

ACKNOWLEDGMENTS

Thanks to Dr. Nels Forsman, Department of Geology and Geological Engineering, UND and Dr. Edward C. Murphy, North Dakota Geological Survey, for providing direction and preliminary information on zeolites in western North Dakota. I would also like to thank Dr. Angel Ugrinov, NDSU Chemistry and Molecular Biology XRD lab, Scott Payne, assistant director, and Jayma Moore, laboratory manager, NDSU Electron Microscopy Center, and Dr. Ellery Frahm, University of Minnesota EML, Department of Geology and Geophysics. Dr. Bernhardt Saini-Eidukat, NDSU Department of Geosciences was my advisor for this project, and the committee members: Dr. Kenneth Lepper, Dr. Achintya Bezbaruah, and Dr. Lisa Montplaisir. NDSU undergraduate students Dilion Dolezal, and Sharon (Brozo) Feit helped with field and analytical work. Thanks also to the land owners: Craig Dvirnak, Brian Benz, Sheila Murphy, Kenny Urlacher, and Marry Dennis for allowing access to their property for sample collection, and Wendell and Linda Vigen for all the hospitality and a place to stay during our sampling trip. A special thanks to my loving wife Heidi Triplett for the endless support she has given me throughout this project and my career. This project was supported by grants from the National Center for Research Resources (5P20RR016471-12) and the National Institute of General Medical Sciences (8 P20 GM103442-12) from the National Institutes of Health.

TABLE OF CONTENTS

LIST OF TABLES

LIST OF FIGURES

LIST OF APPENDIX TABLES

LIST OF APPENDIX FIGURES

CHAPTER 1. INTRODUCTION AND BACKGROUND

1.1 Introduction

During the late 1970's, an epidemic of mesothelioma was discovered in three villages in the Cappadocian region of central Turkey (Baris et al., 1978; Artvinli and Baris, 1979). Subsequent studies investigated the link between the high frequency of deaths within the group caused by malignant pleural mesothelioma (MPM) and the occurrence of a naturally occurring fibrous zeolite mineral known as erionite found in the region's bedrock (Baris et al., 1987). In fact, emigrants from the region were found to have increased risk of MPM and 49% or more of the deaths in the Cappadocian region of Turkey due to MPM had a potential link to erionite fiber exposure (Metintas et al., 1999). Supporting studies on rats have shown that inhaled erionite fibers resulted in increased incidence of mesothelioma in those animals (Wagner et al., 1985). Increasing interest in the subject prompted many more studies on the health effects of erionite, as well as new investigations into its carcinogenic potential, the identification and classification of the zeolite erionite, erionite mineral structure, and the similarities between the mineral erionite and other closely related zeolites. A summary is provided by Carbone et al. (2007).

In 1986, Dr. Nels Forsman reported the discovery of zeolitic mineral fibers within the pores and vugs of tufaceous ash units of the Killdeer Mountain region, Western North Dakota. Based on standard powder X-Ray Diffraction (XRD) analysis and electron microprobe analysis (EMPA) on single mineral crystals, Forsman (1986) concluded that erionite composed the majority of the zeolite content in the samples collected from the Killdeer Mountains.

The concern with the carcinogenic potential of erionite has sparked an interest within North Dakota and other areas believed to have erionite present in regional bedrock. Specifically, there are formations spread throughout western North Dakota which can be correlated to the

sedimentary units of the Killdeer Mountains in which Forsman (1986) conducted his work. Some of these areas include other high butte formations scattered across western North Dakota as well as the badland formations of North Dakota, South Dakota, and Montana (Goodman and Pierson, 2010 and Murphy, pers.comm., 2008).

Due to the possible health risks associated with erionite, hazard mapping (Forsman, 2006) was undertaken by the North Dakota Department of Health (NDDoH), in cooperation with the North Dakota Geological Survey (NDGS) and the Environmental Protection Agency (EPA). These investigations led to gravel quarry restrictions, gravel use restrictions, dust control measures, and guidance plans to control and reduce the overall exposure by businesses and private landowners working in close proximity to the bedrock formations and/or gravel quarries which potentially contain erionite (NDDoH, 2009).

With increasing commercial, agricultural, and mining development in western North Dakota, the questions of potential erionite exposure and the potential health risks associated with this exposure have become of increasing concern. This investigation focuses on acquiring a better understanding of the location of zeolite-bearing strata in western North Dakota, along with analysis of the chemical composition of the North Dakota zeolite occurrences. The goals of this investigation are; 1) to determine the exact location of zeolite bearing rock strata within high butte regions of western North Dakota known to have a zeolite presence which can then be correlated to other similar rock strata throughout the region, and 2) characterize and identify chemical composition of the fibrous zeolites found in identified regions by powder x-ray diffraction (XRD), scanning electron microscopy/energy dispersive spectroscopy (SEM/EDS), and electron microprobe analyzer (EMPA). The results presented here will help in identifying

zeolite presence in North Dakota and in understanding what precautions may need to be taken when working in regions identified as being near zeolite bearing rock units.

1.2 Zeolites

Zeolites are the largest single group of silicate minerals with over 80 natural species (Armbruster and Gunter, 2001) and 600 synthetic (Nesse, 2000) zeolite minerals being identified. There are a variety of ways of defining a zeolite. Armbruster and Gunter (2001) provide the general definition, "a zeolite mineral is a crystalline substance with a structure characterized by a framework of linked tetrahedra, each consisting of four O atoms surrounding a cation. This framework contains open cavities in the form of channels and cages. These are usually occupied by H_2O molecules and extra-framework cations that are commonly exchangeable...", while Nesse (2000) provides the general mineralogical formula $M_x D_y (Al_{x+2y}Si_{n-x-2y}O_{2n}) \cdot mH_2O$, where M is monovalent Na or K and D is Ca, Mg, or other divalent cations, both dependent on the charge difference among the Al^{+3} and Si^{+4} within the crystalline structure, and the amount of water (*m*) being variable (Nesse, 2000).

Zeolites are classified as hydrated framework alumino-silicate minerals composed of interlocking tetrahedra mostly formed from chemically altered, glass rich volcanic ash by water infiltration under differing pressures and temperatures (Nesse, 2000). The tetrahedra consist of SiO_4 and AlO_4 with an (Si+Al)/O ratio equal to ½ (Mumpton, 1977) and are referred to as tectosilicates or framework silicates due to the framework structure created by the interlocking tetrahedra. The microporous framework structure becomes negatively charged (anionic), which allows large cations such as Mg^{2+}, Ca^{2+}, Na^{+}, K^{+} and others to enter the "cages" produced by the connecting tetrahedra. This structure creates a molecular sieve that can be used in industry as an absorbent (Sheppard, 1996) for the treatment of waste water, a soil conditioner, as a catalyst by

ion exchange in the fuel industry (Kokotailovo and Fyfe, 1995), along with other commercial applications.

1.2.1 Erionite and offretite

Erionite (Figure 1.1) and offretite (Figure 1.2) are both naturally occurring zeolites that are usually found associated with volcanic rocks. In addition, erionite can be found in volcanoclastic (transported or reworked volcanic material) silicic and/or tufaceous layers that have been altered in continental and/or marine environments.

Figure 1.1. K-Erionite crystals in vug (Barthelmy, 2011a)


Figure 1.2. Offretite crystal on matrix (Barthelmy, 2011b)

The erionite general formula is $(K_2\ Na_2\ Ca_3)\ [Al_{10}\ Si_{26}\ O_{72}]\cdot 30H_2O$ (Passaglia et al., 1998) with a hexagonal space group symmetry $P6_3/mmc$ and unit cell parameters $a \approx 13.15$ and $c \approx 15.05$ Å (Passaglia et al., 1998). In erionite, the total of Si + Al [$+Fe^{3+}$] should be equal to 36 atoms based on 72 oxygen atoms. There have been three erionite species identified, erionite-Ca, Na, and K. Dogan and Dogan (2008) report the erionite Ca general formula is $(Ca^{2+}_{3.56}\ K^{+}_{1.95}\ Na^{+}_{0.27}\ Mg^{+2}_{0.30})(Si_{25.78}\ Al_{10.28}Fe^{3+}_{0.01})O_{72}$, the erionite Na general formula is $(Ca^{2+}_{1.13}\ K^{+}_{2.40}\ Na^{+}_{4.00}\ Mg^{+2}_{0.24})(Si_{26.69}\ Al_{9.11}Fe^{3+}_{0.22})O_{72}$, and the erionite K general formula is $(Ca^{2+}_{1.03}\ K^{+}_{2.80}\ Na^{+}_{1.66}\ Mg^{+2}_{0.51})(Si_{28.21}\ Al_{7.39}Fe^{3+}_{0041})O_{72}$. In this work, the general term "erionite" will be used for all erionite species.

The offretite general formula is $(Ca\ K\ Mg)\ [Al_5\ Si_{13}\ O_{36}]\cdot 16H_2O$ (Passaglia et al., 1998) with a hexagonal space group symmetry P6m2 and unit cell parameters $a \approx 13.30$ and $c \approx 7.60$ Å (Gualtieri et al., 1998). In offretite, the total of Si + Al [$+Fe^{3+}$] should be equal to 18 atoms based on 36 oxygen atoms.

Erionite can commonly be found associated with clinoptilolite $(Ca\ Na_2\ K_2)_2\ [Al_4\ SiO_8\ O_{24}]\cdot 12H_2O$ (Sheppard, 1996) and can be overgrown on levyne, $(Ca_{0.5}\ Na\ K)_6\ [Al_6\ Si_{12}\ O_{36}]\cdot 18H_2O$, while offretite can be commonly found overgrown on chabazite, $(Ca_{0.5}\ Na\ K)_4\ [Al_4\ Si_8\ O_{24}]\cdot 12H_2O$, levyne and chabazite both being six-member ring structured zeolites (Armbruster & Gunter, 2001) like erionite and offretite. Because of wider ranges in formation though, erionite is the more common of the two zeolite species (Passaglia et al., 1998).

Distinction between the two zeolites is hindered due to uncertain definite parameters distinguishing the two zeolites, because of the structural and chemical similarities between themselves and other zeolites (Passaglia et al., 1998), and due to the possibility of intergrowth of the two species within each crystal (Tschernich, 1992). XRD patterns of erionite and offretite

(Figures 1.3 - 1.5) are very similar and there is the possibility of certain peaks being masked when found in association with smectite clay or clinoptilolite.

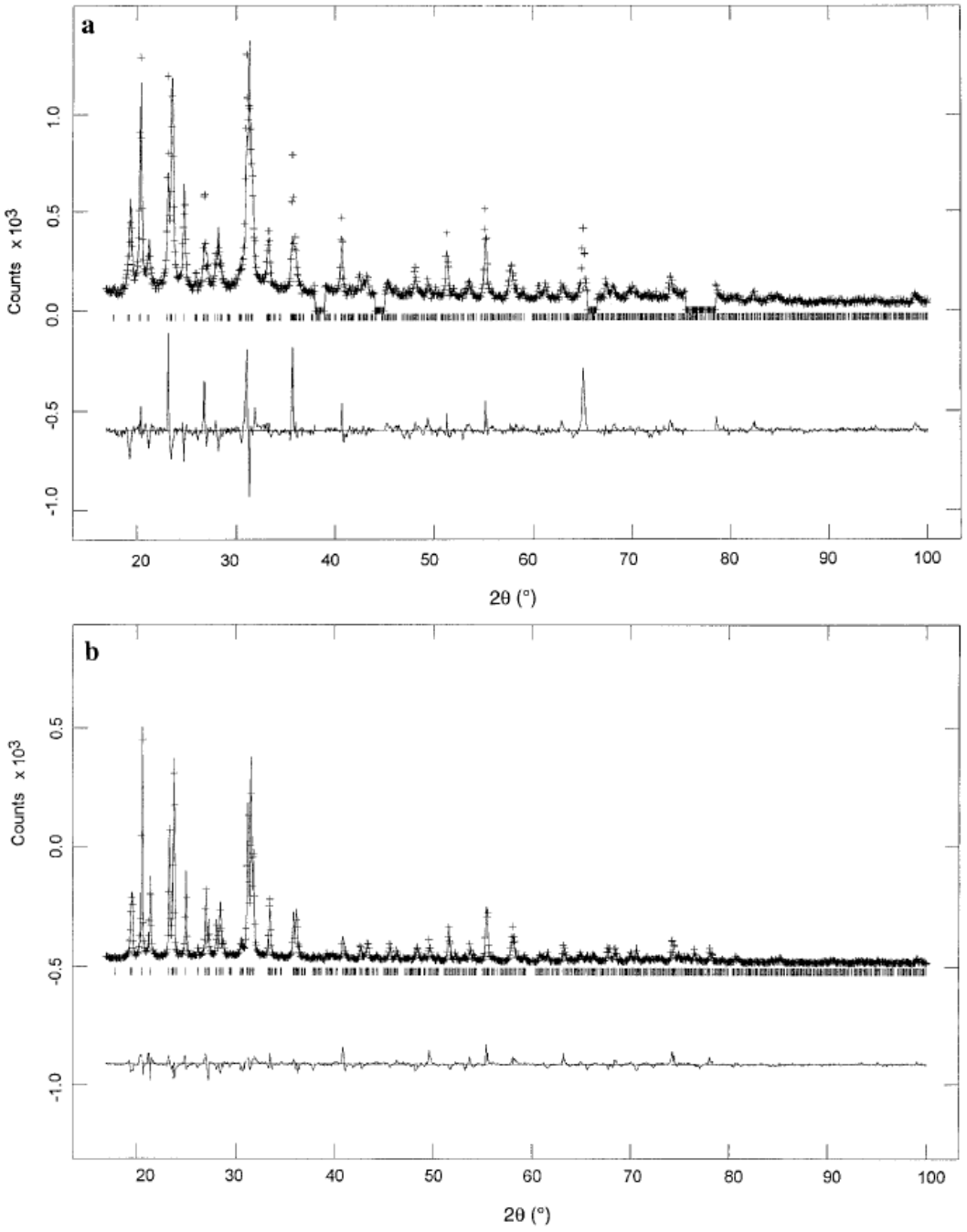

Figure 1.3. Conventional powder X-ray diffraction patterns for (a) erionite and (b) offretite (Gualtieri et al., 1998)

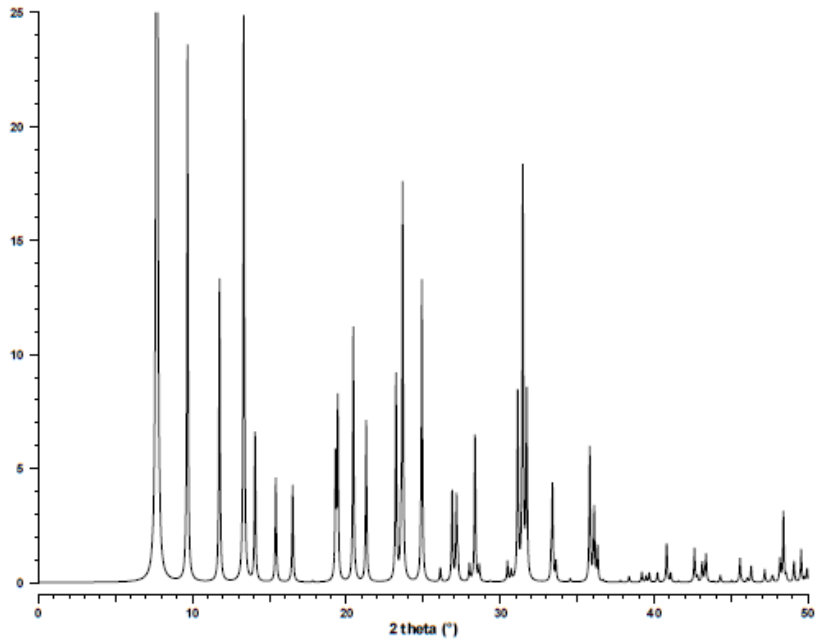

Figure 1.4. Synthetic erionite powder XRD pattern (Treacy and Higgins, 2001)

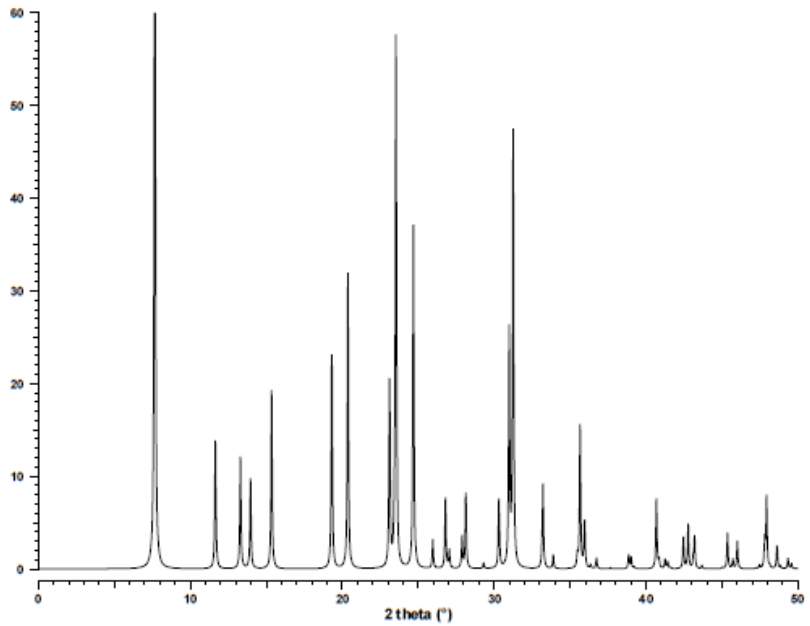

Figure 1.5. Synthetic offretite powder XRD pattern (Treacy and Higgins, 2001)

Unless samples are pure, it is sometimes very difficult to distinguish and/or properly identify the two in mixed rock or mixed mineral samples.

Erionite and offretite are both hexagonal zeolite minerals which contain connected, double six-member ring tetrahedra, Figure 1.6 and 1.7 (Gualtieri et al., 1998), which creates cancrinite cages, Figure 1.8 (Kokotailo and Fyfe, 1995) which orient themselves to form larger cage structures. Framework cages usually are occupied by Ca and K, but Na, Mg, and other metallic ions may also be present depending on the size of the cage structure produced. The presence of water in the cages of hydrated minerals regulates occupied cation sites versus dehydrated minerals due to the presence of hydrogen bonding (Alberti et al., 1997). Specific details on crystal structure can be found in Armbruster and Gunter (2001) and Gualtieri et al. (1998).

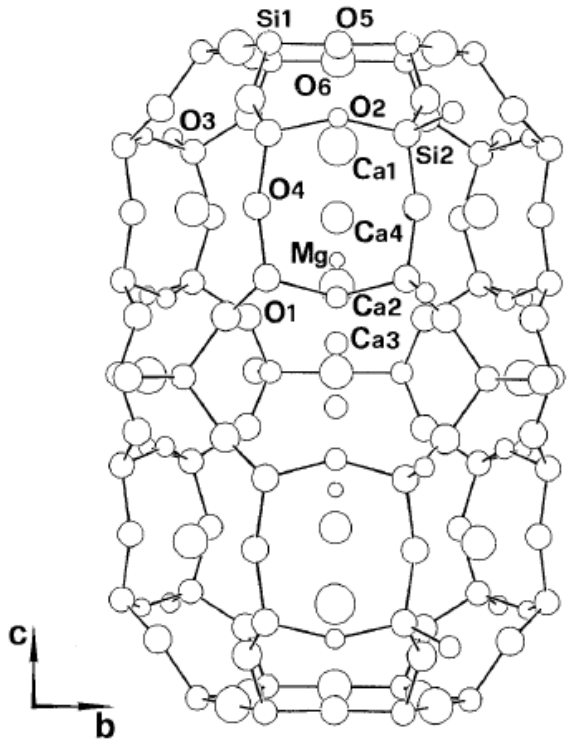

Figure 1.6. Erionite cage minus H_2O molecules (Gualtieri et al., 1998)

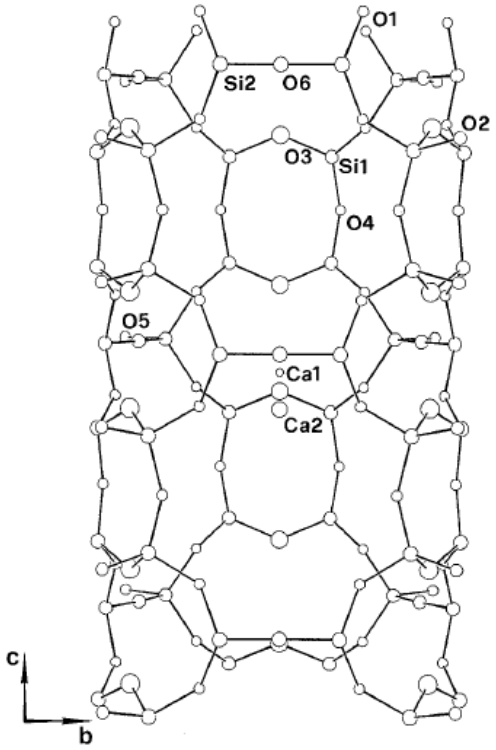

Figure 1.7. Offretite cage minus H_2O (Gualtieri et al., 1998)

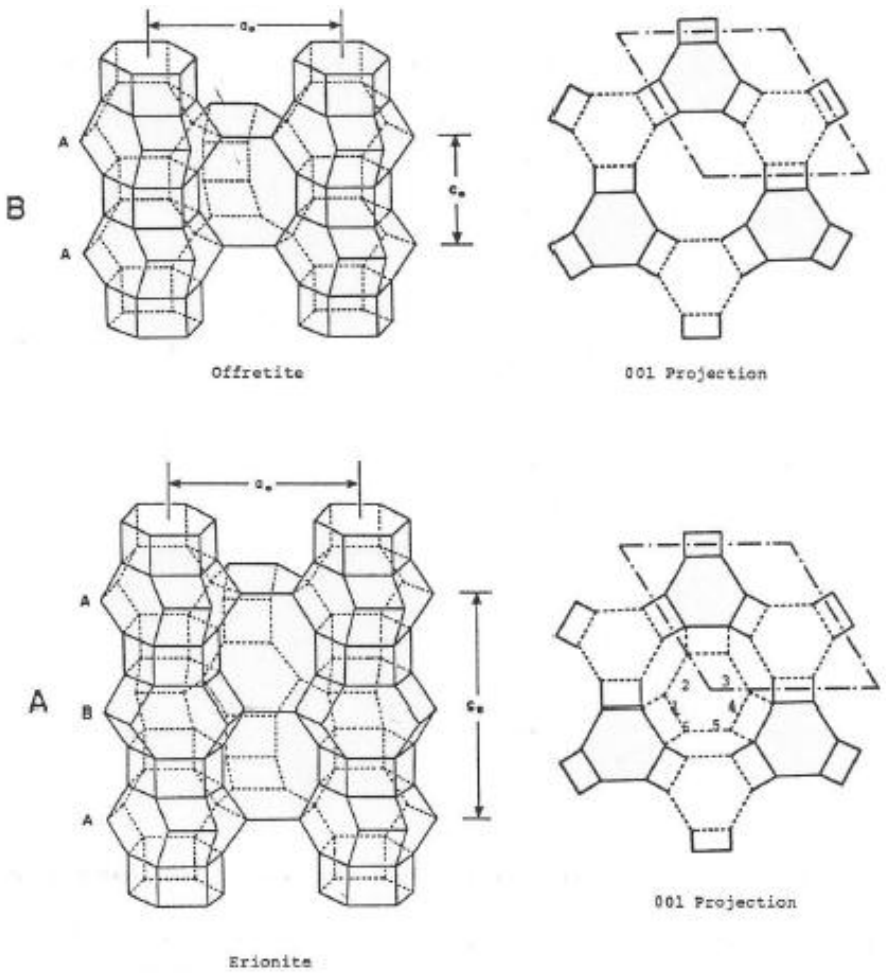

Figure 1.8. Erionite (A) and offretite (B) cage structures (Kokotailo and Fyfe, 1995).

The chemical attribute most relevant to distinguishing erionite from offretite is the ratio of Mg to Ca(+Na). Erionite is more calcium rich, whereas offretite is more magnesium rich. Passaglia et al. (1998) defined the ratio of Mg to Ca (+Na) = 0.30 as the boundary between the two minerals. The reliability of chemical analysis used to determine the zeolite species should be evaluated by using the balance error formula (Dogan and Dogan, 2008):

$$E=[(Al+Fe^{3+}) – (Na+K) + 2(Ca+Mg+Sr+Ba)]/[(Na+k) + 2(Ca+Mg+Sr+Ba)] \times 100,$$

or if there is a low Sr and Ba cation content, the modified formula can be used:

$$E=[(Al+Fe^{3+}) – (Na+K) + 2(Ca+Mg)]/[(Na+k) + 2(Ca+Mg)] \times 100.$$

Chemical analysis results for erionite are only considered to be reliable if the balance error (E%) is equal to or less than 10% (Passaglia, 1998). If the calculated E% from chemical analysis is greater than ±10%, the mineral cannot be erionite as defined by this rule. If the E% falls within the set conditions, then the mineral may be erionite or may still be another closely related zeolite with similar chemical composition. This being one of the major issues in properly identifying the zeolite species. Figs. 1.9 and 1.10 show ternary diagrams from Gualtieri et al. (1998) and Passaglia et al. (1998) used to distinguish erionite from offretite by chemical analysis.

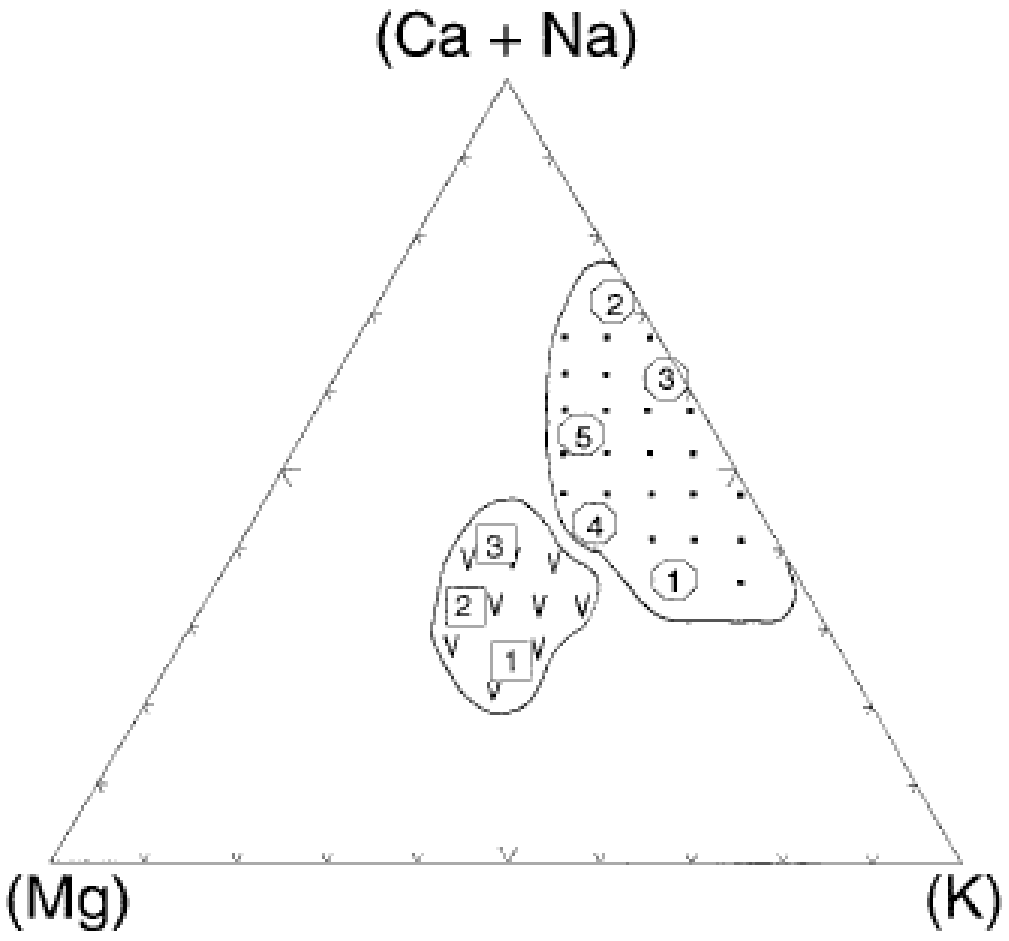

Figure 1.9. Ternary compositional diagram showing where erionite and offretite are expected to plot, open squares: offretite, open circles: erionite (Gualtieri et al., 1998).

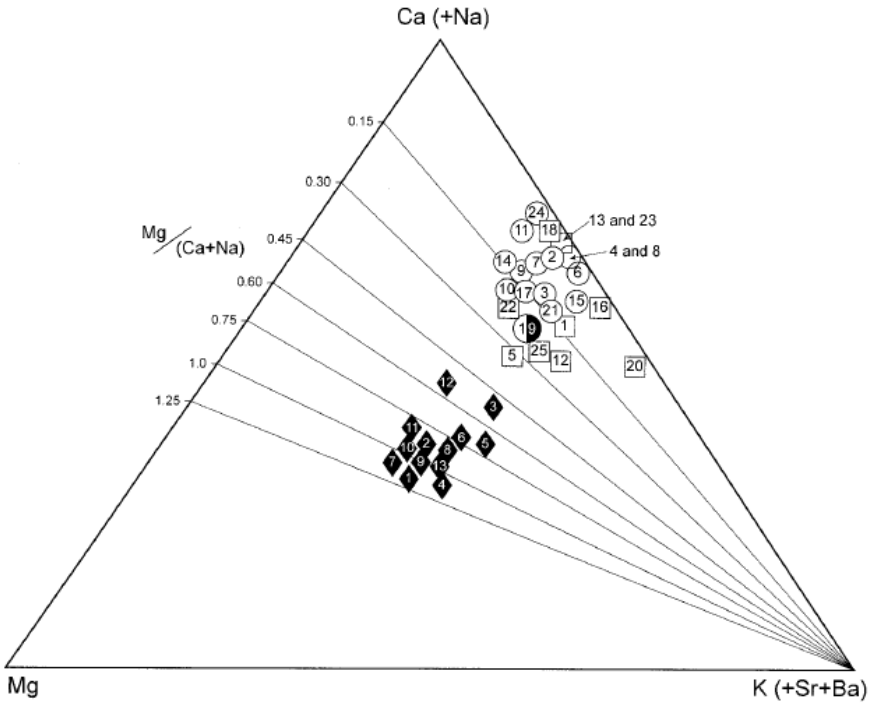

Figure 1.10. Ternary compositional diagram showing the Mg - Ca(+Na) - K(+Sr+Ba) content of erionite and offretite, open circles: erionites associated with levyne; open squares: isolated erionites and solid diamonds: offretite. (Passaglia et al., 1998)

1.3 Background of Erionite and Human Health

The fibrous zeolite mineral erionite has been shown to have greater carcinogenic qualities than crocidolite ($Na_2Fe^{2+}{}_3Fe^{3+}{}_2Si_8O_{22}(OH)_2$) and chrysotile ($Mg_3Si_2O_5(OH)_4$) asbestos (EPA, 2010). It has been classified as a Group I carcinogen by the International Agency for Research on Cancer (IARC, 1987).

The health issues related to erionite were first discovered in the central Anatolia region of Turkey, specifically the Cappadocia region, in the villages of Old Sarihdir, Tuzkoy, Karain, and the surrounding areas. These villages were associated with volcanic bedrock in which erionite was present. The villages were located on top of, built out of, and sometimes built into the soft volcanic tuffs which contained the erionite fibers. Villagers in these regions were exposed to the zeolite bearing bedrock on a daily basis. In the village of Karain, Turkey, a 32 year observation

was conducted of 162 villagers that had lived in the village for more than 10 years. It was recorded that 78% of the deaths that had occurred in the study group were due to malignant mesothelioma. It is estimated that 50% of the total deaths in the area can be attributed to mesothelioma (Metintas, 1999; Emri et al., 2002).

Mesothelioma is a rare cancer caused by genetic mutations that occur in the thin layer of the tissue that covers the body's internal organs, and is usually associated with exposure to fibrous minerals, especially amphibole asbestos. The most common type of mesothelioma is pleural malignant mesothelioma which affects the tissue around the lungs. Other types include peritoneal mesothelioma (tissue of the abdomen) and pericardial mesothelioma (tissue of the heart) (Kleymenova et al., 1999; Mayo Clinic, 2011).

Asbestos fiber (Figure 1.11) exposure and its relation to mesothelioma have been well established. But non-asbestos, fibrous mineral exposure and the relation to mesothelioma is not well known. After recent studies, it is believed that the non-asbestos, zeolite mineral erionite (Figure 1.12) could be potentially more toxic than amphibole asbestos. Experimental studies show erionite has up to 300-800 times more carcinogenic potency and may be 20-40 times more active than some asbestos forms. Physical and chemical differences between the minerals could explain these differences (Kleymenova et al., 1999; Emri et al., 2002).

There are different hypotheses for the increased carcinogenic effect of erionite. One theory identifies the possibility of the balance between cell proliferation, growth and production of cells, and apoptosis, genetically regulated death of cells, as a contributing factor. It is believed that a lower amount of erionite compared with crocidolite ($Na_2Fe^{2+}{}_3Fe^{3+}{}_2Si_8O_{22}(OH)_2$) asbestos is required to induce c-Jun mRNA, a mechanism that has been linked to fiber carcinogenesis (Dogan et al., 2006). A second theory is that the toxicity of erionite could be associated with iron

that accumulates on its surface after it is deposited within the respiratory epithelium which then produces hydroxyl radicals (Fach et al., 2002). And a third theory is that the carcinogenic effects may be due in part to a genetic predisposition within select populations (Dogan et al., 2006; Kliment et al., 2008).

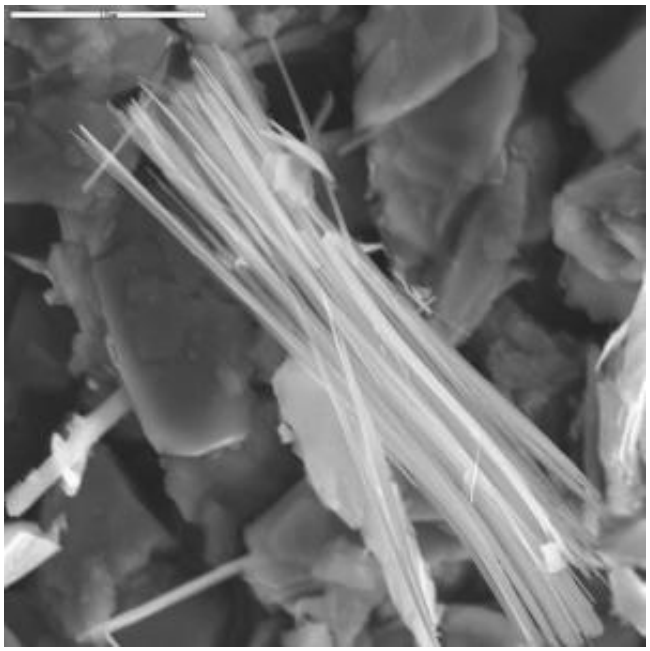

Figure 1.11. Tremolite asbestos, $Ca_2(Mg,Fe)_5Si_8O_{22}(OH)_2$ (Meeker, 2011)

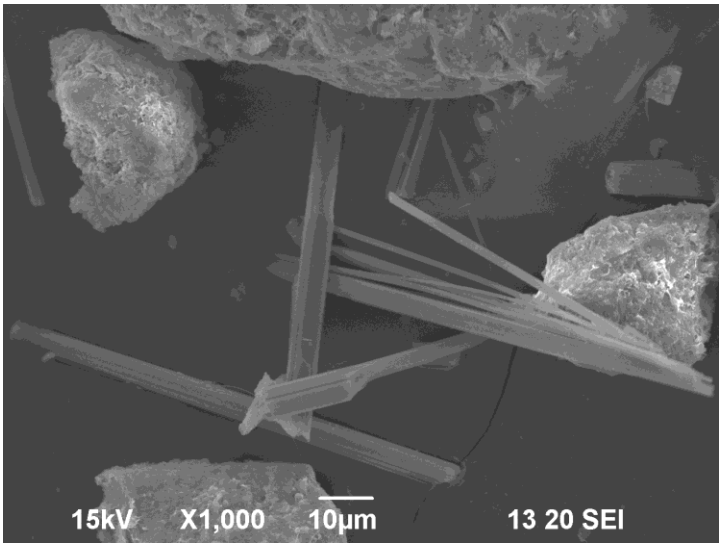

Figure 1.12. Possible erionite fibers from this study, $Na_2\,K_2\,Ca_3\,[Al_{10}Si_{26}O_{72}]\cdot 30\,H_2O$ (NDSU SEM)

1.4 Previous Work on Erionite in North Dakota

Forsman (1986) reported the discovery of the fibrous mineral erionite in volcanic tuffs located in the Killdeer Mountains of western North Dakota's Dunn County. Since then, other locations within the state which are believed to potentially contain erionite have been identified by others, including by state Geologist Dr. Ed Murphy (Murphy, pers. comm., 2008). These other locations correlate to high butte formations similar to the Killdeer Mountains. Because of the potential carcinogenic health affects posed by this zeolite mineral, and the high risk of exposure and transmission in the western part of the state, officials from the NDDoH, NDGS, and the EPA became concerned with exposure and transmission of airborne dusts and particulates possibly containing erionite fibers from gravel pits, roads, parking lots, playgrounds, feed lots, building and construction, mining operations, oil extraction, and farming/ranching operations.

In 2007, the EPA requested a study by the USGS on 20 soil and roadbed samples collected from western North Dakota for zeolite identification. The SEM/EDS analysis determined the zeolite as intermediate between erionite and offretite as determined by Passaglia et al. (1998), and it coincides with zeolites that are associated with high incidences of malignant diseases in Turkey (Dogan et al., 2006). The EPMA data plot within the offretite field and agree with the EPMA data collected by Forsman (1986). X-ray diffraction data support the presence of erionite, but because both minerals have similar diffraction patterns, offretite cannot be ruled out (Passaglia et al., 1998; Lowers and Meeker, 2007).

Studies conducted by the Energy & Environmental Research Center (EERC) at the University of North Dakota identified erionite by XRD and SEM in sandstones and siltstones from buttes in Dunn, Stark, and Slope Counties of North Dakota. No definitive correlation was

determined through comparative mapping between the states erionite occurrences and health effects that may be attributed to erionite. Further health risk assessments were recommended (EERC, Eylands et al., 2009).

In October, 2010, the U.S. EPA published the follow up report to the 2007 study. In this study, 34 volunteers who are current or past residents of western North Dakota with exposure to road gravels and erionite containing rock units partook in chest X-rays and sensitive high resolution computed tomography (HRCT) scans to detect pleural and interstitial changes associated with fiber exposure. Chest X-ray results did not indicate a significant increase in interstitial or localized pleural changes. The HRCT scans did indicate an increase in interstitial changes. Results of this study do suggest that exposure to erionite containing rock units and road gravels could increase the risk of pleural and interstitial changes in the body that are commonly associated with asbestos exposure (U.S. EPA, October, 2010:Ryan et al. 2011).

CHAPTER 2. GENERAL GEOLOGY OF WESTERN NORTH DAKOTA

2.1 North Dakota Geologic Time and Setting

This chapter provides a description of the general geology (surface geology of North Dakota, Figure 2.1), the geologic time setting (North Dakota geologic time scale, Figure 2.2), and the past geologic processes that resulted in the formations and stratigraphy found in the study area that has occurred over the past 150 million years. Most of this discussion is summarized from Bluemle, 2000, Murphy et al., 1993, and Murphy, 2001.

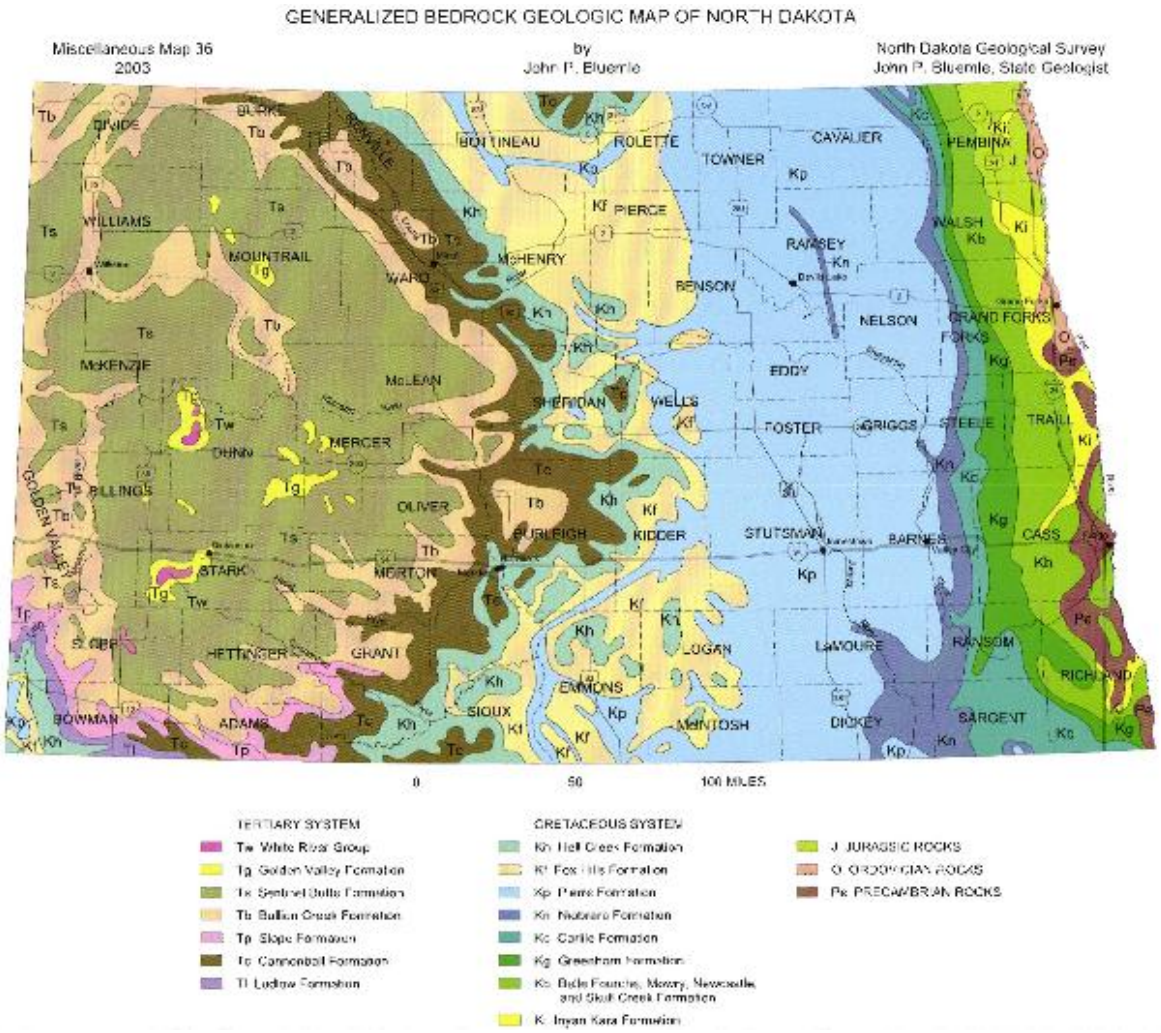

Figure 2.1. Geologic map of North Dakota (Bluemle, 2003)

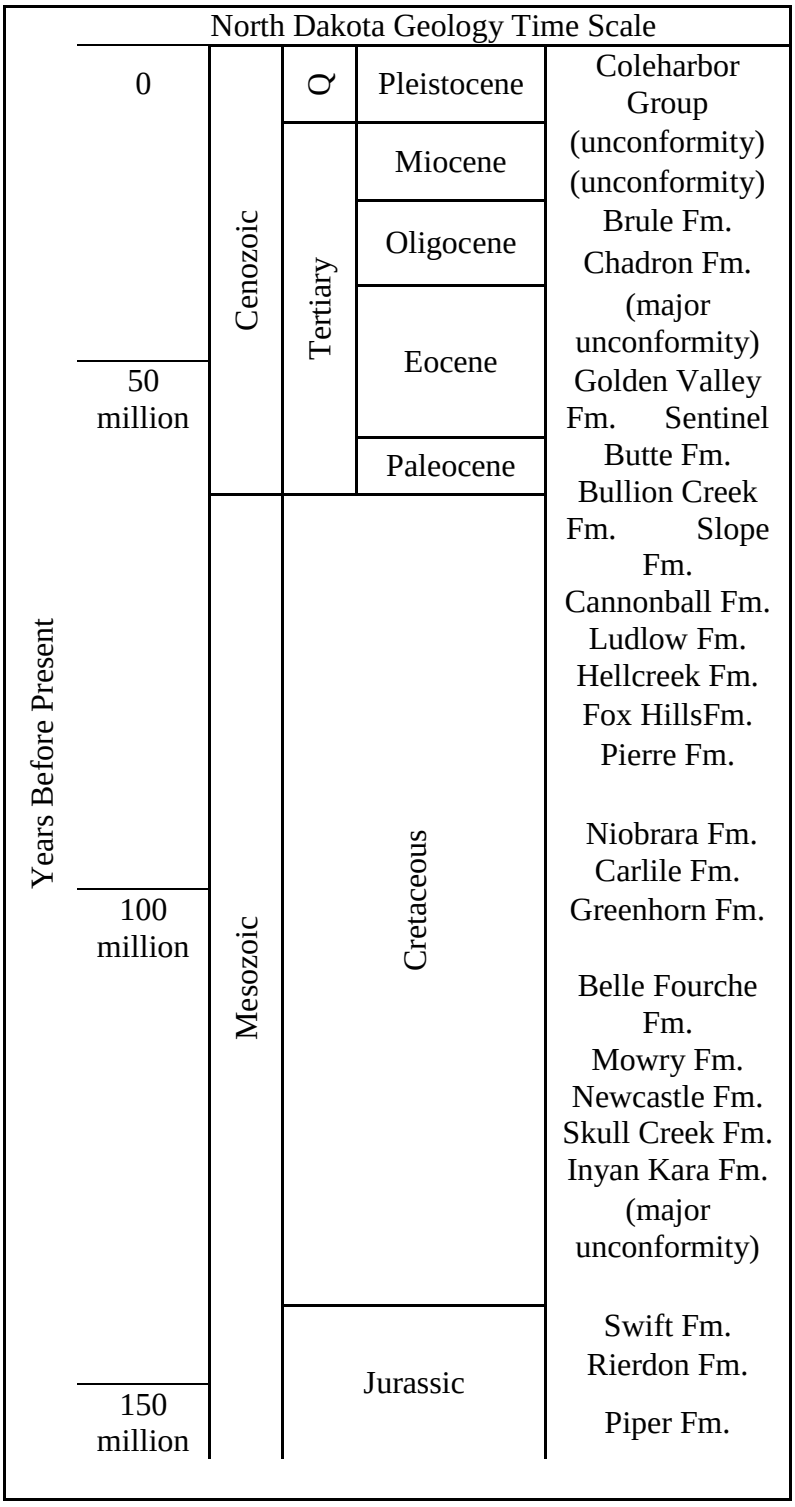

Figure 2.2. North Dakota's geologic history, last 150 million years (edited from Bluemle, 2000)

Geologic units sampled for this study include the Golden Valley, Chadron, Brule, and Arikaree Formations (Figure 2.3), all of which are believed to be represented in the sampling locations of the North and South Killdeer Mountains, the Rainy Butte complex, and Chalky Butte complex (White Butte) described in Chapter 3 Sampling and Analysis.

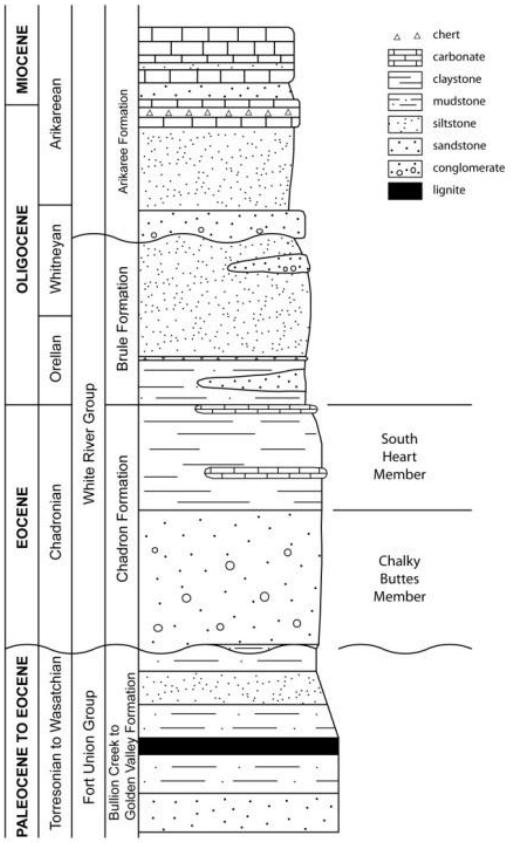

Figure 2.3. Generalized stratigraphic column for Tertiary strata of North Dakota including the Arikaree, Brule, Chadron, and Golden Valley formations (Murphy et al., 1993)

2.2 General Geology of Western North Dakota

Western (southwestern) North Dakota in general is described as the area of North Dakota that is located south and west of the Missouri River. It is an area distinguished by a wide variety of different surface formations including rolling uplands, hills, buttes and mesas, wetlands and river valleys, and scattered areas of badlands (Bluemle, 2000). Specifically known as the

Missouri Slope Upland portion of the North Dakota Great Plains, it is separated from the Central Lowlands of eastern North Dakota by the Missouri Coteau/Missouri Escarpment, a product of recurrent glaciation, initiated by a preglacial, erosional escarpment (Bluemle, 2000). The Missouri Slope Uplands are made up of large expanses of rolling hills and plains, except in regions associated with the badlands which contain many prominent buttes and mesas (Bluemle, 2000) scattered throughout the region. The rolling Missouri upland is a landscape formed primarily from weathering and erosion by wind and water along with subsequent mass wasting processes. Unlike most of North Dakota, these southwestern areas were either never glaciated, or the glaciation occurred so long ago that nearly all definitive evidence of glaciation has been destroyed and removed by the continuing erosional processes (Bluemle, 2000).

The majority of the bedrock in the area consists of layers of sand, silt, clay, and lignite deposited during Paleocene and Eocene times, 55 to 65 million years ago, and belongs to the Fort Union Group. During the Oligocene, rivers and streams cut into the Fort Union sediments, ultimately depositing coarse gravel and sand beds which would become a part of the Chalky Buttes member of the Chadron Formation. Presently, river and stream erosion along with mass wasting is still the primary form of erosion affecting the southwestern North Dakota landscape (Bluemle, 2000).

2.3. Geology of the Killdeer Mountains, Rainy Buttes, and Chalky Butte

2.3.1. The Killdeer Mountains, Dunn County, North Dakota

The Killdeer Mountains consist of two predominant buttes/mesas located in northern Dunn County of western North Dakota. The two mesas rise about 700 ft. (213.4 m) above the surrounding landscape and cover an area of approximately 4,800 acres. The large buttes/mesas are located in an area that was believed to be covered by a large lake or a series of many smaller

lakes during the Miocene time, 20 - 25 million years ago. The cap rock on top of the Killdeer Mountains consists of a thick, resistant layer of limestone that contains volcanic ash believed to have originated from volcanic eruptions in Montana and Wyoming (Bluemle, 2000). The ash was deposited across western North Dakota by eolian processes and then transported to the lake systems by fluvial processes, eventually accumulating to approximately a hundred foot thickness in locations. After the lakes dried up, the ash-rich, tuffaceous sediment settled and hardened into tuffaceous limestone beds (Bluemle, 2000). About five million years ago, the erosional cycle in the area resulted in down cutting, which removed large amounts of surrounding sediment. The resistant tuffaceous limestone beds remained as the cap rock of the Killdeer Mountains, marking the locations of the ancient Miocene lake(s) (Bluemle, 2000). The geologic setting of the area has been described as "inverted lake beds" (Murphy et al., 2001). Figure 2.4 and 2.5 show the Killdeer Mountains, South (Figure 2.4) and North (Figure 2.5).

Figure 2.4. South Killdeer Mountain as viewed from North Killdeer Mountain (photo by JWT)

Figure 2.5. North Killdeer Mountain as viewed from the rim of the southern quarry exposure on North Killdeer Mountain (photo by JWT)

2.3.1.1. Killdeer Mountain stratigraphic units. The Killdeer Mountains contain rock units from the Arikaree formation, Chadron formation (Chalky butte member) and the Golden Valley formation (Bear Den member and Camel Buttes member). No Brule Formation appears to be present in this location (Murphy, 2001). A stratigraphic section of South Killdeer Mountain compared to the general stratigraphy of North Dakota is provided in Figure 2.6 (NDGS, 2006 and Murphy, pers. comm., 2008).

The Arikaree formation constitutes the caprock of the Killdeer Mountain complex and consists of approximately 330 ft. (100.6 m) of tuffaceous siltstones, sandstones, and carbonates, with the sandstones and siltstones being calcareous. The vast majority of the units contain some amount of volcanic glass (Forsman, 1986), characterizing this as slightly to highly tuffaceous.

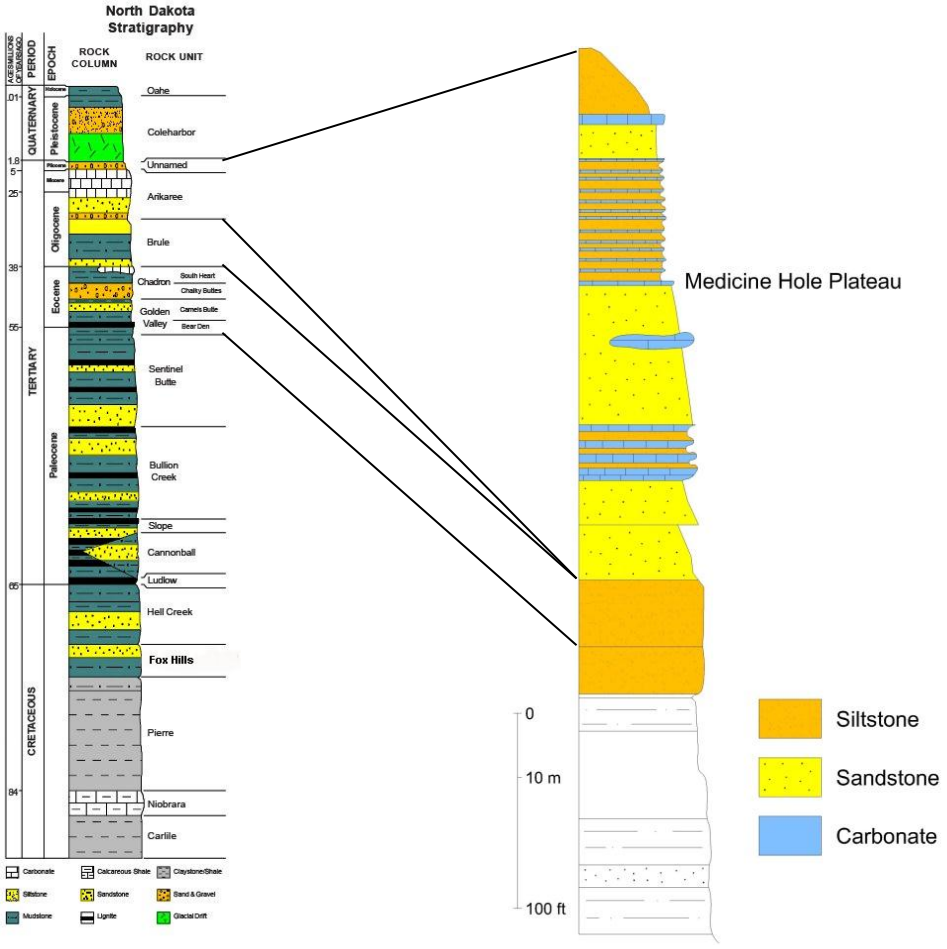

NDGS, 2006 Murphy, 2008

Figure 2.6. General stratigraphy of North Dakota and correlation with the Killdeer Mountains (modified from NDGS (2006) and Murphy, 2008)

The most predominant unit of the Killdeer Mountain caprock contains interbedded tuffaceous sandstone and siltstone layers with carbonate lenses. This unit has been termed the "burrowed marker unit" (BMU) by Forsman (1986) for the presence of an abundance of what he classified as fossilized burrows of unknown origins (Murphy et al, 1993). What these "fossilized burrows" are and the origins of them is still in question.

The Chadron Formation is made up of yellow/green sandy siltstone and clayey sandstone which is not well exposed in the Killdeer Mountains. Due to poor surface exposures, characterization and identification of lithologies beneath the caprock (Arikaree formation) is difficult (Murphy et al, 1993). Nonetheless, these units are believed to be lithologically similar to the Chalky Buttes member of the Chadron Formation found in other parts of southwest North Dakota (Murphy, 2001).

The Fort Union group or Golden Valley formation consists of the Bear Den member and overlying Camel Buttes member. The Bear Den member lies conformably on the Sentinel butte Formation and consists of 20 to 40 ft. (6.1 to 12.2 m) of kaolinitic rich sandstone, siltstone, siltstone, and shale, often with iron staining and gypsum-filled polygons (Murphy, 2001). The Camel Buttes member is an early Eocene unconformity (Murphy, 2001) composed of alternating beds of brown to gold micaceous sandstones and siltstones with thin lignite bands (Murphy et al, 1993) and can be identified by way of the visible mica grains.

2.3.2. Rainy Buttes, Slope County, North Dakota

The Rainy Butte complex consists of four total buttes; East Rainy Butte (Figure 2.7) and West Rainy Butte (Figure 2.8), Baldy Butte, and an unnamed butte located just to the north of East Rainy Butte.

The Rainy Butte complex is located in Slope County of southwestern North Dakota. The Rainy Buttes are a pair of very large butte/mesa formations which rise above the landscape about 500 feet (152.4 m) and cover an area of approximately 972 acres (Murphy et al, 1993).

2.3.2.1. Rainy Buttes stratigraphic units. East and West Rainy Buttes consist of rock units from the Arikaree formation, Brule Formation, Chadron Formation, and Golden Valley Formation. (Murphy et al, 1993)

Figure 2.7. East Rainy Butte and surrounding landscape as viewed from west side (photo by JWT)

Figure 2.8. West Rainy Butte as viewed from the southeast side of the butte (photo by JWT)

The Arikaree Formation found at the Rainy Butte complex composes the caprock which consists of well cemented sandstone on top of West Rainy Butte and well cemented sandstone and shales on top of East Rainy Butte. The sandstones are fine to coarse grained, conglomerated, cross-bedded, burrowed, and contain clay clasts. At East Rainy Butte, the cap rock is underlain by a green siliceous claystone. (Murphy et al, 1993)

The Brule Formation is made of 150 to 180 feet (45.7 to 54.9 m) thick, pink/brown siltstones containing thin, white siliceous or tuffaceous beds. They are fine to medium grained in the middle of the unit, conglomeratic at the base, and are cross bedded throughout. The sandstones at West Rainy Butte appear to thin and thicken throughout the unit and appear to be composed of multiple sandstones due to varying degrees of cementation. Formation very similar to Brule identified strata in the Little Badlands. (Murphy et al, 1993)

The Chadron Formation is identified at the Rainy Buttes as about 10 ft. (3.1 m) of sandy siltstone overlain by smectitic shale of the south heart member (which caps nearby Baldy Butte). At East and West rainy buttes, the south heart member is capped by a thin carbonate lens. (Murphy et al, 1993)

The Golden Valley Formation composes the surrounding surfaces out from the buttes base. Exposures are limited to knolls and road cuts. These exposures are identified as white, micaceous siltstones less than 30 ft. (9.1 m) in thickness and are reported as the Bear Den member of the Golden Valley formation (Murphy et al, 1993).

2.3.3. Chalky Buttes (White Butte), Slope County, North Dakota

White Butte, the highest point in North Dakota, is a part of the Chalky butte complex (Figure 2.12) located in Slope County of western North Dakota. The Chalky buttes are a series of

buttes and mesas which rise over the landscape about 500 ft. (152.4 m) and cover an area of approximately 3,251 acres (Murphy et al, 1993).

Figure 2.9. Chalky Butte complex as approached from the southeast (photo by JWT)

2.3.3.1. White Butte stratigraphic units. White Butte consists of rock units from the Arikaree, Brule, Chadron, and Sentinel Butte Formations.

At White Butte, the Arikaree formation is a 125 ft. (38.1 m) thick unit composed of limestones, sandstones, siltstones, and shales. The sandstones at the base are generally a type of conglomerate containing a mixture of igneous rock, siltstone, and shale pebbles. The Brule Formation at this location is a 25 ft. (7.6 m) layer of pink to buff colored siltstones. It is believed that a large portion of the Brule has been removed due to erosion prior to Arikaree deposition by comparison to the thickness of the Brule in other nearby formations (Murphy et al, 1993). The Chadron formation is well exposed unit and contact is easily distinguished by contrast in color from others. It is mainly composed of white sandy siltstone and pebbly sandstones. The upper portion of the unit consists of gray/green smectite clays with thin limestone beds. The basal unit of White Butte is the Sentinel Butte Formation which is approximately a 200 ft. (61.0 m) thick

layer consisting of shale and sandstone. The shale is a purple-white to light medium brown with an expansion/contraction popcorn texture. The sandstone is a light gray to dazzling white color with a silty to clayey texture. Some very fine to medium quartz grains which are poorly cemented are present along with some iron oxide layers (Murphy et al, 1993).

For reference, Figure 3.1 is a regional map showing the locations of the butte complexes described.

CHAPTER 3. SAMPLING AND ANALYSIS

3.1. Preliminary Samples and Analysis

Preliminary analysis was conducted in 2008 on Killdeer Mountain rock samples generously provided by Dr. Forsman from his 1986 collection. Samples, with sample identification numbers and field notes, were obtained from Dr. Forsman during a personal visit to his lab at the University of North Dakota in preparation for field and lab work. No processing was done to the Forsman samples during preliminary analysis. Material was introduced onto SEM/EDS stubs as described in the section on sample preparation. Ten different samples containing fibrous material were analyzed at NDSU using SEM/EDS. The analysis was conducted on multiple fibers using 25 various points. Table 3.1 shows the samples tested, the number of scan points per fiber, and the results of analyses of these samples. See Appendix Table 2 and Appendix Table 3 for further information on Forsman samples.

Table 3.1. Atom % composition Forsman sample zeolite fibers. (NDSU SEM/EDS)

SEM #	Sample ID	Scan	O %	Na %	Mg %	Al %	Si %	Cl %	K %	Ca%	Fe %	% total
172	NM #3(2) pt1	NA										
172	NM #3(2) pt2		60.52	0.22	1.31	7.05	27.14		2.05	1.7		99.99
172	NM #3(1) pt 1	Area	60.65	0.33	1.45	6.73	26.83		2.52	1.48		99.99
173	NM #2 pt1		60.04	0	1.21	7.59	27.73		2.09	1.33		99.99
173	NM #2 pt2		57.16	0.27	1.67	7.99	30.35		1.56	0.99		99.99
174	MH1a(1) pt1		54.86	0.11	0.27	7.83	31.81		2.13	2.99		100
174	MH1a(1) pt2		55.78	0.28	0.46	7.89	30.85		2.06	2.68		100
175	MH3(1) pt1		60.09	0	0.61	7.36	28.1		1.62	2.23		100.01
175	MH3(1) pt2		58.63	0.1	0.57	7.33	29.19		1.74	2.45		100.01
311	MH 1B(2) pt1		50.7	0.59	1.66	8.42	34.67		2.9	1.07		100.01
311	MH 1B(2) pt2		54.76	0.34	1.58	8.17	31.88		2.24	1.02		99.99
311	MH 1B(2) pt3		53.75	0.44	1.2	8.19	32.72		2.67	1.04		100.01
313	MH 2(1) pt1	NA										0
313	MH 2(1) pt2		50.11	0.13	0.66	8.63	34.64		2.66	3.17		100
313	MH 2(1) pt3		51.18	0.2	0.71	7.8	33.15		2.23	4.72		99.99
315	MH 5B pt1		54.99	1.1	5.25	2.41	21		0.95	5.73	8.4	99.83
315	MH 5B pt2		53.25	1.14	5.7	3.3	21.18		0.64	5.82	8.57	99.6
315	MH 5B pt3		57.91	0.91	4.49	2.83	20.51		0.22	5.41	7.11	99.39
315	MH 5B(2) pt1		57.64	1.12	1.46	6.78	30.12		2.03	0.85		100
315	MH 5B(2) pt2		55.31	0.59	1.57	3.22	24.79		8.03	6.49		100
315	MH 5B(2) pt3		56.92	0.95	2.09	4.4	19.92	0.41	2.07	2.12	11.12	100
317	MH 9A	NA										
319	MH 9B(1) pt1		57.6	0	0.29	7	29.84		2.41	2.86		100
319	MH 9B(1) pt2		59.69	0.16	0.51	7.36	28.17		1.83	2.27		99.99
319	MH 9B(1) pt3		57.6	0	0.48	7.54	29.29		2.21	2.87		99.99

3.2. Field Locations and Sample Site Descriptions

Field work and sampling was completed during the summer of 2008. During the 4 day field trip, we visited three locations relative to the high butte formations described by State Geologist Dr. Ed Murphy that were expected to have the zeolite erionite present within the rock profile. Sampling was conducted where possible at North and South Killdeer Mountains, West and East Rainy Buttes, and White Butte (Chalky Butte complex). A total of 37 rock and soil samples were gathered and cataloged from these locations. Figure 3.1 is a county map showing the regions within the state and specific sampling locations visited during field work.

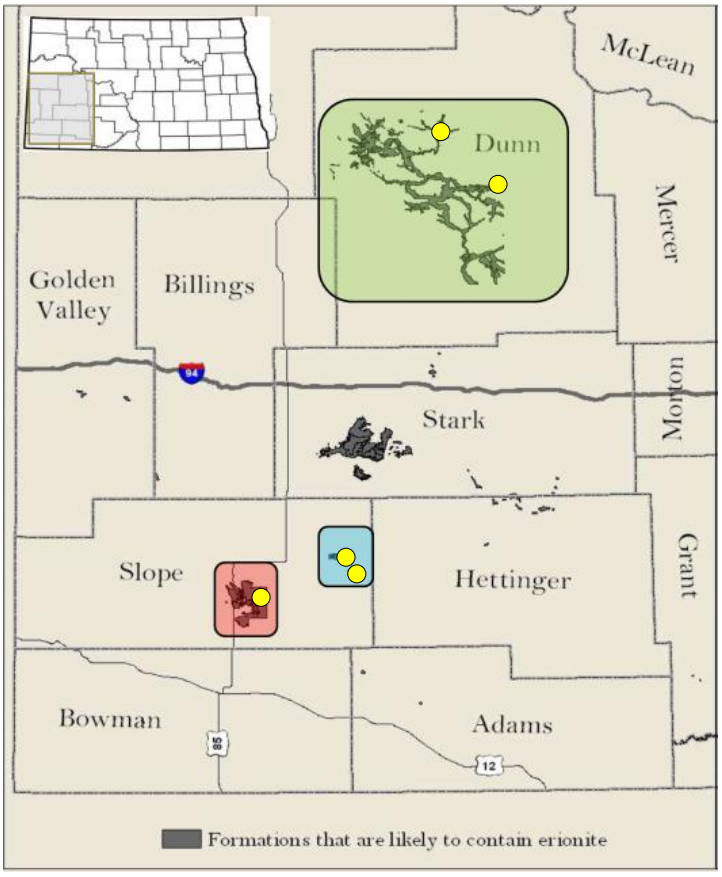

Figure 3.1. Regional map showing sampling locations, (Modified from NDDoH, 2007) North & South Killdeer Mountains, Dunn County, ND (green), East & West Rainy Buttes, Slope County, ND (blue), and White Butte, Slope County, ND (red)

At all sites, sampling consisted of gathering hand samples from undisturbed outcrops, recording latitude, longitude and elevation, measuring elevation (distance) between samples, bagging the hand samples, assigning a sample number to each sample and recording it in a field journal and on the sample bag, and taking a picture of exact sample site with reference scale (see Appendix Table 1 and Appendix Figure 3). Sample numbers were assigned according to the collector, collection date, and daily sequential sample number. For example, jwt080602-01 correlates to a sample collected by Jason W. Triplett (jwt) on 2008 year, 06 month, 02 day, and it was the first (01) sample collected that day. Table 3.2 lists all samples by number and gives sample site and a brief field description.

Table 3.2. Sample list with location and field descriptions

Sample ID – jwt	Sample Site	Field Description (BSE)
080602-01*	SKDM	fine gravel, silty clay. black hammer pic. Light grn color, below drk grn. ~6' below 080602-02
080602-02*	SKDM	fine gravel, silty clay. red hammer pic. Light grn color, below drk grn w/ concretions. ~6' above 080602-01
080602-03	SKDM	Medicine Hole entrance. White color. One sample pic w/ hammer and one w/ Jason. Unit 12 Murphy etal 8-1' carbonate lense interbed 5' siltstones
080603-01	SKDM	2 jwt's (135.25") below base of BMU. Sandy-silt
080603-02	SKDM	5 jwt's (338.125") below base of BMU. Greenish siltstone
080603-03	SKDM	8 jwt's (541") below base of BMU. White, clayey fine-grained siltstone below calcareous ledge unit
080603-04	SKDM	10 jwt's (676.25") below base of BMU. Whitish clayey siltston above cm-banded calcareous unit
080603-05	SKDM	11 jwt's (743.875") below base of BMU. Whitish clayey siltstone directly below cm-banded calcareous unit.
080603-06	SKDM	13 jwt's (879.125") below base of BMU. Whitish silty layer below 2'0" Concretion rich unit. Possibly same as 080602-02,01
080603-07*	SKDM	15 jwt's (1014.38") below base of BMU. Greenish clay-bearing siltstone, possible slump, but don't think so…
080603-08	SKDM	(16' BMU) 8' or 1/2 way up BMU. Friable material between harder calcareous layers
080603-09	SKDM	(16' BMU) 8' or 1/2 way up BMU. Calcareous material. Interior softer, fine grained. Friable core.
080603-10	SKDM	10 jwt's (676.25") above top of BMU. Calcareous, medium grained white sandstone. (believe unit is "unit 10" Murphy etal.)
080603-11	SKDM	25 jwt's (1690.63") above top of BMU. Sandstone Unit #13 Murphy etal. Fine grained siltstone overlain by carbonate (Unit 14 Murphy etal)
080604-01	NKDM(wqe)	Whitish, fine grained, powdery w/ burrow like structures
080604-02	NKDM(wqe)	Massive carbonate cemented ash w/ vugs (pores), chemical alteration (x<20cm across, dark patches), lithic fragments (3mm-5cm)
080604-03	NKDM(wqe)	Whitish carbonate layer above clay (080604-06) and massive ash
080604-04	NKDM(wqe)	Soil Sample
080604-05	NKDM(wqe)	Lithic fragment from 080604-02
080604-06	NKDM(wqe)	Clay layer directly on top of massive unit
080604-07	NKDM(eqe)	Siltstone 4' from base
080604-08	NKDM(eqe)	Silty clay 13' from base
080604-09	NKDM(eqe)	Burrowed calcareous unit 11' from base
080604-10	WRB	Fine grained white siltstone. Golden Valley. 3100' elevation GPS
080604-11	WRB	Top of South Heart member of chadron. Distinct carbonate layer. 3200' elevation
080604-12	WRB	Base of the brule. Pink to brown silty clay. ~3215' elevation GPS
080604-13	WRB	Possibly Unit #6 Murphy etal. Mudstone in Brule. Light pink/brown. Moderatley indurated (chisel)
080604-14	WRB	~10' above 080604-13, Float, small chips of light green clay (?Brule?) 3258' elevation GPS
080604-15	WRB	Small clay bed in among coarse grained crossbedding. Base of caprock. 3260' elevation GPS
080604-16	WRB	Sandstone Caprock. We believe Arikaree.
080605-01	ERB	Top of brule, brown siltstone w/ some clay, directly below dendritic chert layer 3320' elevation GPS
080605-02	ERB	Clay lense - Sandstone/siltstone crossbeding with clay lenses (~1' in length) ~20' below caprock 3250 ' elevation GPS
080605-03	ERB	White powdery siltstone below Sandstone layer. Ashy? 3260" elevation GPS
080605-04	WB	~10' below main chalky butte member whitish with light brown oxidation.
080605-05	WB	Bentonite (very wet, popcorn look on outside, dry 1/2 inch under)

Notes: SKDM - South Killdeer Mountain NKDM - North Killdeer Mountain: wqe - West Quarry entrance, eqe - East Quarry entrance
WRB - West Rainy Butte ERB - East Rainy Butte WB - White Butte

Sample Number with "*" denotes possible slump

3.2.1. Killdeer Mountains, North and South Killdeer Mountain complexes

Figure 3.2 shows satellite image of South Killdeer Mountain and Figure 3.3 shows South Killdeer Mountain and surrounding landscape from the northwest looking towards Medicine Hole Plateau.

Figure 3.2. Satellite image of South Killdeer Mountain, 47°26”38’ north latitude and 102°53”40’ west longitude. Sampling conducted from bottom of trail (white ridge) on east side going upward to the west (Google Earth)


Figure 3.3. South Killdeer Mountain, Medicine Hole Plateau, viewed from the northwest (photo by JWT)

3.2.1.1. South Killdeer Mountain. At South Killdeer Mountain, a systematic sampling scheme was used. Sampling began at the BMU strata (Figure 3.4), named by Dr. Forsman (1986), and proceeded downward, collecting and recording location and elevation at exposed units, and upwards from the BMU collecting and recording location and elevation at exposed units. Due to overgrowth on the surface and abundant slump formations along the slopes of South Killdeer Mountain, it was impossible to identify and collect samples from all units described by Murphy et al. (1993), so samples were taken from outcrop exposures determined to be undisturbed and when possible, different from those already collected. Figure 3.5 is a stratigraphic profile showing locations of all samples collected for South Killdeer Mountain

Figure 3.4. Sampling and measurements taken from the middle of burrowed marker unit (BMU, Forsman, 1986) (photo by BSE)

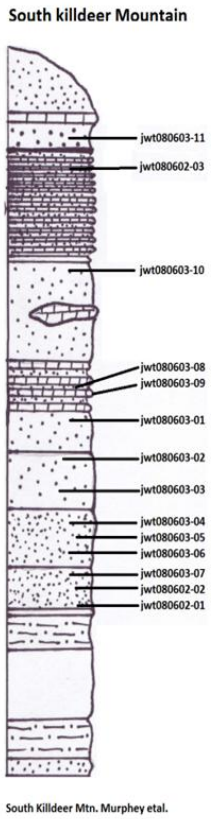

Figure 3.5. Stratigraphic profile and sample location of South Killdeer Mountain (modified from Murphy et. al., 1993)

3.2.1.2. North Killdeer Mountain. Approximately 3.8 miles (6.1 km) north of Medicine Hole plateau stands the North Killdeer Mountains and quarry site. Figure 3.6 shows satellite image of North Killdeer Mountain. At North Killdeer Mountain (Figure 3.7) an excellent stratigraphic profile was recorded due to past quarry activity at the sample site (Figure 3.8). The North Killdeer Mountain was sampled at two locations relative to the quarry entrance (Figure 3.9). The west quarry entrance (Figure 3.10) had units exposed upward approximately 22 feet (6.7 m) above the quarry floor. The east quarry entrance (Figure 3.11) had units exposed downward approximately 25 feet (7.6 meters) below the quarry floor. Specific measurements of profile were recorded and samples were taken from all recognized rock units down the entire profile.

Figure 3.6. Satellite photo North Killdeer Mountain and quarry (white areas), 47°29”53’ north latitude and 102°53”36’ west longitude. Sampling location shown in red (Google Earth)


Figure 3.7. North Killdeer Mountain, image taken facing north/northwest from quarry rim (photo by JWT).

Figure 3.8. North Killdeer Mountain quarry looking to the north (photo by JWT)

Figure 3.9. Quarry entrance looking to the north, west and east side of the quarry entrance (photo by JWT)

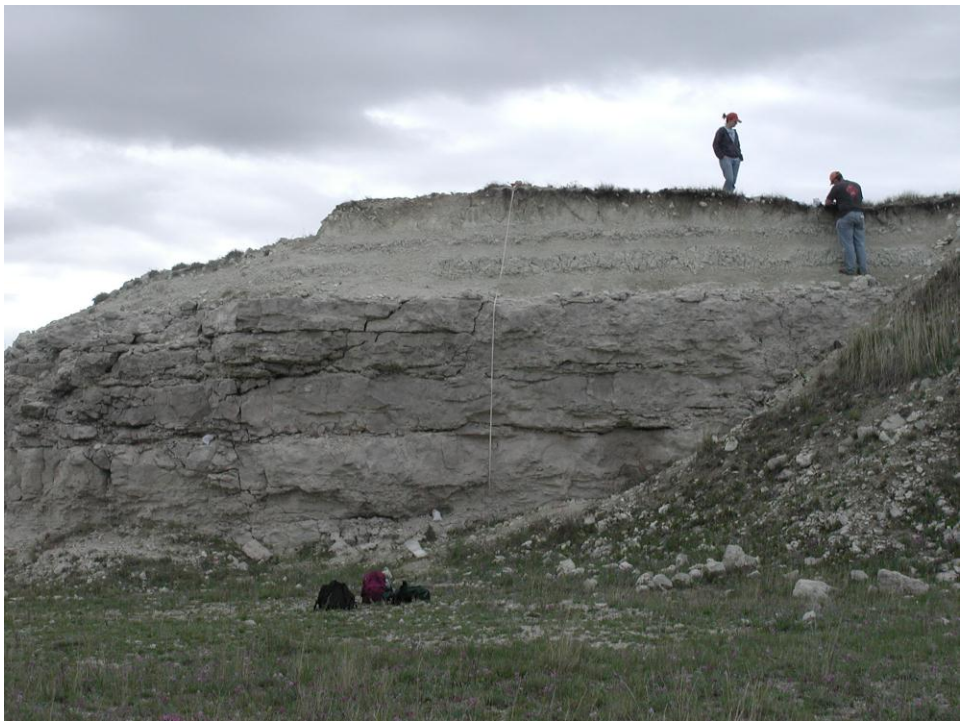

Figure 3.10. North Killdeer Mountain, west quarry entrance. Measuring and recording stratigraphic profile (photo by BSE)

Figure 3.11. North Killdeer Mountain, east quarry entrance, measuring and recording stratigraphic profile (photo by BSE)

We were able to easily correlate the two sides of the North Killdeer Mountain quarry entrance due to the close proximity and rock unit similarities. Figure 3.12 is a stratigraphic profile showing sample locations and the correlation between the two sides of the quarry entrance for North Killdeer Mountain.

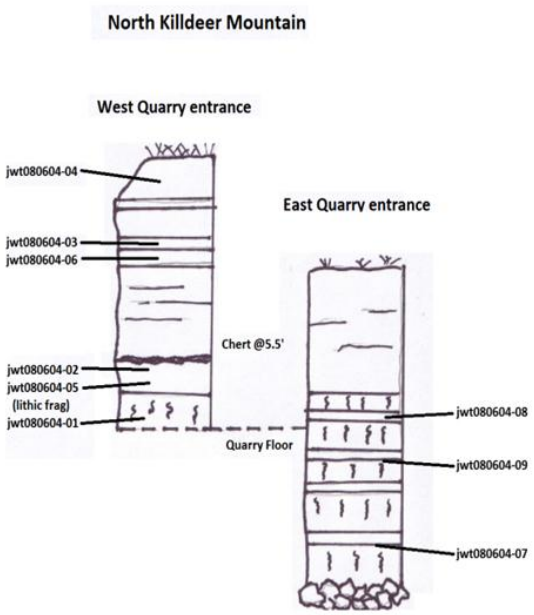

Figure 3.12. Stratigraphic correlation of NKDM sample locations (JWT)

3.2.2. East and West Rainy Butte complexes

Figure 3.13 shows a satellite image of West and East Rainy Buttes. West Rainy Butte is located in the northwest of the image, and East Rainy Butte is located in the southwest.

3.2.2.1. East Rainy Butte. At East Rainy Butte (Figure 3.14) sampling was done similarly as at South Killdeer Mountain. Beginning at the top caprock of each butte/mesa, samples were taken wherever any outcrops were exposed and were undisturbed. Steep sides with numerous slides and slumps, abundant flora, and wet conditions made sampling at the Rainy Buttes difficult. Lack of exposed outcrops below the caprock was the most problematic circumstance in sampling at East and West Rainy Buttes.

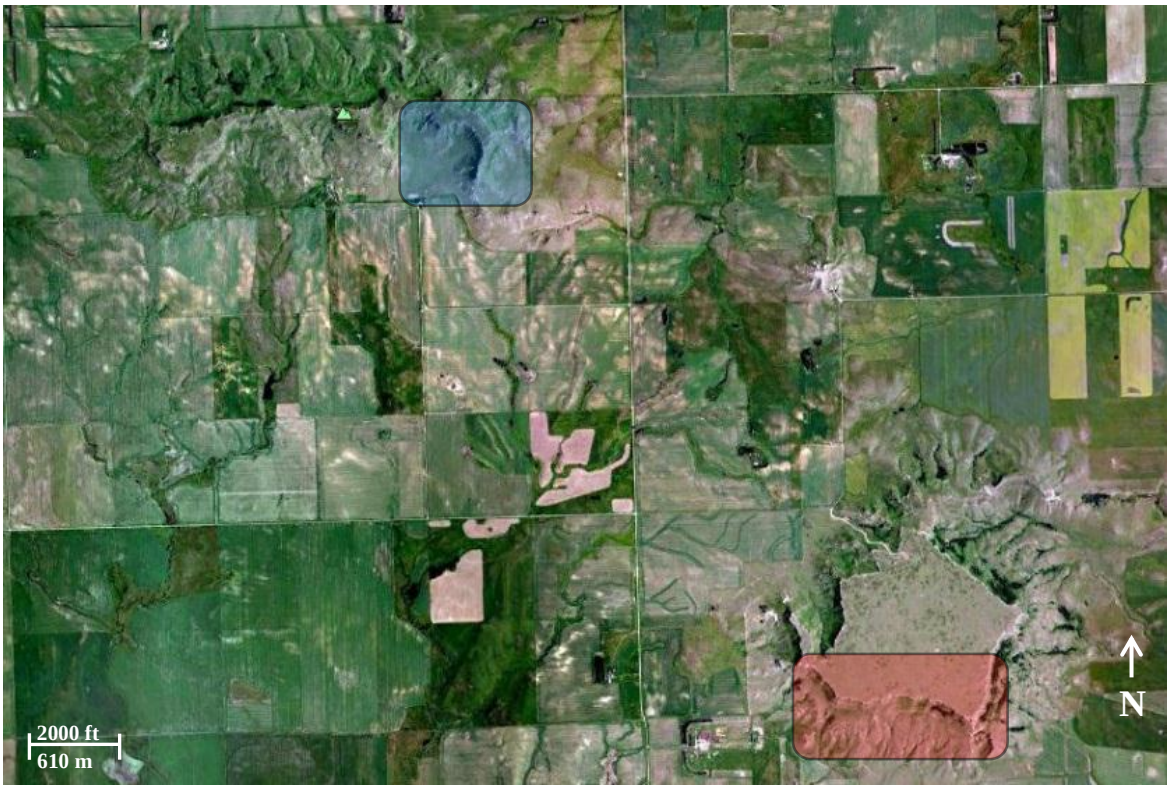

Figure 3.13. West and East Rainy Butte Complex Satellite image, 46°27”34’ north latitude and 102°55”58’ west longitude, East Rainy butte sampling location in red, West Rainy Butte sampling location in blue (Google Earth)


Figure 3.14. East Rainy Butte and surrounding landscape looking to the east (photo by JWT)

3.2.2.2. West Rainy Butte. Sampling was conducted at West Rainy Butte (Figure 3.15) in the same manner as at East Rainy Butte. Sample collection began at the top caprock of the butte and taken wherever any outcrops were exposed and undisturbed. The majority of the butte surface was covered with vegetation and similar to East Rainy Butte, exposed outcrops were difficult to identify. Outcrops that were investigated were exposed near the top of the butte on the east side.

Figure 3.15. West Rainy Butte and surrounding landscape looking to the west (photo by JWT)

3.2.3. Chalky Butte complex (White Butte)

Figure 3.16 shows a satellite image of the Chalky Butte complex (White Butte) and Figure 3.17 shows White Butte as approached from the southwest. At White Butte, only limited sampling was carried out.

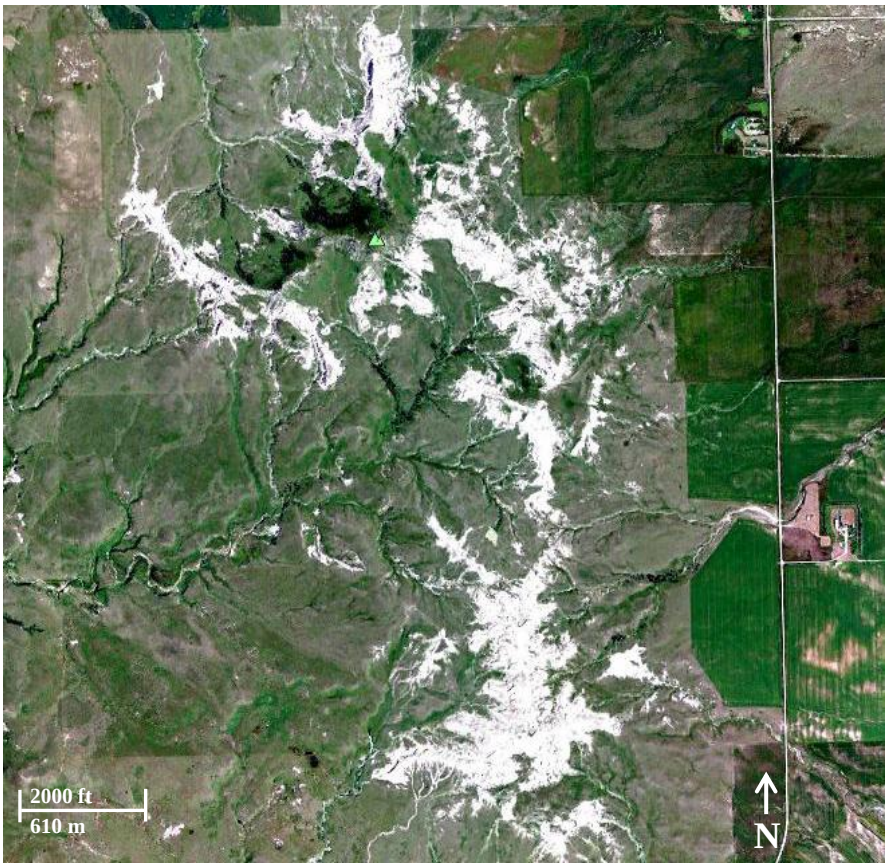

Figure 3.16. Chalky Butte complex satellite image, 46°22”57’ north latitude and 103°17”43’ west longitude (Google Earth)


Figure 3.17. Chalky Butte complex, White Butte (photo JWT)

CHAPTER 4. ANALYTICAL METHODS

4.1. Forsman Samples

Preliminary analysis was conducted on Killdeer Mountain rock samples provided by Dr. Forsman from his 1986 collection. In a fume hood, material from each sample was placed on a piece of carbon tape. To determine the best technique of placing this type of material on the tape, three different methods were used. For the first method, the carbon tape rounds were pressed directly onto the rock sample. Loose material was blown off using compressed air. For the second method, the carbon tape round was pressed into the loose material from the bottom of the sample bag. Loose material was blown off using compressed air. For the third method, a metal spatula was used to scrape material from the rock onto the carbon tape round. Loose material was blown off with compressed air. It was found that pressing the carbon tape rounds directly to the rock did not transfer as much material as desired, probably due to the cementation of the rocks and the intergrowth of the zeolite fibers within the voids between the rock sediment. It was also found that pressing the carbon tape rounds directly into the loose material in the sample bag could also be problematic. If the rounds were pressed too hard, more material than needed was transferred, and the carbon rounds had a too dense coverage, which led to analysis problems. Scraping the rock to obtain a powder sample with the spatula was not the easiest method due to the differing cementation, nor was it believed to be the best due to the possibility of breaking/destroying the fibers we intended to analyze. Through a trial and error approach, it was found that when the carbon tape rounds were pressed into the loose material in the sample bag very lightly, an adequate amount of material was transferred that had the proper density of material and hopefully fibers that were the least altered. These samples were then analyzed by SEM/EDS at NDSU. From this analysis, we were able to confirm visually the presence of

fibrous zeolites, hypothesize on the location of zeolite rich rocks in the field, and we were able to obtain preliminary chemistry data to compare to our own SEM/EDS analysis as well as analysis work done by Dr. Forsman in 1986. This allowed us to get an idea of where and how to best collect our samples, as well as how to most efficiently process and test our samples collected from our sampling field work.

4.2. Lab Preparation

4.2.1. Preliminary sample preparation

All samples were packaged on sight in the field as carefully as possible to limit any contamination and confirmation of proper identification numbers was made. Samples were then verified in the lab to identify that site notes matched to identification numbers and that field photos were correctly paired to sample numbers. All samples were also repackaged and placed in double lined plastic bags in the lab due to concerns with excess moisture in the samples and to diminish any concerns with cross contamination and dust/fiber exposure in the lab. The double lined sample bags were given the sample identification number and separately sealed.

Before chemical analysis was conducted, all samples collected from the areas described were visually inspected, classified, and categorized according to grain size, texture, hardness, and color using the Munsel scale. Table 4.1 lists the physical description of each sample. This was done to aid in identifying the geologic formation we were sampling as well as determining a general morphology of each sample. This information gave us the ability to correlate our work to Dr. Forsman's and Dr. Murphy's previous stratigraphic work and determine other possible locations throughout the region which may need to be investigated.

Table 4.1. Visual and physical description of samples collected. (Dilion Dolezal)

Sample Descriptions

Sample # jwt	Location	Formation	Unit # from Hoganson et al 1993	Location/elevation	Lithology	Grain Size	Cementation	Effervescence	Color Code from Munsel	Munsel Color (Dry)	Additional Notes
South Killdeer Mountain											
080602-01	SKDM	AF	5	SKDM Walking path	Siltstone	Silt	Moderate	Weak	10Y 8/1	Light greenish gray	
080602-02	SKDM	AF	6	SKDM Walking path	Siltstone	Silt	Poor	Weak	5GY 8/1	Light greenish gray	
080602-03	SKDM	AF	12	Medicine hole	Siltstone	Quartz inclusions	Poor	Moderate	10Y 6.5/1	Greenish gray to light greenish gray	Interbedded with harder calcareous beds
080603-01	SKDM	AF	8	11.27 jwt below BMU	Sandstone	Very fine grained	Moderate	Moderate	10Y 7/1	Light greenish gray	Cross bedded with variable weathering
080603-02	SKDM	AF	7	28.17 jwt below BMU	Sandstone	Very fine grained w/ silt	Moderate	None	5GY 7.5/1	Light greenish gray	
080603-03	SKDM	AF	7	45.1 jwt below BMU	Sandstone	Very fine grained w/ silt	Moderate	Weak	10Y 8/1	Light greenish gray	Cross bedding
080603-04	SKDM	AF	6	56.35 jwt below BMU	Siltstone	Silt	Moderate	Strong	10Y 8/1	Light greenish gray	
080603-05	SKDM	AF	6	61.99 jwt below BMU	Siltstone	Silt	Moderate	Strong	10Y 8/1	Light greenish gray	Green nodules present in bed
080603-06	SKDM	AF	6	73.26 jwt below BMU	Siltstone	Silt	Moderate	Moderate	10Y 6/1	Greenish gray	Fibrous crystals
080603-07	SKDM	AF	5	84.53 jwt below BMU	Siltstone	Silt	Moderate	Weak	10Y 7.5/1	Light greenish gray	Fibrous content (some biological?). Spherical concretions in bed
080603-08	SKDM	AF	9	BMU							Friablw layers between tuffs, 080603-09
080603-09	SKDM	AF	9	BMU	Sandstone	Very fine grained w/ silt	Well	Strong	5G 6.5/2 and 5GY 7/1	Pale green and light greenish gray	Fibrous content, burrows present, and tuffaceous
080603-10	SKDM	AF	10	56.35 jwt above BMU	Sandstone	Very fine grained w/ fine grained quartz	Well	Moderate	N 7.5/ and 10YR 8/1	Light gray to white	Massive and calcareous concretions present
080603-11	SKDM	AF	13	140.83 jwt above BMU	Sandstone	Fine grained w/ high quartz content	Poor	Moderate	10Y 6.5/1	Greenish gray to light greenish gray	
North Killdeer Mountain											
080604-01	NKDM	AF		3089'	Siltstone	Silt	Well	Moderate	10YR 8/1	White	Small fibers present. Burrows and white concretions in bed.
080604-02	NKDM	AF		~3092'	Siltstone	Silt	Moderate	Strong	10YR 8/1	White	Small fibers present in some pores.
080604-03	NKDM	AF		~3098'	Siltstone	Silt	Moderate	Weak	5Y 8/1	White	Fibrous material in pores
080604-04	NKDM	AF		~3102'	Siltstone	Silt	Poor	Strong	5Y 8/1	White	Slightly porous. Massive
080604-05	NKDM	AF		3092'	lith fragment						Lithic from same unit as 080604-02
080604-06	NKDM	AF		~3096'	Siltstone	Silt	Moderate	Moderate	5Y 8/1	White	Small fibers present in some pores
080604-07	NKDM	AF		3071'	Sandstone	Very fine grained w/ silt	Poor	None	2.5Y 7.5/2	Light gray to pale yellow	Highly fibrous. Burrows.
080604-08	NKDM	AF		3084'	Sandstone	Very fine grained w/ silt	Well	Strong	5Y 8/1	White	Highly fibrous. Friable
080604-09	NKDM	AF		3082'	Sandstone	Very fine grained w/ silt	Well	Strong	2.5Y 8/1	White	Highly fibrous
West and East Rainy Buttes											
080604-10	WRB	GVF	1	3100'	Sandstone	Very fine grained w/ silt	Poor	None	2.5Y 8/1	White	
080604-11	WRB	CF	3	3200'	Carbonate	Clay within bed	Moderate	Strong	10YR 7/3 and 2.5Y 8/1	Very pale brown to white	Carbonate supports very pale brown clasts
080604-12	WRB	BF	4	3221'	Mudstone	Silty	Poor	None	7.5YR 8/3	Pink	
080604-13	WRB	BF	6	3245'	Mudstone	Clay	Poor	None	7.5YR 8/2.5	Pinkish white to pink	
080604-14	WRB	BF	8	3258'	Mudstone	Clay	Poor	None	10Y 8/1	Light greenish gray	
080604-15	WRB	AF	9	3268'	Sandstone	Fine grained w/ clay	Moderate	None	10YR 8/2 and 5B 7/1	Very pale brown to light bluish gray	Clay varves throughout the sandstone
080604-16	WRB	AF	9	3268'	Sandstone	Fine grained w/ clay	Well	None	2.5Y 7/2	Light gray	Some pebbles present within sandstone
080605-01	ERB	BF	4	3320'	Sandstone	Very fine grained	Poor	Moderate	10YR 7/2.5	Light gray to very pale brown	Dark minerals and feldspar present. Friable. Moderately sorted
080605-02	ERB	BF	4/covered	3250'	Sandstone	Very fine grained	Poor	None	10YR 8/1.5	White to very pale brown	Cross bedding and interbedded with silt. Friable. Moderately sorted
080605-03	ERB	AF	3?	3260'	Sandstone	Very fine grained	Poor	Weak	10YR 7.5/2	Light gray to very pale brown	Calcareous grains present. Friable. Moderately sorted
West and East Rainy Buttes											
080605-04	WB	SB	1	3191'	rkosic sandstor	Medium to course grained	Poor	None	10Y 8/1	Light greenish gray	Oxidation present. Friable. Poorly sorted
080605-05	WB	SB	2	3169'	Clay	Clay	Poor	None	10Y 8/1	Light greenish gray	Popcorn weathering (Bentonite). Friable

Key	
SKDM	South KillDeer Mtn
NKDM	North Killdeer
ERB	East Rainy Butte
WRB	West Rainy Butte
WB	WhiteButte
AF	Arikaree Formation
BF	Brule Formation
CF	Chadron Formation
GVF	Golden Valley Formation
SBF	Sentinel Butte Formation

4.2.2. Sample break down

From our samples collected, a small portion of all samples were broken down into a coarse powder to increase surface area and liberate any zeolite minerals. Some samples were cemented well enough that an agate mortar and pestle was needed, but the majority of the samples were friable enough that they broke apart fairly easy and grinding was not needed. Samples that were friable enough to break apart by hand were placed inside a plastic bag, and broken down within the bag by gently crushing with a hammer or by breaking apart by hand. This was done inside of a plastic Ziploc bag within a fume hood to insure very minimal exposure to dust and fibers as well as avoiding any possibility for cross-contamination between samples. Any of the samples that were too hard to break apart by hand, an agate mortar and pestle was used inside of a fume hood. The ground/broken down materials were individually bagged and labeled. This ground/broken material was used for whole rock SEM/EDS analysis and would be the material that would be further processed for powder XRD analysis, and EMP analysis.

4.3. Analysis Preparation

4.3.1. Whole rock analysis

The first SEM/EDS analysis done on the samples was a whole rock analysis. As done with the original Forsman samples, material was placed on double sided carbon tape rounds by lightly pressing them into the loose material within the sample bag. A whole rock analysis was done to each sample as well as a visual inspection of each sample to determine/identify the presence of zeolite fibers. Samples that had fibers which could be seen by binocular microscope were flagged as having the best potential for zeolite presence for future analysis. After whole rock analysis of each sample was complete, and a list of samples with the best zeolite presence was determined, the samples were processed to try and obtain a zeolite fiber concentrate.

4.3.2. Sample filtration and concentrate acquisition

A simple floatation process was used to separate the zeolite fibers into a concentrate from its parent material. This floatation method was used over other separation methods so the chemical and physical nature of the zeolite fibers remained as consistent and unaltered as possible. The broken, liberated material was placed into a distilled water column within a 1000ml graduated cylinder (Figure 4.1). The sample material and water was agitated to place all material into suspension. The column was then allowed to rest for a period of time to allow the heavier materials to fall out of suspension, leaving the lighter materials, clays and fibers in suspension. Rest time depended on the overall makeup of the original sample material. The more clay material that was in suspension, the longer the column was allowed to rest to try and separate the clay as much as possible for easier filtration later in the process. Samples that contained less clay particles and more sand sized fractions did not require as much time for separation. Each graduated cylinder was covered to prevent contamination and labeled according to sample ID #. After a resting period, a ball pipette was used to transfer all of the suspension, the water and suspended particles, into a vacuum filter system. All of the water from the graduated cylinder was removed by using the pipette. Starting at the top of the water column working down until the water and suspension was removed, and only the heavier, denser material remained. The remaining material was placed into a separate bag and labeled with the ID # of the original sample and set aside for any possible future needs. The material that was removed using the pipette was placed directly into a filter system for water extraction (Figure 4.2). The filter system was composed of an electric vacuum pump and hose, Büchner flask (vacuum flask) and filter holder with a #1, 42.5mm qualitative paper filter.

Figure 4.1. 1000ml beaker with disaggregated sample placed in suspension (photo by JWT)

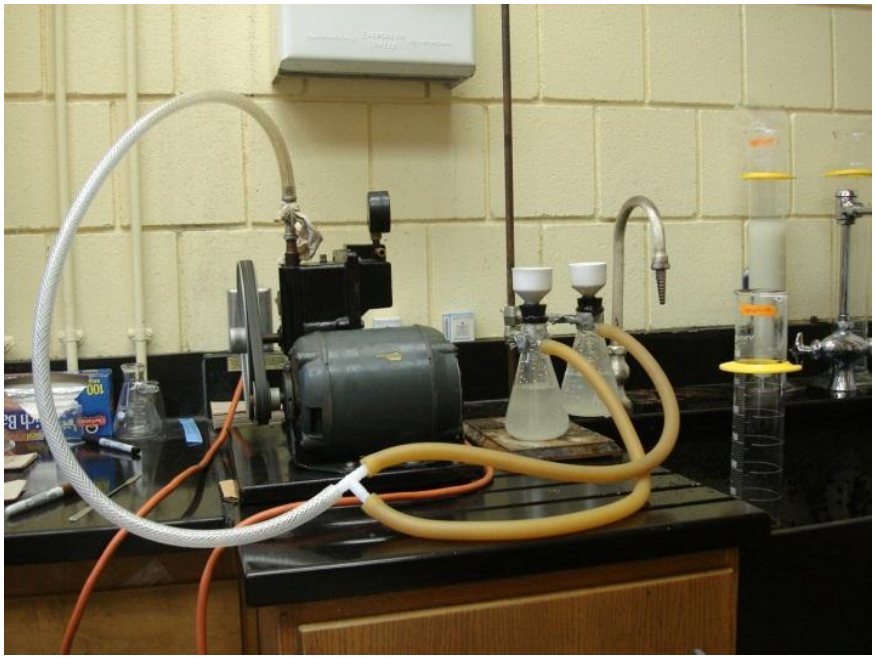

Figure 4.2. Filter system used for producing zeolite concentrate (photo by JWT)

Depending on the amount of clay and fibers in suspension, the filtering process would take from 15 minutes to an hour or more per sample. Due to the time needed to run the filter process, the more clays that could be separated or allowed to settle out of suspension in the settling process the better. Once all the water and suspension had been pipetted from the graduated cylinders and run through the filtering process, the filter papers were removed from the filter holder and placed under labeled petri dishes and dried overnight (Figure 4.3).

Figure 4.3. Filters removed from filter flask placed under petri dishes and allowed to dry (photo by JWT)

Tools and vessels then washed and rinsed for all sample filtrations in preparation for the next sample. After filter and suspended material had dried, it was removed from the filter paper. Usually the dried material on the filter paper peeled away relatively easily from the filter with the aid of a metal spatula. Sometimes the filtered material would need to be scraped off the filter using the metal spatula and rinsed off with a small amount of deionized water. Materials removed from the filters were then placed inside small sample tubes, sealed, and labeled with corresponding sample number. This powder, the concentrate, should now contain only the

smallest particles and fibers present in the sample. Powders derived from the samples using the prep and filter method described, were then used to prep slides for powder XRD, SEM/EDS, and EMPA analysis.

4.4. Powder XRD Slide Preparation

For powder X-ray diffraction, the filtered material was ground into a very fine powder using an agate mortar and pestle (Figure 4.4). Wet mount XRD powder slides were produced by placing a small amount of the finely ground powder on to a new slide labeled with sample number. A few drops of deionized (DI) water were added to the powder to help disperse the powder evenly over the slide. By gently agitating the slide, the wet powder spread out over the slide surface, evenly and randomly dispersing the powder. A heat gun was used to remove surface and excess moisture in the sample. After all slides were prepared, they were individually labeled with sample ID and then analyzed using powdered XRD analysis method (Figure 4.5).

Powder XRD analysis was conducted at North Dakota State XRD lab, Department of Chemistry and Biochemistry on a Phillips X'Pert MPD X-Ray Powder Diffractometer. The data collection is controlled by X'Pert data collector v. 1.2. The PDF-2 database was search-matched using Jade + and X'Pert Highscore software.

Powder XRD analysis of filtered, concentrated samples showed the presence of zeolitic material in numerous samples according to mineral data base. 17 of the 35 samples tested positive for some type, or a combination of zeolites according to XRD data base. Figure 4.6 is an example of one of the XRD scans produced along with the listing of possible minerals present from data base for Forsman sample MH1A. Possible zeolites identified by the data base were erionite, offretite, chabazite, and clinoptilolite.

Figure 4.4. Agate mortar and pestle, powdered sample and sample container (photo by JWT)

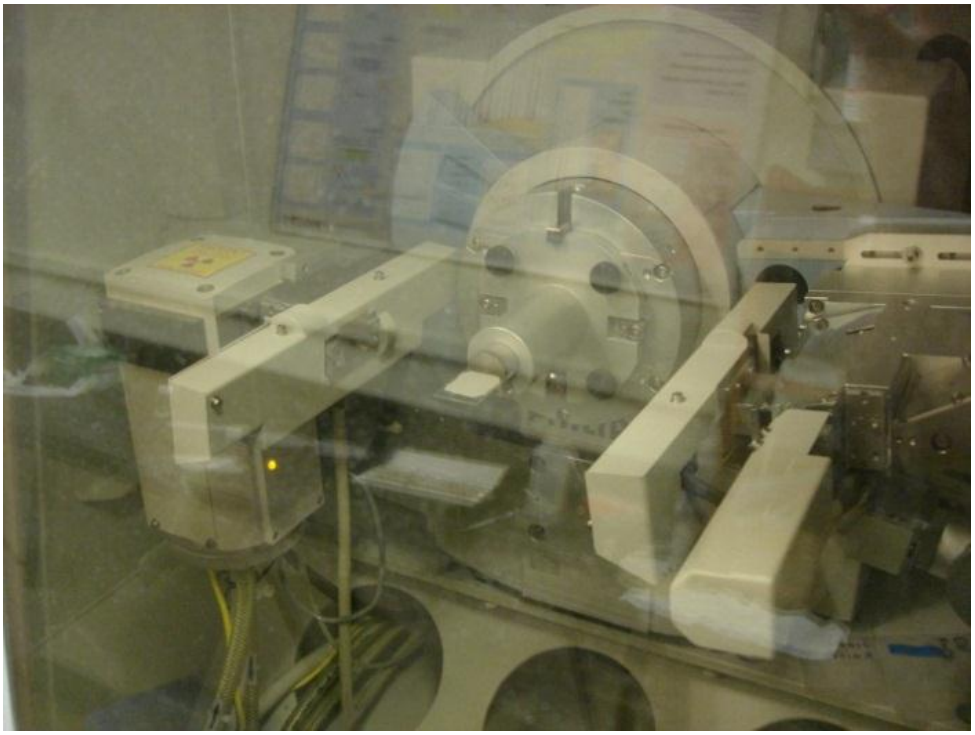
Figure 4.5. Powder wet mount slide in XRD (photo by JWT)

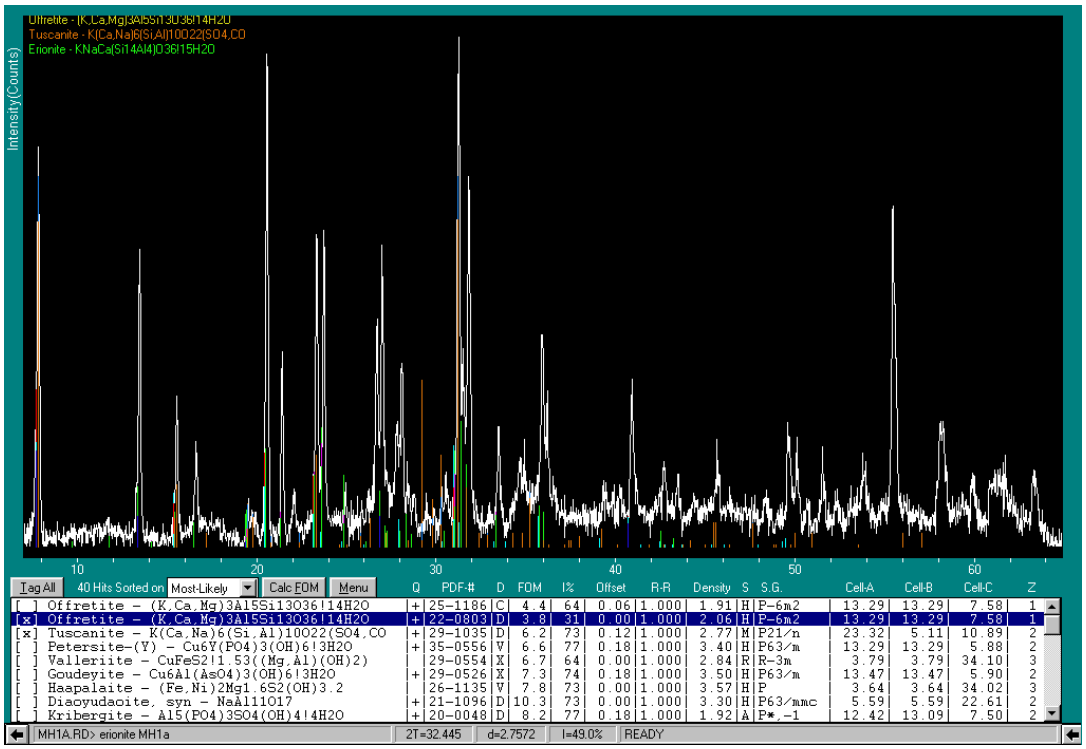

Figure 4.6. XRD scan and data base listing for sample Forsman MH1A (NDSU XRD)

Due to the similarities in XRD patterns, and the differing concentration of zeolitic material within the positive samples, precise identification of erionite by powder XRD is not certain. Specifically, the XRD patterns of the zeolites erionite and offretite are very similar along with the possibility that other zeolites may be present as determined by the data base. Because of overlapping peaks, in addition to specific peaks with low counts, erionite may be present in low amounts, but its peaks may be hidden by larger offretite peaks, and vice versa. A summary of all jwt samples can be seen in Table 4.2. Powder XRD analysis was conducted on all of the collected samples. All the scans were run search-matched with the database to determine mineral content. From the XRD analysis, it was determined which samples showed the best probability for containing zeolite minerals. From the XRD analysis, it can be concluded that erionite and/or offretite are present in some of the samples. All XRD micrographs can be found in Appendix Figure 5.

Table 4.2. Sample ID and location with XRD analysis

Sample ID - JWT	Sample Site	XRD - Data base suggestion
080602-01*	SKDM	Quartz & erionite
080602-02*	SKDM	Calcite & offretite/erionite
080602-03	SKDM	Ankerite & Calcite
080603-01	SKDM	Calcite & erionite
080603-02	SKDM	Offretite & erionite
080603-03	SKDM	Offretite/erionite & Calcite
080603-04	SKDM	Calcite & Erionite
080603-05	SKDM	No definite Match (Off & Eri in list)
080603-06	SKDM	Erionite
080603-07*	SKDM	Calcite & Offretite
080603-08	SKDM	Erionite & Quartz
080603-09	SKDM	Calcite & Quartz
080603-10	SKDM	Dolomite & Quartz
080603-11	SKDM	Calcite & Quartz
080604-01	NKDM (wqe)	Offretite & Calcite
080604-02	NKDM (wqe)	Calcite & Quartz
080604-03	NKDM (wqe)	Cal, Chab, Eri, Quartz
080604-04	NKDM (wqe)	Calcite & Quartz
080604-05	NKDM (wqe)	Calite & Quartz
080604-06	NKDM (wqe)	Cal, Qrtz, Clino, Eri
080604-07	NKDM (eqe)	Offretite
080604-08	NKDM (eqe)	Calcite, Erionite, offretite
080604-09	NKDM (eqe)	Calcite, Quartz, offretite
080604-10	WRB	Quartz, muscovite, kaolinite
080604-11	WRB	Calcite & quartz
080604-12	WRB	Quartz, saponite, albite
080604-13	WRB	Quartz & clay?
080604-14	WRB	Calcite & Quartz
080604-15	WRB	Quartz & Albite
080604-16	WRB	Quartz & Albite
080605-01	ERB	Quartz & Saponite
080605-02	ERB	Saponite & Quartz
080605-03	ERB	Quartz & Saponite
080605-04	WB	Saponite
080605-05	WB	Quartz & saponite

("*" denotes possible slump from field observation.)

4.5. SEM/EDS Sample Preparation

SEM/EDS analysis conducted at North Dakota State University Electron Microscopy Center was done on a JEOL JSM -7600F field-emission scanning electron microscope (SEM). This instrument can magnify up to one million times for visualization and imaging of nanoscale-sized objects and offers 1.5 nm resolutions at 1kV accelerating voltage. In addition to a highly stable probe current and upper and lower secondary-electron detectors, the 7600F is equipped with a retractable in-lens backscatter detector, a low-angle backscatter detector, a scanning

transmission electron (STEM) detector, and it features energy-dispersive X-ray spectrometry with a fine electron probe to determine what elements are present in a sample in an area as small as a few tens of nanometers (NDSU SEM/EDS). SEM/EDS analysis of samples given to us from the Forsman collection were completed first. This allowed us to work with materials that had already been confirmed to contain zeolite fibers. Images and chemical analyses of Forsman samples can be found in Appendix Figure 4 and Appendix Table 2 & 3. Table 4.2 gives the chemical analyses for the Forsman samples acquired at the NDSU SEM/EDS lab.

Table 4.3. SEM/EDS Chemical composition Forsman samples

Element	Molar Mass (g/mol)
Potassium - K	39.098
Sodium - Na	22.99
Magnesium - Mg	24.305
Calcium - Ca	40.078
Aluminum - Al	26.982
Silicon - Si	28.086
Oxygen - O	15.999
Iron - Fe	55.845
Chlorine - Cl	35.453

Oxides
SiO_2 - 60.084 g/mol
Al_2O_3 - 101.961 g/mol
CaO - 56.077 g/mol
K_2O - 94.195 g/mol
MgO - 40.304 g/mol
Na_2O - 61.979 g/mol

Weight % Analysis

Date	SEM #	Sample ID	Scan	O %	Na %	Mg %	Al %	Si %	Cl %	K %	Ca %	Fe %	% total
2/4/2008	172	NM #3(2) pt1	NA										
	172	NM #3(2) pt2		60.52	0.22	1.31	7.05	27.14		2.05	1.7		99.99
	172	NM #3(1) pt 1	pt1 - Area	60.65	0.33	1.45	6.73	26.83		2.52	1.48		99.99
	173	NM #2 pt1		60.04	0	1.21	7.59	27.73		2.09	1.33		99.99
	173	NM #2 pt2		57.16	0.27	1.67	7.99	30.35		1.56	0.99		99.99
	174	MH1a(1) pt1		54.86	0.11	0.27	7.83	31.81		2.13	2.99		100
	174	MH1a(1) pt2		55.78	0.28	0.46	7.89	30.85		2.06	2.68		100
	175	MH3(1) pt1		60.09	0	0.61	7.36	28.1		1.62	2.23		100.01
	175	MH3(1) pt2		58.63	0.1	0.57	7.33	29.19		1.74	2.45		100.01
4/9/2008	311	MH 1B(2) pt1		50.7	0.59	1.66	8.42	34.67		2.9	1.07		100.01
	311	MH 1B(2) pt2		54.76	0.34	1.58	8.17	31.88		2.24	1.02		99.99
	311	MH 1B(2) pt3		53.75	0.44	1.2	8.19	32.72		2.67	1.04		100.01
	313	MH 2(1) pt1	NA										0
	313	MH 2(1) pt2		50.11	0.13	0.66	8.63	34.64		2.66	3.17		100
	313	MH 2(1) pt3		51.18	0.2	0.71	7.8	33.15		2.23	4.72		99.99
	315	MH 5B pt1		54.99	1.1	5.25	2.41	21		0.95	5.73	8.4	99.83
	315	MH 5B pt2		53.25	1.14	5.7	3.3	21.18		0.64	5.82	8.57	99.6
	315	MH 5B pt3		57.91	0.91	4.49	2.83	20.51		0.22	5.41	7.11	99.39
	315	MH 5B(2) pt1		57.64	1.12	1.46	6.78	30.12		2.03	0.85		100
	315	MH 5B(2) pt2		55.31	0.59	1.57	3.22	24.79		8.03	6.49		100
	315	MH 5B(2) pt3		56.92	0.95	2.09	4.4	19.92	0.41	2.07	2.12	11.12	100
	317	MH 9A	NA										
	319	MH 9B(1) pt1		57.6	0	0.29	7	29.84		2.41	2.86		100
	319	MH 9B(1) pt2		59.69	0.16	0.51	7.36	28.17		1.83	2.27		99.99
	319	MH 9B(1) pt3		57.6	0	0.48	7.54	29.29		2.21	2.87		99.99

Sample preparation for SEM/EDS analysis consisted of mounting carbon tape to a 0.5 inch (1.27 cm) diameter aluminum stub and dobbing the carbon tape stub into the ground sample or sprinkling the ground material onto the carbon covered stub. Powder samples were then carbon coated using a carbon string coater.

Each stub was labeled with the original sample ID as well as an SEM lab ID #. SEM analysis confirmed the presence of zeolites in 17 of the 35 samples. Four more samples had potential fibers, but they were difficult to identify due to the very small size and very low concentration. Chemical analysis data for JWT samples are shown in Table 4.3. Visual inspection and classification information for JWT samples can be found in Appendix Table 1 and all SEM/EDS data for JWT sample can be found in Appendix Table 2 and Appendix Table 3.

Table 4.4. SEM/EDS Chemical composition of JWT samples

Sample ID - JWT	NDSU SEM ID #	Sample Site	SEM - Visual	Weight %							
				%Na	% Mg	% Al	% Si	% K	% Ca	% Fe	%O
080602-01*	091798	SKDM	~50% or more fibers, 25-100+ µm	na	1.15	13.02	62.77	13.10	9.96	na	
080602-02*	091799	SKDM	~ 50% fibers, most < 100 µm	na	1.19	15.11	66.48	9.95	7.26	na	
080602-03	092238	SKDM	Scattered fibers	na	1.63	9.05	37.16	3.91	3.95	na	44.3
080603-01	092239	SKDM	~50% or more fibers, 25-100+ µm	0.36	0.83	8.89	34.43	4.52	2.41	na	48.57
080603-02	092240	SKDM	~50% or more fibers, 25-100+ µm	na	0.52	9.05	36.99	4.49	4.27	na	44.68
080603-03	091800	SKDM	~ 50% fibers, most < 100 µm	1.50	1.16	15.21	67.48	9.75	4.91	na	
080603-04	092241	SKDM	< 10 % fibers, most very small	0.42	0.92	9.19	37.50	5.68	3.46	na	42.83
080603-05	092242	SKDM	~50% or more fibers, 25-100+ µm	0.41	0.87	9.56	43.74	9.39	5.58	na	30.45
080603-06	091801	SKDM	~ 50% fibers, most < 100 µm	na	1.27	14.99	65.33	8.32	7.03	3.05	
080603-07*	092243	SKDM	10% fibers, most very small	na	0.75	9.50	38.53	5.62	3.62	0.76	41.24
080603-08	091802	SKDM	< 40% fibers, majority < 100 µm	0.63	0.96	15.16	64.99	11.38	6.89	na	
080603-09	092244	SKDM	no fibers								
080603-10	092245	SKDM	no fibers								
080603-11	092246	SKDM	no fibers								
080604-01	091803	NKDM (wqe)	~ 30% fibers, most < 100 µm	0.78	1.45	15.53	67.04	9.66	5.55	na	
080604-02	092247	NKDM (wqe)	no fibers								
080604-03	091804	NKDM (wqe)	< 10 % fibers, most very small	na	5.20	15.86	58.71	8.79	1.75	9.70	
080604-04	092248	NKDM (wqe)	no fibers								
080604-05	092249	NKDM (wqe)	no fibers								
080604-06	092250	NKDM (wqe)	very few fibers	na	1.16	8.02	31.55	5.00	3.02	na	51.25
080604-07	091805	NKDM (eqe)	~50% or more fibers, 25-100+ µm	na	0.38	15.20	66.54	8.98	8.91	na	
080604-08	092251	NKDM (eqe)	10% fibers, most very small	na	na	9.38	39.88	4.92	7.16	na	38.67
080604-09	092252	NKDM (eqe)	bad fiber analyzed (organic)								
080604-10	092253	WRB	no fibers								
080604-11	092254	WRB	no fibers								
080604-12	092255	WRB	possible fiber, but doubtful???								
080604-13	092256	WRB	no fibers								
080604-14	092257	WRB	no fibers								
080604-15	092258	WRB	no fibers								
080604-16	na	WRB	no fibers								
080605-01	092259	ERB	no fibers								
080605-02	092260	ERB	no fibers								
080605-03	092261	ERB	no fibers								
080605-04	092262	WB	no fibers								
080605-05	092263	WB	no fibers								

4.6. Electron Microprobe Sample Preparation

Electron microprobe analysis was conducted at the University of Minnesota Electron Microprobe Lab, Department of Earth Sciences, during the summer of 2010. EMP analysis was conducted on the JXA-8900 SuperProbe (Figure 4.7), a high resolution SEM and wavelength dispersive (WDS)/EDS combined electron probe microanalyzer (EPMA). This instrument has the capability of using up to 5 WDS X-ray spectrometers and an EDS simultaneously. Microprobe analysis was carried out using the following standards; Na – Amelia Albite, Ba –

Barite, K – Microcline (asbestos, Quebec), Mg, Si, Al, Ca and Fe – Kakanui Hornblende. See Appendix Table 8 for complete analysis. H_2O was included by difference in ZAF correction.

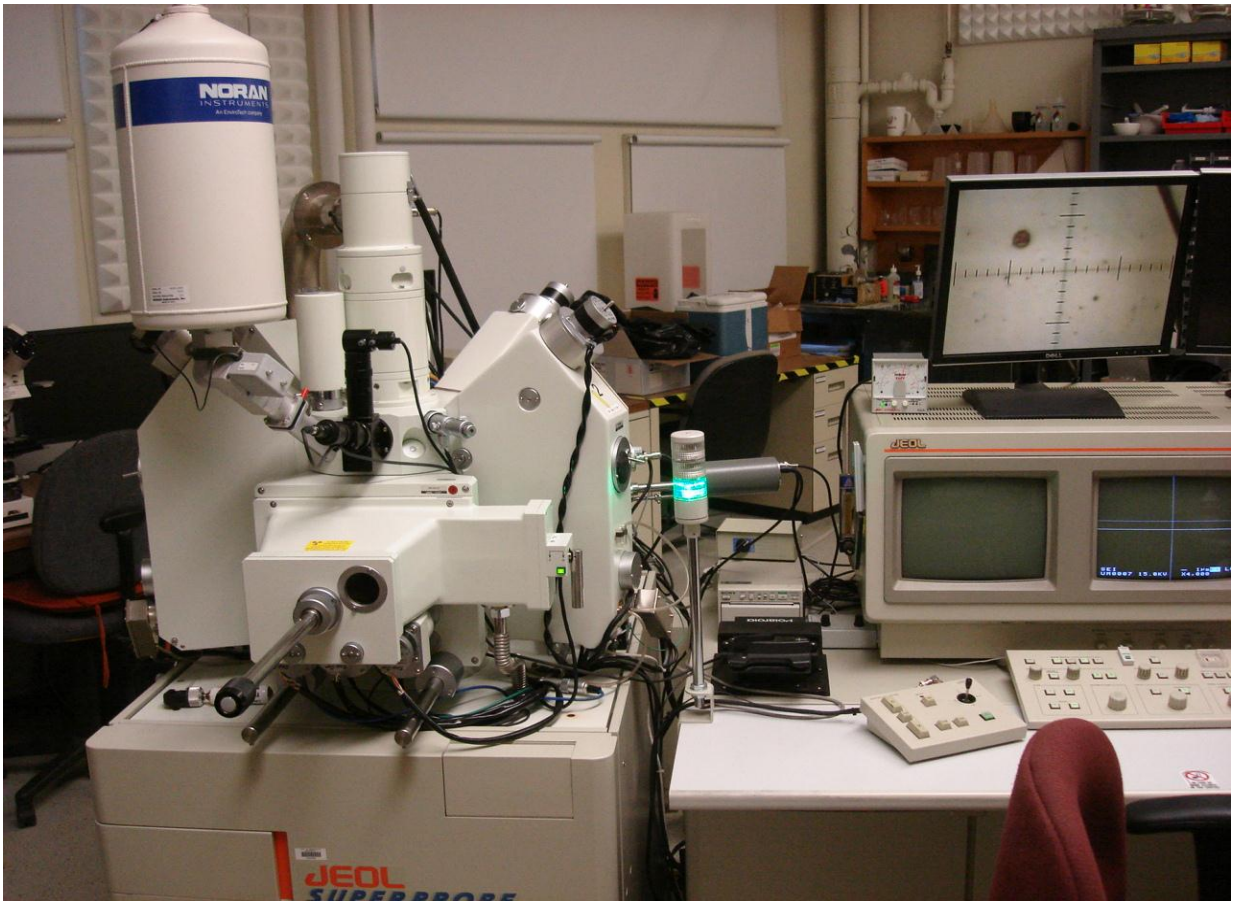

Figure 4.7. JXA-8900 electron probe microanalyzer at the UM (photo by JWT)

Six one-inch aluminum stubs were prepared for EMPA. Samples were prepped for microprobe analysis in a similar fashion as for SEM analysis. Ground, concentrated sample material, was placed on a carbon round which was then placed onto a 1 inch (2.54 cm) diameter aluminum stub and carbon coated with a rotating carbon rod coater.

Each sample round was placed within a specific quadrant (see Appendix Figure 1) for identification and navigation purposes. Figure 4.8 show prepped sample stubs 1-4. Table 4.4 shows the sample numbers correlating to the stub number. Sample numbers begin in top right and continue in order clockwise as listed in Table 4.3.

After the EMPA stubs were prepared, each sample was inspected with a binocular microscope, photographed, and material location mapped/documented. The seventeen samples that were prepped for EMPA were found to contain abundant fibers through powder XRD and SEM/EDS analysis, and were stratigraphically different from each other. Due to time constraints, only 9 of the 17 samples were able to be scanned (Figure4.9).

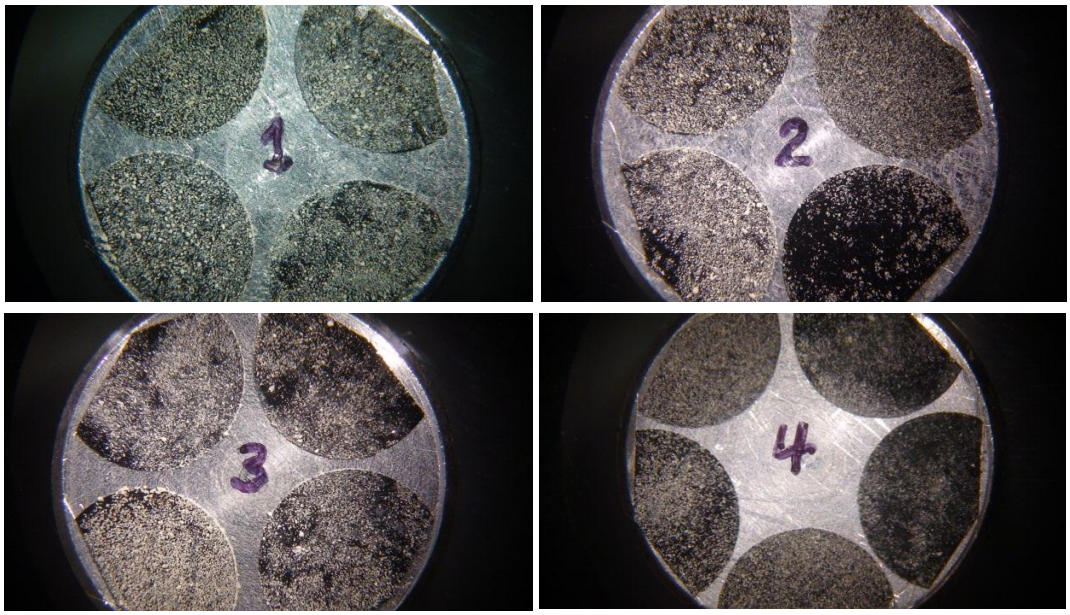

Figure 4.8. Stubs 1-4 prepped for EMPA (photo by JWT)

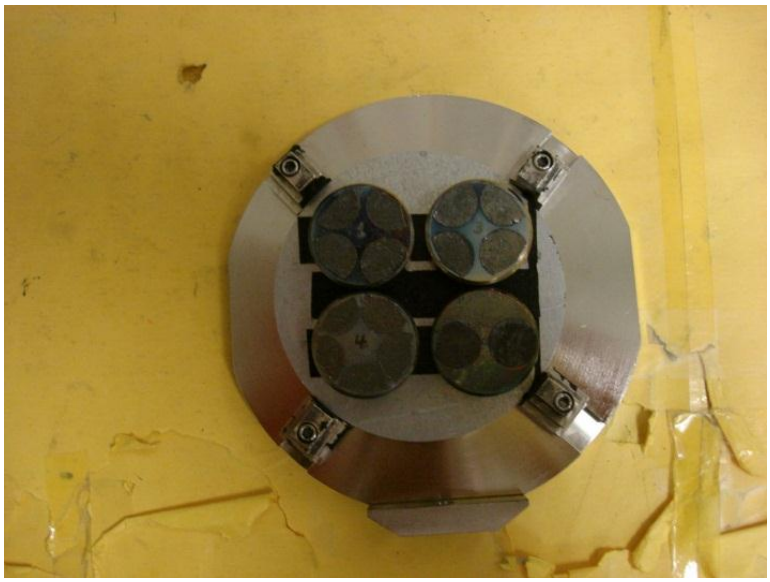

Figure 4.9. EMPA sample holder with carbon coated stubs attached (photo by JWT)

For EMPA, depending on the fiber concentration and the accessibility of the fibers within the surrounding matrix, 1 to 6 mineral crystals/fibers were analyzed from each of the nine samples. The number of scan points per crystal/fiber and beam width depended on the fiber size. Analysis using a 2 to 10 μm electron beam was conducted on 1 to 5 points per crystal/fiber. 27 total fibers were analyzed from 77 total different points. EMPA scan images of all fibers can be found in Appendix Figure 2.

Table 4.5. EMPA stubs and corresponding sample numbers

Stub Number	Sample ID #'s – JWT				
Stub #1	080602-01	080602-02	080602-03	080603-01	
Stub #2	080603-02	080603-03	080603-04	080603-05	
Stub #3	080603-06	080603-07	080603-08	080604-01	
Stub #4	080604-03	080604-06	080604-07	080604-08	080604-09
Stub #5	080603-04				
Stub #6	080603-08	080602-03			

CHAPTER 5. RESULTS AND CONCLUSIONS

5.1. Analytical Results

5.1.1. Macroscopic and binocular microscope

During preliminary visual and microscopic inspection and classification of rock/soil samples collected from the three locations described, several Killdeer Mountain complex samples showed evidence of fibrous content within vugs and pore spaces within the rock matrix, three samples from South Killdeer Mountain (jwt080603-06, -07, and -09), and seven from North Killdeer Mountain (jwt080604-01, -02, -03, -06, -07, -08, and -09). The origin and/or composition of these fibers are not known from this visual inspection, and some may not be fibrous minerals. No fibrous material could be identified in any samples from the Rainy Buttes and/or White Butte samples. Complete visual classifications and descriptions are presented in Table 4.1.

5.1.2. XRD

XRD analysis was conducted on all the samples collected using sample concentrate produced from water column separation and vacuum filtration as described in Chapter 4. Using powdered XRD scanning analysis data base, evidence of some type of zeolite was identified in ten of the fourteen SKDM samples and seven of the nine NKDM samples. Erionite and offretite were the most common zeolite identified, but the zeolites chabazite, heulandite, and clinoptilolite were also identified. No zeolites were positively identified by XRD and data base analysis in any of the Rainy Butte or White Butte samples.

Many of the scans completed returned multiple zeolite identifications from the database. A summary of these results is presented in Table 5.1. XRD micrographs of all samples can be found in Appendix Figure 5. As described previously, the powder XRD patterns of different

zeolites, especially the zeolites in question, erionite and offretite, are similar and difficult to distinguish. In addition, the scans were not of pure mineral samples, which resulted in different background data for different scans. For these reasons, all the scans were visually compared and were labeled with an estimated best mineral/zeolite match.

Table 5.1. Powder XRD identification of zeolites in samples collected

Powder XRD identification					
Sample ID	Zeolite	Possible zeolite??	Other		
jwt080602-01 w/Si	erionite		quartz		
jwt080602-02 w/Si	offretite	erionite?	calcite		
jwt080602-03			ankerite	calcite	
jwt080603-01 w/Si	erionte		calcite		
jwt080603-02	erionite & offretite				
jwt080603-03	offretite	erionite?	calcite		
jwt080603-04	erionite		calcite		
jwt080603-05	no match	erionite & offretite			
jwt080603-06	erionite		calcite	quartz	
jwt080603-07	offretite		calcite		
jwt080603-08	erionite		quartz		
jwt080603-09			calcite	quartz	
jwt080603-10			dolomite	quartz	
jwt080603-11			calcite	quartz	
jwt080604-01	offretite		calcite		
jwt080604-02			calcite	quartz	
jwt080604-03		erionite & chabazite	calcite	quartz	
jwt080604-04		erionite & heulandite	calcite	quartz	
jwt080604-05			calcite	quartz	
jwt080604-06		Clino, eri, off	calcite	quartz	
jwt080604-07	offretite				
jwt080604-08		erionite & offretite	calcite		
jwt080604-09	offretite		calcite	quartz	
jwt080604-10			quartz	kaolinite	muscovite
jwt080604-11			calcite	quartz	
jwt080604-12			quartz	saponite	albite
jwt080604-13			quartz	sauconite	selenium
jwt080604-14			calcite	quartz	
jwt080604-15		very low eri & clino	quartz	albite	
jwt080604-16			quartz	albite	cliftonite?
jwt080605-01			quartz	saponite	
jwt080605-02			saponite	quartz	
jwt080605-03			quartz	saponite	
jwt080605-04			saponite		
jwt080605-05			quartz	saponite	fraipontite??

Through data base analysis and visual, comparative analysis, the following determinations were made: 5 sample scans were determined to be erionite in combination with calcite and/or quartz (jwt080602-01, jwt080603-01, -04, -06, and -08), 6 scans were determined

to be offretite (jwt080602-02, jwt080603-03, -07, jwt080604-01, -07, and -09) plus 2 in combination with erionite (jwt080602-02 and 080603-03) along with calcite and/or quartz, 1 scan was identified as erionite and/or offretite (080603-02), and 3 scans had other zeolites, chabazite, heulandite, and clinoptilolite as possibilities along with erionite and/or offretite (080604-03, -04, -06). 18 scans were determined to be composed of, or a combination of quartz, calcite, albite, saponite, dolomite, ankerite and/or other with no positive presence of zeolites. Two scans were inconclusive (080603-05 and 080604-08), though erionite and offretite were identified as possibilities. A total of 17 samples were identified as having zeolites present by XRD, 2 of which were questionable.

5.1.3. SEM/EDS

Samples that showed positive zeolite results from powder XRD examination were analyzed using SEM/EDS. SEM visual analysis was conducted, and a preliminary chemical composition of the identified zeolite fibers was determined. Appendix Table 2 and Appendix Table 3 contains chemical data for all samples analyzed by SEM/EDS. All samples from SKDM except 080603-09, -10, and -11 contained fibers at differing abundances. Six of the nine samples collected from NKDM contained fibers. The three that did not were samples jwt080604-02, -04, and -05. A complete listing of SEM/EDS analysis of fibers from the KDM complex can be found in Appendix Table 6. No fibers were positively identified for samples from WRB, ERB, and WB. In sample jwt080604-12 from WRB, there was one possible fiber found, but it was too small and covered by other material to determine if it was a mineral fiber or some other material.

SEM/EDS analyses showed most fibers to be classified as offretite when compared on ternary diagrams edited from Passaglia et al. (1998) and Gualtieri et al. (1998) shown in Figure 5.1. See Appendix Table 3 for EDS ternary diagram data.

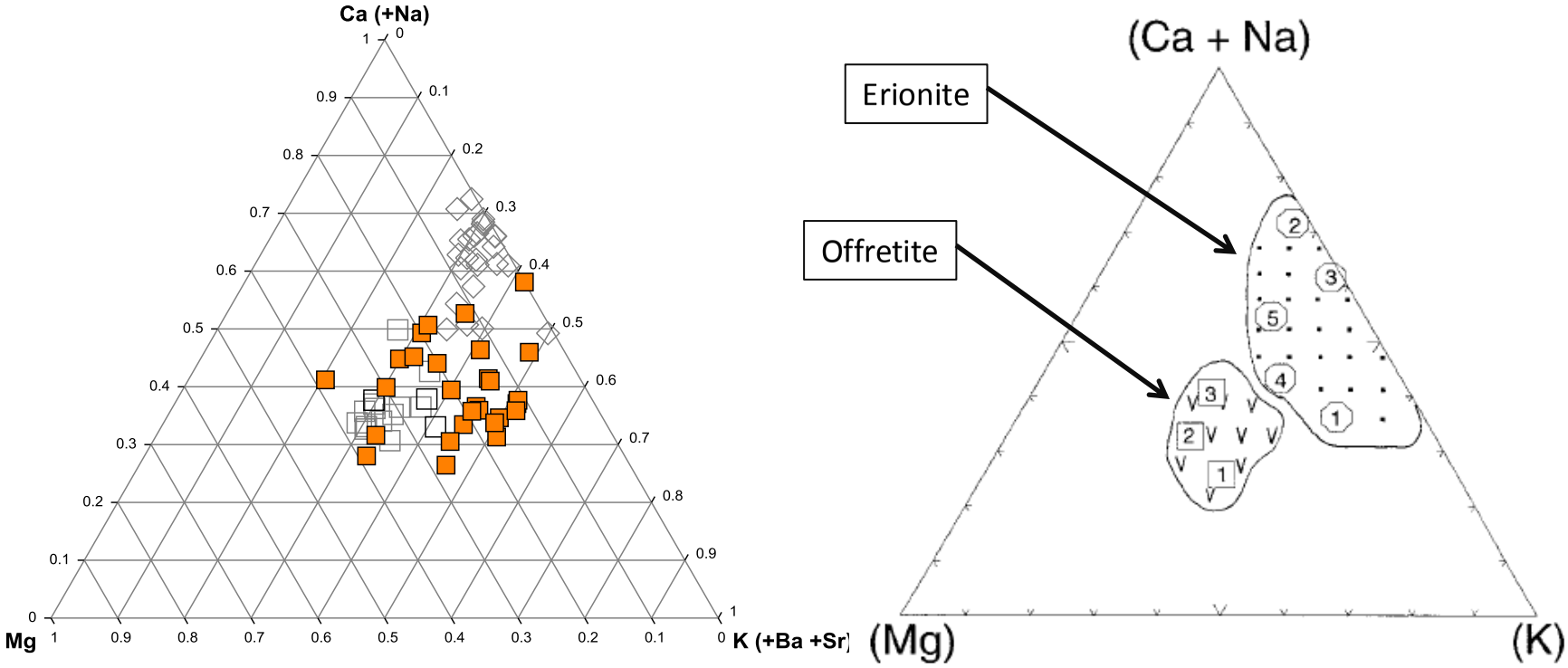

Figure 5.1. Comparison of SEM/EDS analyses. Passaglia et al. (1998): erionite (open diamond) and offretite (open box), Forsman (1986): erionite (bold, open box), Triplett et al. (2009): erionite/offretite (filled box). Gualtieri et al. (1998)

5.1.4. EMPA

EMP analysis was conducted on 9 samples with high zeolite concentration based on XRD and SEM/EDS analysis. From the 9 samples, a total of 28 individual fibers (77 points) were analyzed (see Appendix Table 4 for EMPA point data). From the microscopic mapping images done prior to EMPA, it is known that some of the fibers measured using EMPA were the identical fibers measured by SEM/EDS (see Appendix Table 7).

Using E% as described by Passaglia (1998) to determine which sets of analysis data could be used for comparison, and then [Mg/(Ca+Na)] ratio, it was determined that only four of the fourteen fiber analysis could be classified as erionite. Due to the close relation between the two zeolites, it is difficult to attain a definite identification if the E% is not in the accepted range. Summarized data are presented in Table 5.2 and a plot of the EMPA data is shown in Figure 5.2. The EMPA data indicate that most of the zeolite fibers we identified and examined would be classified as offretite (Figure 5.2). Complete EMPA data and figures can be found in Appendix Table 8 and Appendix Figure 2 and EMPA ternary data in Appendix Table 5.

Table 5.2. E% and Mg/(Ca+Na) ratio for zeolite fibers based on microprobe data

Sample No.	080603-08 1-1	080603-08 2-1	080603-08 2-2	080603-08 2-3	080603-08 3-1	080603-07 2-2	080603-07 3-1
E%	6.96	3.04	-1.16	10.77	-8.88	10.78	0.67
Mg/(Ca+Na)	0.81	0.38	0.30	0.34	0.26	0.61	1.81
Zeoliote	offretite	offretite	erionite	offretite	erionite	offretite	offretite

Sample No.	080603-01 1-1	080603-01 1-3	080603-07 4-1	080603-07 4-2	080603-07 4-3	080604-09 1-4	080603-07 3-3
E%	2.03	-5.16	10.77	0.29	3.06	-10.15	2.95
Mg/(Ca+Na)	0.56	0.27	0.37	0.47	0.30	0.78	3.40
Zeoliote	offretite	erionite	offretite	offretite	erionite	offretite	offretite

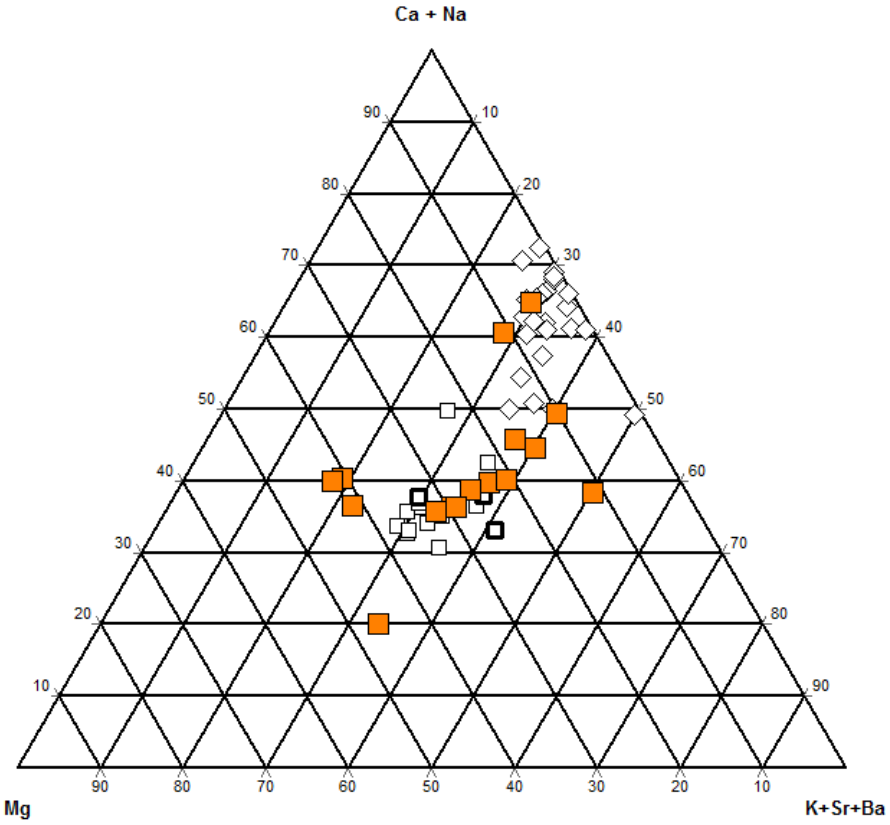

Figure 5.2. Ternary Mg, K, Ca+Na plot of EMPA analyses of zeolite fibers, Passaglia et al. (1998): erionite (open diamond) and offretite (open box), Forsman (1986): erionite (bold, open box), Triplett et al. (2009): erionite/offretite (filled box)

From this analysis, it was determined that only 4 of the 28 zeolite fibers could be classified as erionite according to identification guidelines set by Passaglia (1998). Following said guidelines, the other 24 fibers would be classified as offretite. That being stated, because of the close relation between erionite and offretite, it is possible that some of the 24 offretite fibers may still be erionite, or some of the 4 erionite fibers may be offretite.

5.2. Zeolite Identification in the Study Area

From the analyses described above, it can be determined which locations visited during sampling field work contain fibrous zeolites within the bedrock. Positive identification of fibrous zeolitic material was confirmed for the Killdeer Mountain complex. Due to sampling limitations

at the Rainy Buttes and at White Butte, we can only be report that the presence of fibrous zeolite material in the samples collected for this project from the Rainy Buttes and from White Butte was negative.

5.2.1. Killdeer Mountain complex zeolite locations

5.2.1.1. South Killdeer Mountain. Zeolite material was determined by XRD, SEM/EDS, and EMPA to be present in all but four of the fourteen samples. Specific sampling locations for South Killdeer Mountain are discussed in Chapter 3. At South Killdeer Mountain, samples jwt080602-01, -02, -03, jwt080603-01, -02, -03, -04, -05, -06, -07, and -08 showed positive results for zeolites.

Sample jwt080602-01 is a siltstone that was determined by XRD to be composed of primarily quartz in combination with erionite. Sample jwt080602-02 is a siltstone composed of calcite and contained offretite/erionite. It was noted on site that these two samples could have been part of possible slump formations. Sample jwt080602-03 was collected from the Medicine Hole crevasse entrance located on the top of Medicine Hole Plateau. This sample was identified as siltstone by visual inspection and as ankerite and calcite by XRD. Fibers present were identified by EMPA to not be erionite. Meaning it may be offretite or some other related zeolite. This sample is believed to correspond to the top of unit 12 as described by Murphy et al. (1993), a 62 foot (18.9 m) unit consisting of eight - 1 foot (0.3 m) thick carbonate lenses interbedded with 5 foot (1.5 m) thick siltstone beds. Sample jwt080603-01 was determined to be very fine grained sandstone composed of calcite with erionite. Sample jwt080603-02 was determined to be very fine grained sandstone with silt containing offretite and erionite. Sample jwt080603-03 was determined to be very fine grained sandstone with silt determined to be calcite containing offretite/erionite. Sample jwt080603-04 is a siltstone composed of calcite and contained erionite.

Sample jwt080603-05 is a siltstone, but no definite match by XRD of a zeolite. Offretite and erionite were suggested by the XRD data base and fibers were visible by SEM. Sample jwt080603-06 is a siltstone containing erionite. Sample jwt080603-07 is a siltstone composed of calcite and contains offretite. This sample was a part of a possible slump formation. Sample jwt080603-08 was a very friable sand/siltstone layer composed of quartz and contained erionite.

Samples jwt080603-09, jwt080603-10, and jwt080603-11 did not contain zeolite fibers. Sample jwt080603-09 corresponds to the well cemented carbonate lenses in unit 9 as described by Murphy et al. (1993) and termed the BMU by Forsman (1986). These 6-8 inch (15 - 20 cm) lenses are mostly well cemented, calcareous, tufaceous, and contain differing sizes of putative burrows (Murphy et al., 1993). Powder XRD analysis showed the main mineral content of these separating layers to be mainly calcite and quartz. Sample jwt080603-10 corresponds to the fine grained sandstone of Murphy et al.'s (1993) unit 10 described by them as a massive, buff to white, fine grained, moderately to well cemented sandstone which overlies unit 9, the BMU. Powder XRD analysis concluded the rock unit consisted mainly of dolomite and quartz. Sample jwt080603-11 corresponds to unit 13 of Murphy et al. (1993) and is described as a light gray to green, very fine grained, poorly cemented sandstone. This unit sits approximately 50 feet (15.2 m) below the top surface of South Killdeer Mountain. Powder XRD analysis showed the sample taken from the rock unit to be mostly calcite and quartz. One fiber was located in this sample during SEM/EDS analysis. The EDS analysis showed a high carbon content, indicating this fiber is probably organic.

This study shows that there are zeolite containing rock units throughout South Killdeer Mountain as far down as unit 5 of Murphy et al. (1993), a 25 foot (7.6 m) moderately cemented siltstone with sand lenses and concretions approximately 307 feet (93.6 m) from the top of the

butte. Four samples did not contain zeolite fibers: the entrance to Medicine Hole, the massive unit 10, the calcareous portion of unit 9, and near the top of the butte in unit 13. Because this was the extent of the sampling for this study, it is possible that the zeolite bearing rock units extend below the Arikaree formation into the Chadron and Golden Valley Formations. Figure 5.3 is a stratigraphic profile of SKDM highlighting the units with a positive zeolite presence.

5.2.1.2. North Killdeer Mountain. At North Killdeer Mountain, zeolite material was determined by XRD, SEM/EDS, and EMPA to be present in six of the nine samples. Specific sampling locations for NKDM are discussed in Chapter 3 Sampling. Samples jwt080604-01, -03, -06, -07, -08, -09 were positive for containing zeolitic material.

Sample jwt080604-01 was identified visually as a whitish, fine grained (powdery) siltstone with burrow like structures and was identified as calcite containing offretite by XRD. Sample jwt080604-03 is a whitish carbonate siltstone layer above clay (080604-06) and massive ash layer and identified by XRD as calcite and quartz containing chabazite and erionite. Sample jwt080604-06 is a clay/siltstone layer directly on top of massive unit and was identified by XRD as calcite and quartz containing clinoptilolite and erionite. Sample jwt080604-07 is a silt/sandstone 4 ft. (1.2 m) from base of quarry floor containing offretite as identified by XRD. Sample jwt080604-08 is a silty/clay sandstone 13 ft. (4.0 m) from base of quarry floor identified as calcite containing erionite and offretite by XRD. Sample jwt080604-09 is a burrowed, calcareous sandstone unit 11 ft. (3.4 m) from base of quarry floor and was identified as calcite and quartz containing offretite by XRD.

Samples jwt080604-02, jwt080604-04, and jwt080604-05 did not contain zeolitic material. Sample jwt080604-02 corresponds to what we identified as the massive unit 10 found at the South Mountain and described by Murphy et al. (2003) as a massive, fine grained sandstone,

buff to white, fine grained, moderately to well cemented. We described the unit in the field as a massive carbonate cemented ash w/ vugs (pores), chemical alteration (x<20cm across, dark patches), with lithic fragments (3mm-5cm). Powder XRD analysis showed that the sample concentrate consisted mainly of calcite and quartz, which is a similar mineral content as that in Unit 10, dolomite and quartz. The lack of fibrous minerals in this sample also supports the idea that the two units are correlative. Sample jwt080603-10 from South Killdeer Mountain unit 10 lacked fibrous minerals in our analysis. As with the South Killdeer Mountain sample, the NKDM sample was overlying a unit that would be correlative to the unit 9 (Murphy et al., 2003) BMU. However, the BMU unit at North Killdeer Mountain was not as distinct or compacted as was found at the south mountain. The BMU unit at North Killdeer Mountain had numerous burrows of different sizes throughout, but did not have the distinct 6-8 inch (15-20 cm) lenses with friable sandstone separating each as seen at SKDM. Unlike the SKDM carbonate lense sample (jwt080603-09), the carbonate lenses at NKDM (jwt080604-08) did contain a very limited amount of very small fibers in the sample concentrate. Sample jwt080604-05 was a 4-5 cm lithic fragment removed from the same massive unit as was collected in sample jwt080604-02 described above. Powder XRD analysis showed the lithic fragment to be composed of calcite and quartz and no fibrous zeolite was identified. Sample jwt080604-04 was a soil collected from the very top layer of the rim of the North Killdeer Mountain quarry. Powder XRD analysis of filtered concentrate showed that the majority of the mineral content in the sample was calcite and quartz. The PDF database also listed erionite and heulandite (a very common and well known zeolite) as possible components, but no fibers were discovered in the SEM/EDS analysis of the filtered concentrate.

These results show that there are zeolite containing rock units from just below the uppermost soil of NKDM down to the massive unit, unit 10 of Murphy et al. (2003) and additionally from the bottom of the massive unit down to the stratigraphically lowest outcrop of the NKDM east quarry wall. That unit is interpreted to be the bottom of unit 9 or the top of unit 8, the stratigraphically lowest sampling for this project at North Killdeer Mountain. All of these samples would correlate to Arikaree in age. Because this was the extent of our sampling, it is possible that stratigraphically lower rock units may contain zeolite. Figure 5.4 shows the location of zeolite containing units at NKDM as they relate to the overall stratigraphy.

5.2.2. Rainy Butte and Chalky Butte complexes

No zeolites were positively identified at the Rainy Butte and Chalky Butte complexes.

5.3. Conclusions

The first primary objective of this study was to determine the presence or absence of zeolite fibers within the stratigraphic profile of specific high butte formations in western North Dakota.

The presence of zeolitic material was confirmed for the Killdeer Mountain complex, both North and South Killdeer Mountains. Though the profile of each Killdeer Mountain is slightly different in terms of thicknesses and the distinction of each layer, the zeolite bearing strata of each mountain match up and align very well. The same numbers of relative units containing zeolite fibers were the same, giving an excellent understanding of how the two profiles relate. The possibility that zeolitic material can be found in lower stratigraphic units is plausible, but cannot be confirmed by this study. Specific stratigraphic locations of zeolitic materials are shown in Figure 5.3 and Figure 5.4

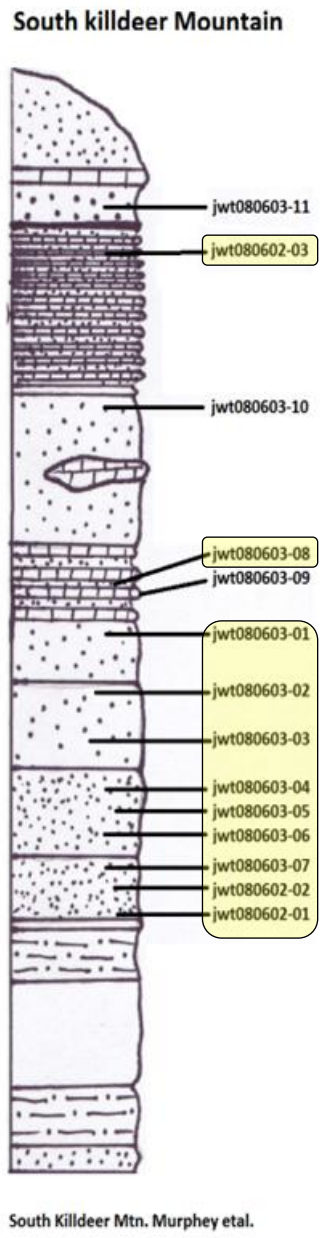

Fig 5.3. Stratigraphic profile of SKDM showing positive zeolite samples (highlighted) (modified from Murphy et. al., 1993)

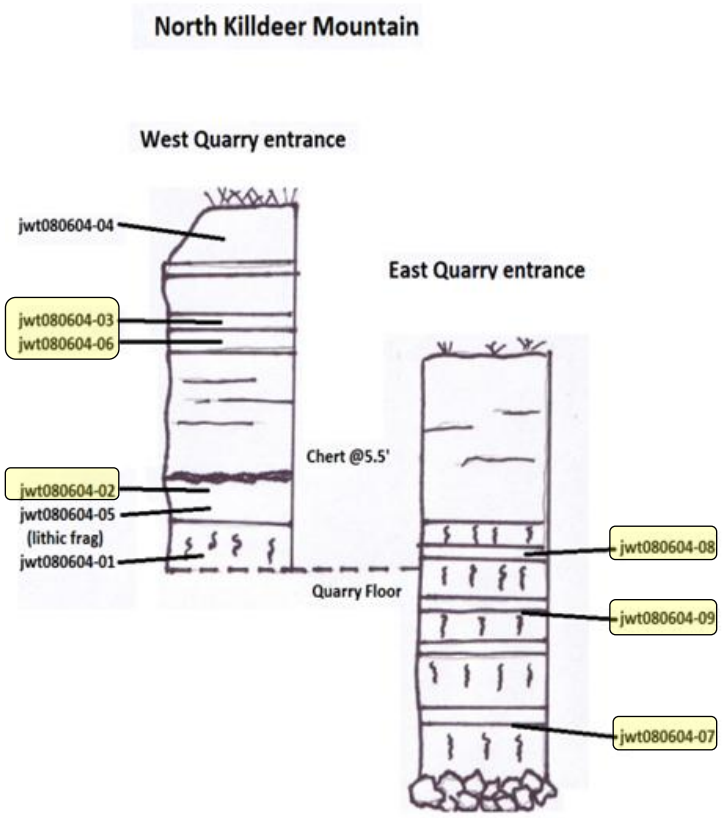

Figure 5.4. Stratigraphic profile of NKDM showing positive zeolite samples (highlighted) (JWT)

Due to sampling limitations at the Rainy Buttes and White Butte, it cannot be reported that these areas do not contain fibrous zeolites. It can only be reported that the presence of fibrous zeolite material in our Rainy Butte and White Butte samples was negative.

The second objective of the study was to identify and characterize any fibrous zeolites found using XRD, SEM, and EMPA. Through XRD analysis, it was determined that 17 samples contained zeolite material. Of those 17 samples, erionite was determined to be present in 5, offretite in 6, a combination of erionite and/or offretite in 3, and 3 were classified as erionite or offretite along with other different zeolites. SEM/EDS and EMPA analysis produced similar results. By comparing the chemical composition of the individual fibers, specifically the [Mg/Ca (+Na)] ratio, and by implementing the E% filter as described by Passaglia et al., 1998, a majority

of the zeolite fibers analyzed were calculated to be offretite fibers rather than erionite. SEM/EDS analysis determined 3 fibers to be erionite and 23 fibers to be offretite. One fiber was determined to fall on the calculated boundary directly in the middle of erionite and offretite. EMPA analysis determined 4 fibers to be erionite and 24 fibers to be offretite. From this analytical investigation, it was determined that a majority of the fibrous zeolites discovered would be classified as offretite.

REFERENCES CITED

Alberti, A., Martucci, A., Galli, E., and Vezzalini, G. (1997) A reexamination of the crystal structure of erionite. Zeolites 19:349-352, 1997

Armbruster, T. and Gunter, M. E. (2001) Crystal Structures of Natural Zeolites. Mineralogical Society of America.

Artvinli, M., and Baris, Y.I. (1979) Malignant Mesothelioma in a Small Village in the Anatolian Region of Turkey: An Epidemiologic Study. J. Natl. Canc. Inst., 63, 17 - 22.

Baris, Y.I., Sahin, A.A., Ozesmi, M., Kerse, I., Ozen, E., Kolacan, B., Altinörs, M., and Göktepeli, A. (1978) An outbreak of pleural mesothelioma and chronic fibrosing pleurisy in the village of Karain/Ürgüp in Anatolia. Thorax, 33, 181-192.

Baris, I., Artvinli, M., Saracci, R., Simonato, L., Pooley, F., Skidmore, J., and Wagner, C. (1987) Epidemiological and environmental evidence of the health effects of exposure to erionite fibres: A four-year study in the Cappadocian region of Turkey. International Journal of Cancer, 39(1), 10-17.

Barthelmy, D. (2011a) Erionite-K Mineral Data, http://webmineral.com/data/Erionite-K.shtml, accessed Dec. 27, 2011.

Barthelmy, D. (2011b) Offretite Mineral Data, http://webmineral.com/data/Offretite.shtml, accessed Dec. 27, 2011.

Bluemle, J.P. (2000) The Face of North Dakota - third edition.

Bluemle, J.P. (2003) Geologic Surface Map of North Dakota, NDGS. www.dmr.nd.gov/ndgs/Publication_List/pdf/MIS%20MAPS/MM-36.pdf. Accessed Feb. 20, 2012.

Carbone, M., Emri, S., Dogan, A.E., Steele, I., Tuncer, M., Pass, H.I., and Baris, Y.I. (2007) A mesothelioma epidemic in Cappadocia: scientific developments and unexpected social outcomes. Nature Reviews Cancer, 7, 147-154

Dogan, A.U., Baris, Y. I., and Dogan, M. (2006) Mesothelioma Epidemic in Turkey Genetic Predisposition to Fiber Carcinogenesis Causes, Cancer Res 66:5063-5068. Published online May 16, 2006.

Dogan, A.U. and Dogan, M. (2008) Re-evaluation and re-classification of erionite series minerals. Received: 1 November 2006 / Accepted: 15 December 2007 / Published online: 20 March 2008

Emri, S., Demir, A., Dogan, M., Akay, H., Bozkurt, B., Carbone, M., Baris, I. (2002) Lung diseases due to environmental exposures to erionite and asbestos in Turkey. Toxicology Letters 127, 251-257

Eylands, K.E., Azenkeng, A., Mibeck, B.A., and Raymond, L.J. (2009) Subtask 1.1 – Characterization of Erionite. 2009-EERC-12-06

Fach, E., Waldman, W. J., Williams, M., Long, J., Meister, R. K., and Dutta, P. K. (2002) Analysis of the Biological and Chemical Reactivity of Zeolite-Based Aluminosilicate Fibers and Particulates. Environmental Health Perspectives, Volume 110, Number 11, November 2002.

Forsman N.F. (1986) Documentation and Diagenesis of Tuffs in the Killdeer Mountains, Dunn County, North Dakota. Report of Investigation No. 87 North Dakota Geological Survey.

Forsman, N.F. (2006) Erionite in tuffs of North Dakota: the need for erionite hazard maps. GSA Abstracts with Programs, 38(7), 366.

Goodman, B.S. and Pierson, M.P. (2010) Erionite, a naturally occurring fibrous mineral hazard in the tri-state area of North Dakota, South Dakota, and Montana. GSA Abstracts with Programs, 42:3, 5.

Gualtieri, A., Artioli, G., Passaglia, E., Bigi, S., Viani, A., and Hanson, J.C. (1998) American Mineralogist, Volume 83, pages 590–606, 1998. Crystal structure-crystal chemistry relationships in the zeolites erionite and offretite

Hoganson, J. W., Murphy, E. C., and Forsman, N.F. (1998) Lithostratigraphy, paleontology, and biochronology of the Chadron, Brule, and Arikaree Formations in North Dakota. Geological Society of America Special Paper 325.

Hoganson, J.W., Murphy, E.C., Forsman, N.F. (2007). https://www.dmr.nd.gov/ndfossil/Research/Short%20Papers/white_river.asp. Accessed Nov. 4, 2011.

IARC (1987) Overall evaluations of carcinogenicity: an updating of IARC Monographs volume 42. IARC Monographs on the Evaluation of Carcinogenic Risks Humans, Suppl. 7: 225.

Kleymenova, E.V., Horesovsky, G., Pylev, L.N., Everitt, J. (1999) Mesotheliomas induced in rats by the fibrous mineral erionite are independent from p53 alterations. Cancer Letters 147, 55-61

Kliment, Corrine R., Clemens, Kristen and Oury, Tim D. (2008) North American Erionite-Associated Mesothelioma with Pleural Plaques and Pulmonary Fibrosis: A Case Report Department of Pathology, University of Pittsburgh School of Medicine, Pittsburgh, PA, USA and 2RJ Lee Group, 350 Hochberg Road, Monroeville, PA, USA Received 9 October 2008; Accepted 15 October 2008; Available online 25 November 2008

Kokotailo, G.T. and Fyfe, C.A. (1995) Zeolite structure analysis with powder X-Ray diffraction and solid-state NMR techniques. The Rigaku Journal. Vol. 12, No. 1, 1995.

Lowers, H.A., and Meeker, G.P. (2007) Denver microbeam laboratory administrative report 14012007: U.S. Geological Survey Administrative Report, 11 p.

Mayo Clinic. http://mayoclinic.com/health/mesothelioma/DS00779, Accessed Dec. 8, 2011.

Meeker, G., Tremolite asbestos, Death Valley, California. http://usgsprobe.cr.usgs.gov/picts2.html, Accessed Dec. 9, 2011.

Metintas, M., Hillerdal, G., and Metintas, S. (1999) Malignant mesothelioma due to environmental exposure to erionite: follow-up of a Turkish emigrant cohort. Eur Respir J., 13(3), 523-6.

Murphy, E.C., Hoganson, J.W., and Forsman, N.F. (1993) The Chadron, Brule, and Arikaree Formationsin North Dakota. Report of Investigation No. 96 North Dakota Geological Survey.

Murphy, E.C. (2001) Geology of Dunn County. Bulletin 68 – Part 1, North Dakota Geological Survey.

Murphy, E.C. (2008) personal communication.

Mumpton, F.A. (1977) Natural Zeolites. Mineralogy and Geology of Natural Zeolites. Mineralogical Society of America Short Course Notes Vol 4, pgs 1-17.

North Dakota Department of Health, http://www.health.state.nd.us/EHS/Erionite/. Accessed Aug. 17, 2009.

North Dakota Geological Survey, Department of Mineral Resources. (2006) www.dmr.nd.gov/ndfossil/Poster/sentinalB/Sentinel%20Butte.pdf . Accessed Feb. 20, 2012.

Nesse, W.D. (2000) Introduction to Mineralogy. Oxford University Press, Inc.

Passaglia, E., Artioli, G., and Gualtieri, A. (1998) Crystal chemistry of the zeolites erionite and offretite. American Mineralogist, Volume 83, pages 577–589, 1998

Ryan, P.H., Dihle, M., Griffin, S., Partridge, C., Hillbert, T.J., Taylor, R., Adjei, S. and Lockey, J.E. (2011) Erionite in road gravel associated with interstitial and pleural changes-an occupational hazard in western United States. Journal of Occupational Enviornmental Medicine. vol. 53(8) pg 892-898.

Sheppard, R.A. (1996) Occurrences of Erionite in Sedimentary Rocks of the Western United States. U.S. Department of the Interior and U.S. Geological Survey, Denver, Colorado.

Treacy, M.M.J. and Higgins, J.B. (2001) Collection of Simulated XRD Powder Patterns for Zeolites Fourth Revised Edition. Published on behalf of the Stucture Commision of the International Zeolite Association.

Tschnerich, R.W. (1992) Zeolites of the World, pp. 156-166, 380-391.

U.S. EPA (2010) Radiographic Changes Associated with Exposure to Erionite in Road Gravel in North Dakota. Report EP-R8-06-02/TO#0804, 2010. pp. 90

Wagner, J.C., Skidmore, J.W., Hill, R.J., and Griffiths, D.M. (1985) Erionite exposure and mesotheliomas in rats. Br J Cancer, 51(5), 727-730.

Table 1. Sample Site Description and Location

Sample ID - JWT	Sample Site	Field Description (BSE)	Sample ID - JWT	N Lat.	W Long.	Elevation (ft)	Time (Central)	Date sampled
080602-01*	SKDM	fine gravel, silty clay. black hammer pic. Light grn color, below drk grn. ~6' below 080602-02	080602-01*	47 26.685 N	102 53.211 W	3010 ft	4:42:15 PM	6/2/2008
080602-02*	SKDM	fine gravel, silty clay. red hammer pic. Light grn color, below drk grn w/ concretions. ~6' above 080602-01	080602-02*	47 26.683 N	102 53.215 W	3017 ft	4:56:45 PM	6/2/2008
080602-03	SKDM	Medicine Hole entrance. White color. One sample pic w/ hammer and one w/ Jason. Unit 12 Murphy etal 8-1' ca	080602-03	47 26.656 N	102 53.464 W	3180 ft	5:34:35 PM	6/2/2008
080603-01	SKDM	2 jwt's (135.25") below base of BMU. Sandy-silt	080603-01	47 26.679 N	102 53.222 W	3067 ft	12:03:24 PM	6/3/2008
080603-02	SKDM	5 jwt's (338.125") below base of BMU. Greenish siltstone	080603-02	47 26.669 N	102 53.219 W	3063 ft	11:59:58 AM	6/3/2008
080603-03	SKDM	8 jwt's (541") below base of BMU. White, clayey fine-grained siltstone below calcareous ledge unit	080603-03	47 26.665 N	102 53.219 W	3046 ft	12:20 PM	6/3/2008
080603-04	SKDM	10 jwt's (676.25") below base of BMU. Whitish clayey siltston above cm-banded calcareous unit	080603-04	47 26.662 N	102 53.220 W	3035 ft	12:51 PM	6/3/2008
080603-05	SKDM	11 jwt's (743.875") below base of BMU. Whitish clayey siltstone directly below cm-banded calcareous unit.	080603-05	47 26.660 N	102 53.219 W	3018 ft	12:51 PM	6/3/2008
080603-06	SKDM	13 jwt's (879.125") below base of BMU. Whitish silty layer below 2'0" Concretion rich unit. Possibly same as 0	080603-06	47 26.656 N	102 53.215 W	3007 ft	12:52 PM	6/3/2008
080603-07*	SKDM	15 jwt's (1014.38") below base of BMU. Greenish clay-bearing siltstone, possible slump, but don't think so…	080603-07*	47 26.651 N	102 53.213 W	3079 ft	1:15 PM	6/3/2008
080603-08	SKDM	(16' BMU) 8' or 1/2 way up BMU. Friable material between harder calcareous layers	080603-08	47 26.675 N	102 53.234 W	3090 ft	2:59:16 PM	6/3/2008
080603-09	SKDM	(16' BMU) 8' or 1/2 way up BMU. Calcareous material. Interior softer, fine grained. Friable core.	080603-09	"	"	3090 ft	2:59:16 PM	6/3/2008
080603-10	SKDM	10 jwt's (676.25") above top of BMU. Calcareous, medium grained white sandstone. (believe unit is "unit 10" Mu	080603-10	47 26.722 N	102 53.392 W	3178 ft	3:55:26 PM	6/3/2008
080603-11	SKDM	25 jwt's (1690.63") above top of BMU. Sandstone Unit #13 Murphy etal. Fine grained siltstone overlain by carb	080603-11	47 26.623 N	102 54.046 W	3260 ft	5:09:56 PM	6/3/2008
080604-01	NKDM(wqe)	Whitish, fine grained, powdery w/ burrow like structures	080604-01	47 30.004 N	102 53.674 W	3089 ft	10:28 PM	6/4/2008
080604-02	NKDM(wqe)	Massive carbonate cemented ash w/ vugs (pores), chemical alteration (x<20cm across, dark patches), lithic fragme	080604-02	"	"	~3092 ft	10:47 PM	6/4/2008
080604-03	NKDM(wqe)	Whitish carbonate layer above clay (080604-06) and massive ash	080604-03	"	"	~3098 ft	11:10 PM	6/4/2008
080604-04	NKDM(wqe)	Soil Sample	080604-04	"	"	~3102 ft	11:10 PM	6/4/2008
080604-05	NKDM(wqe)	Lithic fragment from 080604-02	080604-05	"	"	~3088 ft	10:46 PM	6/4/2008
080604-06	NKDM(wqe)	Clay layer directly on top of massive unit	080604-06	"	"	~3096 ft	10:51 PM	6/4/2008
080604-07	NKDM(eqe)	Siltstone 4' from base	080604-07	47 30.007 N	102 53.642 W	3071 ft	12:53 PM	6/4/2008
080604-08	NKDM(eqe)	Silty clay 13' from base	080604-08	"	"	3084 ft	12:53 PM	6/4/2008
080604-09	NKDM(eqe)	Burrowed calcareous unit 11' from base	080604-09	"	"	3082 ft	12:53 PM	6/4/2008
080604-10	WRB	Fine grained white siltstone. Golden Valley. 3100' elevation GPS	080604-10	46 29.529 N	103 01.424 W	3100 ft	8:25 PM	6/4/2008
080604-11	WRB	Top of South Heart member of chadron. Distinct carbonate layer. 3200' elevation	080604-11	46 29.581 N	103 01.435 W	3200 ft	8:34 PM	6/4/2008
080604-12	WRB	Base of the brule. Pink to brown silty clay. ~3215' elevation GPS	080604-12	46 29.530 N	103 01.458 W	3221 ft	8:45:13 PM	6/4/2008
080604-13	WRB	Possibly Unit #6 Murphy etal. Mudstone in Brule. Light pink/brown. Moderatley indurated (chisel)	080604-13	46 29.532 N	103 01.461 W	3245 ft	8:56 PM	6/4/2008
080604-14	WRB	~10' above 080604-13, Float, small chips of light green clay (?Brule?) 3258' elevation GPS	080604-14	46 29.532 N	103 01.464W	3258 ft	9:08:14 PM	6/4/2008
080604-15	WRB	Small clay bed in among coarse grained crossbedding. Base of caprock. 3260' elevation GPS	080604-15	46 29.537 N	103 01.471 W	3268 ft	9:16:42 PM	6/4/2008
080604-16	WRB	Sandstone Caprock. We believe Arikaree.	080604-16	46 29.537 N	103 01.471 W	3268 ft	9:16:42 PM	6/4/2008
080605-01	ERB	Top of brule, brown siltstone w/ some clay, directly below dendritic chert layer 3320' elevation GPS	080605-01	46 27.216 N	102 58.648 W	3220 ft	11:50 PM	6/5/2008
080605-02	ERB	Clay lense - Sandstone/siltstone crossbeding with clay lenses (~1' in length) ~20' below caprock 3250 ' elevation	080605-02	46 27.214 N	102 58.609 W	3274 ft	12:20:09 PM	6/5/2008
080605-03	ERB	White powdery siltstone below Sandstone layer. Ashy? 3260" elevation GPS	080605-03	46 27.282 N	102 58.834 W	3260 ft	1:31:48 PM	6/5/2008
080605-04	WB	~10' below main chalky butte memberwhitish with light brown oxidation.	080605-04	46 23.590 N	103 18.162 W	3191 ft	4:54:10 PM	6/5/2008
080605-05	WB	Bentonite (very wet, popcorn look on outside, dry 1/2 inch under)	080605-05	46 23.639 N	103 18.116 W	3169 ft	5:22:34 PM	6/5/2008

Notes:
SKDM - South Killdeer Mountain
NKDM - North Killdeer Mountain: wqe - West Quarry entrance, eqe - East Quarry entrance
WRB - West Rainy Butte
ERB - East Rainy Butte
WB - White Butte
"*" Denotes possible slump

APPENDIX SEM/EDS CHEMICAL ATOM %

Table 2. SEM/EDS Chemical Atom %

SEM #	Sample ID	C	O	Na	Mg	Al	Si	Cl	K	Ca	Ti	Fe	Total
091798	JWT080602-01(1)_pt1	0.00	0.00	0.00	1.41	14.41	66.75	0.00	10.01	7.42	0.00	0.00	100.00
091799	JWT080603-02(1)_pt1	0.00	0.00	0.00	1.44	16.41	69.38	0.00	7.46	5.31	0.00	0.00	100.00
091800	JWT080603-03(1)_pt1	0.00	0.00	1.89	1.38	16.33	69.63	0.00	7.23	3.55	0.00	0.00	100.01
091801	JWT080603-06(1)_pt1	0.00	0.00	0.00	1.55	16.46	68.88	0.00	6.30	5.20	0.00	1.62	100.01
091802	JWT080603-08(1)_pt1	0.00	0.00	0.80	1.16	16.49	67.95	0.00	8.54	5.05	0.00	0.00	99.99
091803	JWT080604-01(1)_pt1	0.00	0.00	0.98	1.73	16.73	69.36	0.00	7.18	4.02	0.00	0.00	100.00
091804	JWT080604-03(1)_pt1	0.00	0.00	0.00	6.41	17.63	62.70	0.00	6.74	1.31	0.00	5.21	100.00
091805	JWT080604-07(1)_pt1	0.00	0.00	0.00	0.46	16.57	69.68	0.00	6.76	6.54	0.00	0.00	100.01
092238	JWT080602-03 (1)_pt1	0.00	59.00	0.00	1.43	7.14	28.19	0.00	2.13	2.10	0.00	0.00	99.99
092238	JWT 080602-03(1)_pt1	0.00	59.57	0.00	0.46	7.16	28.09	0.00	2.45	2.27	0.00	0.00	100.00
092239	JWT 080603-01 (1)_pt1	0.00	63.03	0.33	0.71	6.84	25.45	0.00	2.40	1.25	0.00	0.00	100.01
092241	JWT 080603-04 (1)_pt1	0.00	57.69	0.39	0.82	7.34	28.77	0.00	3.13	1.86	0.00	0.00	100.00
092242	JWT 080603-05 (1)_pt1	0.00	44.80	0.42	0.84	8.34	36.66	0.00	5.65	3.28	0.00	0.00	99.99
092243	JWT 080603-07(1)_pt1	0.00	56.29	0.00	0.67	7.69	29.95	0.00	3.14	1.97	0.00	0.30	100.01
092244	JWT 080603-09(1)_pt1	40.17	31.01	0.00	0.19	0.34	1.02	0.00	0.17	27.10	0.00	0.00	100.00
092244	JWT 080603-09(1)_pt1	0.00	51.93	0.00	0.34	0.60	1.75	0.00	0.27	45.11	0.00	0.00	100.00
092245	JWT 080603-10(1)_pt1	0.00	66.56	0.00	9.61	1.36	8.38	0.00	0.29	13.07	0.00	0.74	100.01
092246	JWT 080603-11(1)_pt1	68.63	23.87	0.47	0.35	1.25	3.23	0.00	0.12	1.86	0.00	0.21	99.99
092246	JWT 080603-11(1)_pt2	49.82	35.42	0.00	1.67	1.53	9.03	0.00	0.48	1.36	0.00	0.68	99.99
092247	JWT 080604-02(1)_pt1	43.60	36.86	0.00	0.24	0.00	0.00	0.00	0.00	19.30	0.00	0.00	100.00
092247	JWT 080604-02(1)_pt2	42.57	35.73	0.00	0.34	0.00	0.17	0.00	0.00	21.18	0.00	0.00	99.99
092244	JWT 080604-04(1)_pt1	0.00	57.17	0.00	1.09	6.23	23.13	0.00	1.96	9.63	0.00	0.79	100.00
092249	JWT 080604-05(1)_pt1	0.00	59.51	0.00	1.34	5.22	22.30	0.00	2.19	7.44	0.24	1.45	99.99
092249	JWT 080604-05(1)_pt2	48.46	33.63	0.00	0.20	0.00	0.27	0.00	0.00	17.44	0.00	0.00	100.00
092250	JWT 080604-06(1)_pt1	0.00	65.71	0.00	0.98	6.09	23.04	0.00	2.63	1.55	0.00	0.00	100.00
092251	JWT 080604-08(1)_pt1	0.00	53.84	0.00	0.00	7.74	31.63	0.00	2.80	3.98	0.00	0.00	99.99
092252	JWT 080604-09(1)_pt1	0.00	59.61	0.00	2.70	5.62	22.04	0.00	1.64	5.65	0.25	2.48	99.99
092253	JWT 080604-10(1)_pt1	0.00	48.38	0.34	0.68	17.36	24.45	0.00	6.75	0.00	0.59	1.45	100.00
092254	JWT 080604-11(1)_pt1	0.00	59.94	0.00	0.38	0.95	2.79	0.00	0.36	35.57	0.00	0.00	99.99
092254	JWT 080604-11(1)_pt2	0.00	67.96	0.00	0.59	2.21	23.44	0.00	0.55	4.53	0.00	0.70	99.98
092255	JWT 080604-12(1)_pt1	0.00	60.59	1.60	1.08	6.68	26.86	0.00	0.88	0.78	0.22	1.32	100.01
092255	JWT 080604-12(1)_pt2	0.00	52.86	1.27	0.92	8.96	28.67	0.00	4.42	0.87	0.32	1.71	100.00
092256	JWT 080604-13(1)_pt1	0.00	57.95	0.27	1.65	7.64	27.89	0.00	1.73	0.60	0.24	2.03	100.00
092256	JWT 080604-13(1)_pt2	0.00	55.87	0.00	1.90	9.35	27.16	0.00	2.28	0.81	0.00	2.62	99.99
092257	JWT 080604-14(1)_pt1	0.00	27.34	0.00	0.97	4.41	52.21	0.00	2.79	1.96	0.00	10.32	100.00
092258	JWT 080604-15-2,1_pt1	0.00	54.93	2.27	0.74	8.35	28.66	0.00	0.89	2.11	0.00	2.05	100.00
092259	JWT 080605-01(1)_pt1	0.00	56.06	0.00	2.92	6.34	28.24	0.00	0.53	1.78	0.23	3.91	100.01
092260	JWT 080605-02(1)_pt1	0.00	51.75	0.38	2.50	7.71	29.63	0.00	0.64	3.48	0.32	3.58	99.99
092261	JWT 080605-03(1)_pt1	0.00	56.44	0.00	2.78	7.92	28.60	0.00	0.50	1.69	0.18	1.91	100.02
092262	JWT 080605-04(1)_pt1	0.00	50.31	1.99	1.56	12.12	28.64	0.00	0.35	1.25	0.53	3.24	99.99
092263	JWT 080605-05(1)_pt1	0.00	52.84	0.88	0.51	11.28	29.28	0.00	1.28	0.56	0.44	2.92	99.99
172	NM #3(2) pt1	0.00	73.30	0.28	1.16	4.83	18.47	0.00	1.25	0.71	0.00	0.00	100.00
172	NM #3(2) pt2	0.00	0.00	0.00	0.00	0.00	0.00	0.00	0.00	0.00	0.00	0.00	0.00
172	NM #3(1) pt 1	0.00	73.18	0.18	1.04	5.06	18.70	0.00	1.01	0.82	0.00	0.00	99.99
173	NM #2 pt1	0.00	72.76	0.00	0.97	5.45	19.14	0.00	1.03	0.65	0.00	0.00	100.00
173	NM #2 pt2	0.00	70.12	0.23	1.35	5.82	21.21	0.00	0.78	0.48	0.00	0.00	99.99
174	MH1a(1) pt1	0.00	68.62	0.09	0.22	5.81	22.67	0.00	1.09	1.49	0.00	0.00	99.99
174	MH1a(1) pt2	0.00	69.34	0.24	0.38	5.82	21.85	0.00	1.05	1.33	0.00	0.00	100.01
175	MH3(1) pt1	0.00	72.91	0.00	0.49	5.29	19.42	0.00	0.80	1.08	0.00	0.00	99.99
175	MH3(1) pt2	0.00	71.73	0.08	0.46	5.32	20.34	0.00	0.87	1.20	0.00	0.00	100.00
311	MH 1B(2) pt1	0.00	64.54	0.52	1.39	6.35	25.14	0.00	1.51	0.54	0.00	0.00	99.99
311	MH 1B(2) pt2	0.00	68.13	0.29	1.30	6.03	22.60	0.00	1.14	0.51	0.00	0.00	100.00
311	MH 1B(2) pt3	0.00	67.32	0.38	0.99	6.08	23.34	0.00	1.37	0.52	0.00	0.00	100.00
313	MH 2(2) pt1	0.00	70.72	0.98	4.44	1.84	15.38	0.10	0.50	2.94	0.00	3.09	99.99
313	MH 2(2) pt2	0.00	69.12	1.03	4.87	2.54	15.66	0.25	0.34	3.02	0.00	3.19	100.02
313	MH 2(2) pt3	0.00	72.91	0.80	3.72	2.11	14.71	0.34	0.11	2.72	0.00	2.56	99.98
315	MH 5B pt1	0.00	0.00	0.00	0.00	0.00	0.00	0.00	0.00	0.00	0.00	0.00	0.00
315	MH 5B pt2	0.00	0.00	0.00	0.00	0.00	0.00	0.00	0.00	0.00	0.00	0.00	0.00
315	MH 5B pt3	0.00	0.00	0.00	0.00	0.00	0.00	0.00	0.00	0.00	0.00	0.00	0.00
315	MH 5B(2) pt1	0.00	70.53	0.95	1.17	4.92	21.00	0.00	1.01	0.42	0.00	0.00	100.00
315	MH 5B(2) pt2	0.00	70.31	0.52	1.31	2.43	17.95	0.00	4.18	3.29	0.00	0.00	99.99
315	MH 5B(2) pt3	0.00	72.99	0.84	1.76	3.35	14.55	0.24	1.09	1.09	0.00	4.08	99.99
317	MH 9A	0.00	0.00	0.00	0.00	0.00	0.00	0.00	0.00	0.00	0.00	0.00	0.00
319	MH 9B(1) pt1	0.00	71.06	0.00	0.23	5.12	20.97	0.00	1.22	1.41	0.00	0.00	100.01
319	MH 9B(1) pt2	0.00	72.61	0.13	0.41	5.31	19.52	0.00	0.91	1.10	0.00	0.00	99.99
319	MH 9B(1) pt3	0.00	71.00	0.00	0.39	5.51	20.57	0.00	1.12	1.41	0.00	0.00	100.00

APPENDIX TERNARY EDS CHEMICAL DATA

Table 3. Ternary EDS Chemical Data

JWT Sample ID	Mg	K	Ca(+Na)
JWT080602-01(1)_pt1	0.116	0.513	0.371
JWT080603-02(1)_pt1	0.155	0.499	0.346
JWT080603-03(1)_pt1	0.138	0.448	0.414
JWT080603-06(1)_pt1	0.180	0.454	0.366
JWT080603-08(1)_pt1	0.112	0.512	0.377
JWT080604-01(1)_pt1	0.179	0.462	0.359
JWT080604-03(1)_pt1	0.563	0.368	0.070
JWT080604-07(1)_pt1	0.053	0.487	0.460
JWT080602-03 (1)_pt1	0.355	0.329	0.316
JWT080602-03(1)_pt1	0.137	0.453	0.410
JWT080603-01 (1)_pt1	0.215	0.451	0.335
JWT080603-04 (1)_pt1	0.190	0.452	0.358
JWT080603-05 (1)_pt1	0.124	0.518	0.359
JWT080603-07(1)_pt1	0.176	0.511	0.313
JWT080603-09(1)_pt1	0.011	0.006	0.982
JWT080603-09(1)_pt1	0.012	0.006	0.982
JWT080603-10(1)_pt1	0.542	0.010	0.447
JWT080603-11(1)_pt1	0.171	0.036	0.793
JWT080603-11(1)_pt2	0.598	0.107	0.295
JWT080604-02(1)_pt1	0.020	0.000	0.980
JWT080604-02(1)_pt2	0.026	0.000	0.974
JWT080604-04(1)_pt1	0.134	0.150	0.717
JWT080604-05(1)_pt1	0.186	0.189	0.625
JWT080604-05(1)_pt2	0.019	0.000	0.981
JWT080604-06(1)_pt1	0.276	0.460	0.264
JWT080604-08(1)_pt1	0.000	0.419	0.581
JWT080604-09(1)_pt1	0.378	0.143	0.479
JWT080604-10(1)_pt1	0.130	0.801	0.069
JWT080604-11(1)_pt1	0.017	0.010	0.973
JWT080604-11(1)_pt2	0.160	0.093	0.747
JWT080604-12(1)_pt1	0.285	0.144	0.571
JWT080604-12(1)_pt2	0.166	0.496	0.338
JWT080604-13(1)_pt1	0.489	0.319	0.192
JWT080604-13(1)_pt2	0.499	0.372	0.129
JWT080604-14(1)_pt1	0.249	0.446	0.305
JWT080604-15(1)_pt1	0.149	0.111	0.740
JWT080605-01(1)_pt1	0.675	0.076	0.249
JWT080605-02(1)_pt1	0.462	0.074	0.464
JWT080605-03(1)_pt1	0.675	0.076	0.249
JWT080605-04(1)_pt1	0.336	0.047	0.617
JWT080605-05(1)_pt1	0.198	0.309	0.493

Forsman Samples	Mg	K	Ca(+Na)
NM #3(2) pt1	0.435	0.292	0.273
NM #3(1) pt 1	0.442	0.267	0.292
NM #2 pt1	0.484	0.319	0.197
NM #2 pt2	0.570	0.205	0.226
MH1a(1) pt1	0.116	0.357	0.527
MH1a(1) pt2	0.182	0.312	0.507
MH3(1) pt1	0.298	0.303	0.399
MH3(1) pt2	0.254	0.298	0.448
MH 1B(2) pt1	0.434	0.293	0.274
MH 1B(2) pt2	0.495	0.270	0.235
MH 1B(2) pt3	0.387	0.333	0.280
MH 2(2) pt1	0.587	0.041	0.372
MH 2(2) pt2	0.609	0.026	0.365
MH 2(2) pt3	0.592	0.011	0.397
MH 5B(2) pt1	0.383	0.205	0.412
MH 5B(2) pt2	0.203	0.403	0.394
MH 5B(2) pt3	0.441	0.170	0.389
MH 9B(1) pt1	0.125	0.411	0.464
MH 9B(1) pt2	0.230	0.318	0.452
MH 9B(1) pt3	0.201	0.359	0.440

APPENDIX EMPA CHEMICAL ANALYSIS

Table 4. EMPA Chemical Analysis

EMPA ANALYSIS Sample No.	080603-08 1-1	080603-08 2-1	080603-08 2-2	080603-08 2-3	Average 080603-08 2
SiO_2	44.86	51.54	53.11	55.97	53.54
Al_2O_3	12.03	13.83	13.51	14.36	13.90
Fe_2O_3	1.99	0.37	0.14	0.33	0.28
MgO	1.78	1.14	0.97	1.02	1.04
CaO	2.77	3.80	4.12	3.64	3.85
SrO					
BaO	0.04	-0.05	0.11	0.09	0.05
Na_2O	0.16	0.22	0.17	0.27	0.22
K_2O	2.41	3.25	3.22	3.19	3.22
H_2O	34.17	25.93	24.67	21.16	23.92
Si	26.79	27.29	27.63	27.71	27.54
Al	8.47	8.63	8.29	8.38	8.43
Fe^{3+}	0.90	0.15	0.06	0.12	0.11
Mg	1.58	0.90	0.75	0.75	0.80
Ca	1.78	2.16	2.30	1.93	2.13
Sr	0.00	0.00	0.00	0.00	0.00
Ba	0.01	-0.01	0.02	0.02	0.01
Na	0.18	0.23	0.17	0.26	0.22
K	1.84	2.20	2.14	2.02	2.12
H_2O	68.07	45.79	42.82	34.94	41.18
Alth	8.75	8.52	8.44	7.67	8.21
E%	6.96	3.04	-1.16	10.77	4.21
R	0.76	0.76	0.77	0.77	0.77
M=Na+K	2.02	2.43	2.31	2.27	2.34
D=Ca+Mg+Sr+Ba	3.37	3.05	3.07	2.70	2.94
M/(M+D)	0.38	0.44	0.43	0.46	0.44
Ca/D	0.53	0.71	0.75	0.72	0.72
Na/M	0.09	0.10	0.07	0.11	0.09
SiO_2 wt%	44.86	51.54	53.11	55.97	53.54
Si+Al	35.26	35.92	35.92	36.08	35.97
Mg/(Ca+Na)	0.81	0.38	0.30	0.34	0.34
K+Sr+Ba	1.85	2.19	2.16	2.03	2.13
Ca+Mg	3.36	3.05	3.05	2.68	2.93
Ca+Na	1.96	2.39	2.46	2.19	2.35
Mg	1.58	0.90	0.75	0.75	0.80
sum cat (no H_2O)	41.54	41.54	41.35	41.18	41.36
Ca+K+Na	3.80	4.58	4.60	4.21	4.46
Ca/K	0.97	0.98	1.07	0.96	1.01
Ca/Na	9.77	9.36	13.64	7.46	10.15
K/Na	10.12	9.52	12.69	7.78	10.00
Ca/Mg	1.12	2.40	3.06	2.57	2.68
K/Mg	1.16	2.45	2.85	2.68	2.66
Si+Al [+Fe^{3+}]	36.15	36.06	35.98	36.21	36.08
Na+K	2.02	2.43	2.31	2.27	2.34
Ca+Mg	3.36	3.05	3.05	2.68	2.93

Table 4 continued.

EMPA ANALYSIS cont. Sample No.	080603-08 3-1	080603-08 3-2	Average 080603-08 3	080603-07 1-1	080603-07 1-2	Average 080603-07 1
SiO_2	23.54	63.45	43.49	58.84	64.80	61.82
Al_2O_3	8.40	15.66	12.03	14.70	16.79	15.74
Fe_2O_3	0.05	0.05	0.05	0.21	1.11	0.66
MgO	0.53	0.95	0.74	1.46	1.78	1.62
CaO	2.35	3.35	2.85	3.27	3.92	3.59
SrO						
BaO	0.18	0.13	0.15	0.03	0.02	0.02
Na_2O	0.24	0.22	0.23	0.13	0.20	0.16
K_2O	2.89	4.41	3.65	3.09	2.94	3.02
H_2O	61.83	11.80	36.81	18.30	8.56	13.43
Si	25.13	28.08	26.60	27.93	27.53	27.73
Al	10.57	8.17	9.37	8.22	8.41	8.32
Fe^{3+}	0.04	0.02	0.03	0.08	0.36	0.22
Mg	0.84	0.62	0.73	1.03	1.13	1.08
Ca	2.68	1.59	2.14	1.66	1.79	1.72
Sr	0.00	0.00	0.00	0.00	0.00	0.00
Ba	0.07	0.02	0.05	0.01	0.00	0.00
Na	0.51	0.19	0.35	0.12	0.17	0.14
K	3.93	2.49	3.21	1.87	1.59	1.73
H_2O	220.18	17.41	118.80	28.97	12.12	20.55
Alth	11.65	7.15	9.40	7.39	7.59	7.49
E%	-8.88	14.53	2.83	12.23	15.54	13.89
R	0.70	0.77	0.74	0.77	0.77	0.77
M=Na+K	4.44	2.68	3.56	1.99	1.76	1.87
D=Ca+Mg+Sr+Ba	3.60	2.23	2.92	2.70	2.91	2.81
M/(M+D)	0.55	0.55	0.55	0.42	0.38	0.40
Ca/D	0.75	0.71	0.73	0.62	0.61	0.61
Na/M	0.11	0.07	0.09	0.06	0.09	0.08
SiO_2 wt%	23.54	63.45	43.49	58.84	64.80	61.82
Si+Al	35.70	36.24	35.97	36.15	35.94	36.04
Mg/(Ca+Na)	0.26	0.35	0.31	0.58	0.58	0.58
K+Sr+Ba	4.01	2.51	3.26	1.88	1.60	1.74
Ca+Mg	3.53	2.21	2.87	2.70	2.91	2.80
Ca+Na	3.19	1.78	2.48	1.78	1.95	1.86
Mg	0.84	0.62	0.73	1.03	1.13	1.08
sum cat (no H_2O)	43.78	41.17	42.48	40.92	40.97	40.94
Ca+K+Na	7.12	4.27	5.70	3.65	3.54	3.60
Ca/K	0.68	0.64	0.66	0.89	1.12	1.00
Ca/Na	5.30	8.39	6.85	14.28	10.80	12.54
K/Na	7.77	13.16	10.46	16.10	9.64	12.87
Ca/Mg	3.18	2.55	2.86	1.61	1.59	1.60
K/Mg	4.66	3.99	4.33	1.81	1.42	1.61
Si+Al [+Fe^{3+}]	35.74	36.26	36.00	36.23	36.29	36.26
Na+K	4.44	2.68	3.56	1.99	1.76	1.87
Ca+Mg	3.53	2.21	2.87	2.70	2.91	2.80

Table 4 continued.

EMPA ANALYSIS cont. Sample No.	080603-07 2-1	080603-07 2-2	Average 080603-07 2	080603-07 3-1	080603-07 3-3	Average 080603-07 3
SiO_2	47.82	48.30	48.06	23.98	54.70	39.34
Al_2O_3	11.37	12.68	12.03	9.91	14.31	12.11
Fe_2O_3	0.18	0.16	0.17	6.79	6.53	6.66
MgO	1.33	1.37	1.35	2.94	4.73	3.84
CaO	2.29	2.97	2.63	1.12	1.68	1.40
SrO						
BaO	0.08	0.07	0.07	0.19	-0.01	0.09
Na_2O	0.10	0.09	0.09	0.63	0.14	0.39
K_2O	1.97	2.29	2.13	3.25	2.51	2.88
H_2O	34.87	32.09	33.48	51.87	16.07	33.97
Si	28.27	27.60	27.94	21.18	25.80	23.49
Al	7.93	8.54	8.23	10.32	7.96	9.14
Fe^{3+}	0.08	0.07	0.07	4.52	2.32	3.42
Mg	1.17	1.16	1.17	3.87	3.33	3.60
Ca	1.45	1.82	1.64	1.06	0.85	0.96
Sr	0.00	0.00	0.00	0.00	0.00	0.00
Ba	0.02	0.02	0.02	0.07	0.00	0.03
Na	0.12	0.10	0.11	1.07	0.13	0.60
K	1.49	1.67	1.58	3.66	1.51	2.58
H_2O	68.77	61.16	64.97	152.85	25.29	89.07
Alth	6.89	7.77	7.33	14.74	9.98	12.36
E%	16.27	10.78	13.52	0.67	2.95	1.81
R	0.78	0.76	0.77	0.67	0.76	0.72
M=Na+K	1.60	1.76	1.68	4.73	1.64	3.19
D=Ca+Mg+Sr+Ba	2.64	3.00	2.82	5.00	4.17	4.59
M/(M+D)	0.38	0.37	0.37	0.49	0.28	0.38
Ca/D	0.55	0.61	0.58	0.21	0.20	0.21
Na/M	0.07	0.05	0.06	0.23	0.08	0.15
SiO_2 wt%	47.82	48.30	48.06	23.98	54.70	39.34
Si+Al	36.20	36.14	36.17	31.51	33.76	32.63
Mg/(Ca+Na)	0.75	0.61	0.68	1.81	3.40	2.61
K+Sr+Ba	1.50	1.68	1.59	3.73	1.51	2.62
Ca+Mg	2.62	2.99	2.81	4.94	4.17	4.56
Ca+Na	1.57	1.92	1.74	2.14	0.98	1.56
Mg	1.17	1.16	1.17	3.87	3.33	3.60
sum cat (no H_2O)	40.52	40.98	40.75	45.76	41.88	43.82
Ca+K+Na	3.06	3.59	3.32	5.80	2.49	4.14
Ca/K	0.98	1.09	1.04	0.29	0.56	0.43
Ca/Na	12.40	18.80	15.60	0.99	6.48	3.73
K/Na	12.68	17.22	14.95	3.41	11.54	7.47
Ca/Mg	1.24	1.56	1.40	0.27	0.25	0.26
K/Mg	1.27	1.43	1.35	0.94	0.45	0.70
Si+Al [+Fe^{3+}]	36.28	36.21	36.24	36.02	36.07	36.05
Na+K	1.60	1.76	1.68	4.73	1.64	3.19
Ca+Mg	2.62	2.99	2.81	4.94	4.17	4.56

Table 4 continued.

EMPA ANALYSIS cont. Sample No.	080603-07 4-1	080603-07 4-2	080603-07 4-3	Average 080603-07 4	080604-09 3-1	080604-08 1-1
SiO_2	47.35	54.58	44.24	48.72	64.87	67.52
Al_2O_3	12.62	13.72	12.56	12.97	16.36	17.27
Fe_2O_3	0.22	0.53	0.18	0.31	0.12	0.32
MgO	0.96	1.39	0.90	1.08	0.37	0.77
CaO	3.24	3.86	3.87	3.66	6.00	5.95
SrO						
BaO	-0.07	0.09	0.03	0.02	-0.09	0.09
Na_2O	0.17	0.16	0.17	0.17	0.03	0.03
K_2O	2.74	2.91	2.48	2.71	2.35	2.33
H_2O	32.78	22.81	35.60	30.40	10.01	5.76
Si	27.48	27.62	26.96	27.35	27.92	27.78
Al	8.64	8.18	9.02	8.61	8.30	8.38
Fe^{3+}	0.10	0.20	0.08	0.13	0.04	0.10
Mg	0.83	1.05	0.82	0.90	0.24	0.47
Ca	2.02	2.09	2.53	2.21	2.77	2.62
Sr	0.00	0.00	0.00	0.00	0.00	0.00
Ba	-0.01	0.02	0.01	0.00	-0.02	0.01
Na	0.20	0.16	0.20	0.18	0.02	0.03
K	2.03	1.88	1.93	1.94	1.29	1.22
H_2O	63.46	38.50	72.37	58.11	14.37	7.90
Alth	7.88	8.36	8.83	8.36	7.30	7.47
E%	10.77	0.29	3.06	4.71	14.31	13.51
R	0.76	0.77	0.75	0.76	0.77	0.77
M=Na+K	2.22	2.04	2.12	2.13	1.31	1.25
D=Ca+Mg+Sr+Ba	2.83	3.16	3.36	3.12	2.99	3.11
M/(M+D)	0.44	0.39	0.39	0.41	0.30	0.29
Ca/D	0.71	0.66	0.75	0.71	0.92	0.84
Na/M	0.09	0.08	0.09	0.09	0.02	0.02
SiO_2 wt%	47.35	54.58	44.24	48.72	64.87	67.52
Si+Al	36.11	35.80	35.99	35.97	36.22	36.15
Mg/(Ca+Na)	0.37	0.47	0.30	0.38	0.09	0.18
K+Sr+Ba	2.01	1.90	1.93	1.95	1.27	1.24
Ca+Mg	2.85	3.14	3.35	3.11	3.01	3.10
Ca+Na	2.21	2.25	2.73	2.40	2.79	2.65
Mg	0.83	1.05	0.82	0.90	0.24	0.47
sum cat (no H_2O)	41.27	41.20	41.55	41.34	40.56	40.61
Ca+K+Na	4.24	4.13	4.65	4.34	4.08	3.87
Ca/K	1.00	1.11	1.31	1.14	2.15	2.15
Ca/Na	10.33	13.44	12.87	12.21	119.67	101.45
K/Na	10.38	12.08	9.80	10.75	55.76	47.24
Ca/Mg	2.43	2.00	3.09	2.51	11.50	5.54
K/Mg	2.44	1.79	2.35	2.20	5.36	2.58
Si+Al [+Fe^{3+}]	36.21	36.01	36.07	36.10	36.26	36.25
Na+K	2.22	2.04	2.12	2.13	1.31	1.25
Ca+Mg	2.85	3.14	3.35	3.11	3.01	3.10

Table 4 continued.

EMPA ANALYSIS cont. Sample No.	080604-07 2-1	080603-01 1-1	080603-01 1-2	080603-01 1-3	Average 080603-01 1	080603-01 2-1
SiO_2	62.45	59.23	64.34	53.09	58.89	48.20
Al_2O_3	15.14	11.87	15.13	11.70	12.90	10.98
Fe_2O_3	0.57	0.06	0.09	0.09	0.08	0.21
MgO	0.69	1.38	1.84	0.67	1.29	2.35
CaO	4.57	3.27	3.02	3.12	3.14	2.73
SrO						
BaO	0.02	0.03	0.12	0.04	0.07	0.04
Na_2O	0.05	0.09	0.07	0.18	0.11	0.29
K_2O	3.20	1.92	1.60	4.34	2.62	1.28
H_2O	13.36	22.17	13.81	26.77	20.92	33.94
Si	28.05	29.13	28.49	28.47	28.70	28.08
Al	8.01	6.88	7.89	7.39	7.39	7.54
Fe^{3+}	0.19	0.02	0.03	0.04	0.03	0.09
Mg	0.46	1.01	1.21	0.54	0.92	2.04
Ca	2.20	1.72	1.43	1.80	1.65	1.70
Sr	0.00	0.00	0.00	0.00	0.00	0.00
Ba	0.00	0.01	0.02	0.01	0.01	0.01
Na	0.04	0.08	0.06	0.18	0.11	0.32
K	1.84	1.21	0.90	2.97	1.69	0.95
H_2O	20.02	36.37	20.40	47.88	34.89	65.95
Alth	7.21	6.76	6.29	7.84	6.96	8.79
E%	13.84	2.03	25.95	-5.16	7.61	-13.11
R	0.78	0.81	0.78	0.79	0.80	0.79
M=Na+K	1.88	1.29	0.96	3.15	1.80	1.28
D=Ca+Mg+Sr+Ba	2.66	2.74	2.67	2.34	2.58	3.75
M/(M+D)	0.41	0.32	0.26	0.57	0.39	0.25
Ca/D	0.83	0.63	0.54	0.77	0.64	0.45
Na/M	0.02	0.06	0.06	0.06	0.06	0.25
SiO_2 wt%	62.45	59.23	64.34	53.09	58.89	48.20
Si+Al	36.06	36.01	36.38	35.86	36.08	35.62
Mg/(Ca+Na)	0.21	0.56	0.81	0.27	0.55	1.01
K+Sr+Ba	1.84	1.21	0.92	2.98	1.70	0.96
Ca+Mg	2.66	2.73	2.64	2.33	2.57	3.74
Ca+Na	2.24	1.80	1.49	1.98	1.76	2.03
Mg	0.46	1.01	1.21	0.54	0.92	2.04
sum cat (no H_2O)	40.79	40.06	40.03	41.39	40.50	40.74
Ca+K+Na	4.08	3.01	2.39	4.95	3.45	2.98
Ca/K	1.20	1.43	1.59	0.60	1.21	1.79
Ca/Na	52.60	21.20	24.64	9.84	18.56	5.26
K/Na	43.93	14.85	15.50	16.29	15.55	2.94
Ca/Mg	4.75	1.71	1.18	3.34	2.08	0.84
K/Mg	3.97	1.20	0.74	5.53	2.49	0.47
Si+Al [+Fe^{3+}]	36.25	36.03	36.41	35.90	36.11	35.71
Na+K	1.88	1.29	0.96	3.15	1.80	1.28
Ca+Mg	2.66	2.73	2.64	2.33	2.57	3.74

Table 4 continued.

EMPA ANALYSIS cont. Sample No.	080602-03 1-4	080602-03 2-1	080602-03 2-2	Average 080602-03 2	080604-01 1-2	080604-01 3-2
SiO_2	61.46	60.09	58.96	59.53	45.10	64.51
Al_2O_3	14.93	14.41	14.25	14.33	14.44	16.24
Fe_2O_3	0.24	0.22	0.37	0.29	0.17	0.03
MgO	2.52	2.68	2.54	2.61	1.95	1.99
CaO	3.08	3.51	3.18	3.35	2.92	3.42
SrO						
BaO	0.03	-0.01	0.05	0.02	0.01	0.07
Na_2O	0.02	0.08	0.02	0.05	0.08	0.05
K_2O	1.57	1.16	1.45	1.30	2.35	2.79
H_2O	16.17	17.87	19.22	18.55	32.99	10.92
Si	28.06	28.01	27.98	27.99	26.29	27.94
Al	8.04	7.92	7.97	7.95	9.92	8.29
Fe^{3+}	0.08	0.08	0.13	0.10	0.07	0.01
Mg	1.72	1.86	1.80	1.83	1.70	1.28
Ca	1.51	1.75	1.62	1.69	1.82	1.59
Sr	0.00	0.00	0.00	0.00	0.00	0.00
Ba	0.01	0.00	0.01	0.00	0.00	0.01
Na	0.02	0.08	0.02	0.05	0.09	0.04
K	0.92	0.69	0.88	0.78	1.75	1.54
H_2O	24.62	27.79	30.42	29.11	64.14	15.78
Alth	7.40	8.00	7.75	7.87	8.89	7.34
E%	9.71	-0.03	4.63	2.30	12.40	13.01
R	0.78	0.78	0.78	0.78	0.73	0.77
M=Na+K	0.94	0.76	0.90	0.83	1.84	1.58
D=Ca+Mg+Sr+Ba	3.23	3.62	3.42	3.52	3.53	2.88
M/(M+D)	0.23	0.17	0.21	0.19	0.34	0.35
Ca/D	0.47	0.49	0.47	0.48	0.52	0.55
Na/M	0.02	0.10	0.02	0.06	0.05	0.02
SiO_2 wt%	61.46	60.09	58.96	59.53	45.10	64.51
Si+Al	36.10	35.92	35.96	35.94	36.20	36.23
Mg/(Ca+Na)	1.12	1.02	1.10	1.06	0.89	0.79
K+Sr+Ba	0.92	0.69	0.89	0.79	1.75	1.55
Ca+Mg	3.22	3.62	3.42	3.52	3.52	2.87
Ca+Na	1.53	1.83	1.64	1.73	1.91	1.62
Mg	1.72	1.86	1.80	1.83	1.70	1.28
sum cat (no H_2O)	40.35	40.38	40.41	40.40	41.64	40.70
Ca+K+Na	2.44	2.52	2.51	2.52	3.66	3.16
Ca/K	1.64	2.55	1.85	2.20	1.04	1.03
Ca/Na	69.70	23.12	78.83	50.98	20.59	41.76
K/Na	42.46	9.07	42.70	25.88	19.74	40.59
Ca/Mg	0.88	0.94	0.90	0.92	1.07	1.23
K/Mg	0.53	0.37	0.49	0.43	1.03	1.20
Si+Al [+Fe^{3+}]	36.18	36.00	36.09	36.04	36.28	36.24
Na+K	0.94	0.76	0.90	0.83	1.84	1.58
Ca+Mg	3.22	3.62	3.42	3.52	3.52	2.87

APPENDIX TERNARY EMPA CHEMICAL DATA

Table 5. Ternary EMPA Chemical Data

Zeolite Composition

SAMPLE #	Mg	K+Sr+Ba	Na+Ca
080603-08 1-1	0.293	0.343	0.363
080603-08 2	0.152	0.403	0.445
080603-08 3	0.113	0.503	0.383
080603-07 1	0.231	0.371	0.398
080603-07 2	0.259	0.354	0.387
080603-07 3	0.463	0.336	0.200
080603-07 4	0.171	0.372	0.457
080604-09 3-1	0.056	0.296	0.648
080604-08 1-1	0.109	0.284	0.608
080604-07 2-1	0.102	0.405	0.493
080603-01 1	0.210	0.389	0.401
080603-01 2-1	0.405	0.191	0.403
080602-03 1-4	0.412	0.221	0.366
080602-03 2	0.421	0.181	0.399
080604-01 1-2	0.317	0.327	0.357
080604-01 3-2	0.288	0.348	0.364

APPENDIX SEM/EDS VISUAL AND CHEMICAL FIBER ANALYSIS

KILLDEER MOUNTAINS

Table 6. SEMS/EDS Visual and Chemical Fiber Analysis Killdeer Mountains

Sample ID jwt	NDSU SEM ID #	Sample Site	SEM - Visual	Weight % %Na	% Mg	% Al	% Si	% K	% Ca	% Fe	%O
080602-01*	091798	SKDM	~50% or more fibers, 25-100+ µm	na	1.15	13.02	62.77	13.10	9.96	na	na
080602-02*	091799	SKDM	~ 50% fibers, most < 100 µm	na	1.19	15.11	66.48	9.95	7.26	na	na
080602-03	092238	SKDM	Few/Scattered fibers	na	1.63	9.05	37.16	3.91	3.95	na	44.3
080603-01	092239	SKDM	~50% or more fibers, 25-100+ µm	0.36	0.83	8.89	34.43	4.52	2.41	na	48.57
080603-02	092240	SKDM	~50% or more fibers, 25-100+ µm	na	0.52	9.05	36.99	4.49	4.27	na	44.68
080603-03	091800	SKDM	~ 50% fibers, most < 100 µm	1.50	1.16	15.21	67.48	9.75	4.91	na	na
080603-04	092241	SKDM	< 10 % fibers, most very small	0.42	0.92	9.19	37.50	5.68	3.46	na	42.83
080603-05	092242	SKDM	~50% or more fibers, 25-100+ µm	0.41	0.87	9.56	43.74	9.39	5.58	na	30.45
080603-06	091801	SKDM	~ 50% fibers, most < 100 µm	na	1.27	14.99	65.33	8.32	7.03	3.05	na
080603-07*	092243	SKDM	10% fibers, most very small	na	0.75	9.50	38.53	5.62	3.62	0.76	41.24
080603-08	091802	SKDM	< 40% fibers, majority < 100 µm	0.63	0.96	15.16	64.99	11.38	6.89	na	na
080603-09	092244	SKDM	no fibers								
080603-10	092245	SKDM	no fibers								
080603-11	092246	SKDM	no fibers								
080604-01	091803	NKDM(wqe)	~ 30% fibers, most < 100 µm	0.78	1.45	15.53	67.04	9.66	5.55	na	na
080604-02	092247	NKDM(wqe)	no fibers								
080604-03	091804	NKDM(wqe)	< 10 % fibers, most very small	na	5.20	15.86	58.71	8.79	1.75	9.70	na
080604-04	092248	NKDM(wqe)	no fibers								
080604-05	092249	NKDM(wqe)	no fibers								
080604-06	092250	NKDM(wqe)	very few fibers	na	1.16	8.02	31.55	5.00	3.02	na	51.25
080604-07	091805	NKDM(eqe)	~50% or more fibers, 25-100+ µm	na	0.38	15.20	66.54	8.98	8.91	na	na
080604-08	092251	NKDM(eqe)	10% fibers, most very small	na	na	9.38	39.88	4.92	7.16	na	38.67
080604-09	092252	NKDM(eqe)	bad fiber analyzed (organic)								

APPENDIX EDS/EMPA INDIVIDUAL FIBER ANALYSIS AND COMPARISON

Table 7. EDS/EMPA Individual Fiber Analysis and Comparison

	EMPA	EMPA	EMPA average
Sample No.	080603-08 1-1	080603-08 1-2	080603-08 1
Si	64.495	61.489	62.992
Al	20.381	26.249	23.315
Fe^{3+}	2.156	0.020	1.088
Mg	3.805	2.114	2.960
Ca	4.275	4.810	4.542
Sr	0.000	0.000	0.000
Ba	0.022	0.100	0.061
Na	0.437	0.427	0.432
K	4.427	4.790	4.609
	EDS 8/19/10	EDS 8/19/10	EDS Average
Sample No.	080603-08 1-1	080603-08 1-2	080603-08 1
Si	67.87	68.81	68.34
Al	15.18	15.36	15.27
Fe^{3+}	0.00	0.00	0.00
Mg	0.80	0.79	0.80
Ca	7.30	7.03	7.17
Sr	0.00	0.00	0.00
Ba	0.00	0.00	0.00
Na	0.60	0.00	0.30
K	7.91	8.01	7.96

	EMPA	EMPA	EMPA	EMPA average
Sample No.	080603-08 2-1	080603-08 2-2	080603-08 2-3	080603-08 2
Si	65.699	66.823	67.278	66.600
Al	20.772	20.044	20.343	20.386
Fe^{3+}	0.355	0.136	0.300	0.264
Mg	2.161	1.813	1.823	1.933
Ca	5.194	5.554	4.692	5.146
Sr	0.000	0.000	0.000	0.000
Ba	-0.023	0.053	0.041	0.024
Na	0.555	0.407	0.629	0.531
K	5.287	5.170	4.895	5.117
	EDS 8/19/10	EDS 8/19/10	EDS 8/19/10	EDS Average
Sample No.	080603-08 2-1	080603-08 2-2	080603-08 2-3	080603-08 2
Si	70.39	67.93	na	67.93
Al	15.31	15.48	na	15.48
Fe^{3+}	0.00	0.00	na	0.00
Mg	0.83	0.00	na	0.00
Ca	7.30	7.66	na	7.66
Sr	0.00	0.00	na	0.00
Ba	0.00	0.00	na	0.00
Na	0.00	0.00	na	0.00
K	6.17	6.92	na	6.92

Table 7 continued.

	EMPA	EMPA	EMPA average
Sample No.	080603-08 3-1	080603-08 3-2	080603-08 3
Si	57.392	68.192	62.79
Al	24.139	19.833	21.99
Fe^{3+}	0.099	0.043	0.07
Mg	1.928	1.515	1.72
Ca	6.131	3.857	4.99
Sr	0.000	0.000	0.00
Ba	0.170	0.053	0.11
Na	1.157	0.460	0.81
K	8.984	6.048	7.52
	EDS 8/19/10	EDS 8/19/10	EDS Average
Sample No.	080603-08 3-1	080603-08 3-2	080603-08 3
Si	68.92	69.39	69.16
Al	15.24	14.73	14.99
Fe^{3+}	0.00	0.00	0.00
Mg	0.73	0.86	0.80
Ca	7.04	6.48	6.76
Sr	0.00	0.00	0.00
Ba	0.00	0.00	0.00
Na	0.00	0.37	0.19
K	8.06	8.17	8.12

	EMPA	EMPA	EMPA	EMPA	EMPA average
Sample No.	080603-08 4-1	080603-08 4-2	080603-08 4-3	080603-08 4-4	080603-08 4
Si	68.287	67.481	68.05	68.94	68.19
Al	20.035	20.927	21.08	20.86	20.73
Fe^{3+}	0.274	0.277	0.25	0.04	0.21
Mg	1.629	1.614	1.58	1.53	1.59
Ca	4.266	4.351	4.30	4.47	4.35
Sr	0.000	0.000	0.00	0.00	0.00
Ba	-0.031	0.021	-0.03	0.06	0.00
Na	0.337	0.263	0.37	0.35	0.33
K	5.203	5.066	4.40	3.75	4.61
	EDS 8-19-10	EDS 8-19-10	EDS 8-19-10	EDS 8-19-10	EDS Average
Sample No.	080603-08 4-1	080603-08 4-2	080603-08 4-3	080603-08 4-4	080603-08 4
Si	68.190	70.150	na	na	69.170
Al	15.020	15.610	na	na	15.315
Fe^{3+}	0.000	0.000	na	na	0.000
Mg	0.760	0.770	na	na	0.765
Ca	7.390	7.140	na	na	7.265
Sr	0.000	0.000	na	na	0.000
Ba	0.000	0.000	na	na	0.000
Na	0.000	0.000	na	na	0.000
K	8.640	6.330	na	na	7.485

Table 7 continued.

	EMPA	EMPA	EMPA	EMPA average
Sample No.	080603-01 1-1	080603-01 1-2	080603-01 1-3	080603-01 1
Si	72.72	71.15	68.77	70.88
Al	17.17	19.72	17.86	18.25
Fe^{3+}	0.05	0.07	0.09	0.07
Mg	2.52	3.03	1.30	2.28
Ca	4.30	3.58	4.34	4.07
Sr	0.00	0.00	0.00	0.00
Ba	0.02	0.05	0.02	0.03
Na	0.20	0.15	0.44	0.26
K	3.01	2.25	7.18	4.15
	EDS 8-19-10	EDS 8-19-10	EDS 8-19-10	EDS Average
Sample No.	080603-01 1-1	080603-01 1-2	080603-01 1-3	080603-01 1
Si	61.46	64.88	na	63.17
Al	13.82	14.90	na	14.36
Fe^{3+}	1.84	0.00	na	0.92
Mg	1.24	1.29	na	1.27
Ca	5.61	7.14	na	6.38
Sr	0.00	0.00	na	0.00
Ba	0.00	0.00	na	0.00
Na	0.92	0.65	na	0.79
K	15.10	13.06	na	14.08

	EMPA	EMPA	EMPA
Sample No.	080604-01 2-1	080604-01 2-2	080604-01 2-3
Si	69.19	70.54	70.20
Al	20.56	20.35	21.42
Fe^{3+}	0.11	0.06	0.06
Mg	2.84	1.60	1.51
Ca	4.00	4.09	3.86
Sr	0.00	0.00	0.00
Ba	0.00	-0.01	0.05
Na	0.24	0.14	0.06
K	3.08	3.24	2.84
	EDS 8-19-10	EDS 8-19-10	EDS 8-19-10
Sample No.	080604-01 2-1	080604-01 2-2	080604-01 2-3
Si	69.94	69.16	na
Al	15.27	15.35	na
Fe^{3+}	0.00	0.46	na
Mg	1.08	1.14	na
Ca	5.82	5.82	na
Sr	0.00	0.00	na
Ba	0.00	0.00	na
Na	0.00	0.43	na
K	7.89	8.09	na

Table 7 continued.

	EMPA average	EMPA	EMPA	EMPA average
Sample No.	080604-01 2	080604-01 3-1	080604-01 3-2	080604-01 3
Si	69.97	69.00	68.65	68.94
Al	20.77	20.41	20.37	18.71
Fe^{3+}	0.07	0.06	0.02	0.04
Mg	1.98	2.99	3.16	2.43
Ca	3.98	3.74	3.90	4.49
Sr	0.00	0.00	0.00	0.00
Ba	0.01	0.03	0.03	0.02
Na	0.15	0.11	0.09	0.21
K	3.05	3.65	3.79	5.18
	EDS Average	EDS 8-19-10	EDS 8-19-10	EDS Average
Sample No.	080604-01 2	080604-01 3-1	080604-01 3-2	080604-01 3
Si	69.55	69.41	68.21	68.81
Al	15.31	15.61	15.00	15.31
Fe^{3+}	0.23	0.00	0.12	0.06
Mg	1.11	1.16	0.99	1.08
Ca	5.82	4.95	6.37	5.66
Sr	0.00	0.00	0.00	0.00
Ba	0.00	0.00	0.00	0.00
Na	0.22	0.00	0.00	0.00
K	7.99	8.86	9.43	9.15

	EMPA	EMPA	EMPA	EMPA	EMPA average
Sample No.	080604-01 4-1	080604-01 4-2	080604-01 4-3	080604-01 4-4	080604-01 4
Si	70.68	70.05	69.20	69.76	69.92
Al	20.79	21.01	21.27	21.31	21.10
Fe^{3+}	0.05	0.06	0.02	0.17	0.07
Mg	3.42	2.75	2.43	2.07	2.67
Ca	3.14	3.15	3.67	3.39	3.34
Sr	0.00	0.00	0.00	0.00	0.00
Ba	0.03	0.06	0.02	0.01	0.03
Na	0.41	0.29	0.22	0.09	0.25
K	1.48	2.63	3.17	3.19	2.62
	EDS 8-19-10	EDS 8-19-10	EDS 8-19-10	EDS 8-19-10	EDS Average
Sample No.	080604-01 4-1	080604-01 4-2	080604-01 4-3	080604-01 4-4	080604-01 4
Si	67.82	68.69	69.98	na	68.83
Al	15.04	15.04	15.34	na	15.14
Fe^{3+}	0.00	0.00	0.00	na	0.00
Mg	1.22	0.96	1.35	na	1.18
Ca	6.24	7.56	6.44	na	6.75
Sr	0.00	0.00	0.00	na	0.00
Ba	0.00	0.00	0.00	na	0.00
Na	0.23	0.00	0.00	na	0.08
K	9.45	6.89	6.89	na	7.74

APPENDIX EMPA POINT DATA

Table 8. EMPA Point Data

No.	Na_2O	SiO_2	CaO	FeO	MgO	Al_2O_3	K_2O	BaO	H_2O	Total	Comment
1	2.715	40.617	10.486	11.194	12.763	15.036	2.208	0.093	4.889	100.000	hbld019 pnt 1
2	2.740	40.768	10.551	11.100	12.947	15.112	2.254	0.098	4.430	100.000	hbld019 pnt 2
3	2.922	40.766	10.438	11.059	12.958	14.770	2.219	0.120	4.750	100.000	hbld019 pnt 3
4	2.803	40.929	10.176	11.127	12.979	15.012	2.203	0.151	4.621	100.000	hbld019 pnt 4
5	2.845	41.629	10.085	10.657	13.001	15.256	2.192	0.018	4.318	100.000	hbld019 pnt 4
6	2.865	40.876	10.125	11.297	12.997	15.338	2.159	0.098	4.245	100.000	hbld019 pnt 5
7	2.863	40.925	10.487	10.954	13.223	15.122	2.328	0.101	3.997	100.000	hbld019 pnt 6
8	2.930	40.829	10.277	11.259	13.081	15.454	2.211	-0.042	4.001	100.000	hbld019 pnt 7
9	0.157	44.855	2.775	1.794	1.775	12.026	2.413	0.040	34.166	100.000	080603-08 1-1
10	0.101	28.179	2.057	0.011	0.650	10.206	1.721	0.117	56.959	100.000	080603-08 1-2
11	0.225	51.543	3.803	0.333	1.137	13.826	3.251	-0.047	25.929	100.000	080603-08 2-1
12	0.167	53.105	4.119	0.130	0.967	13.514	3.220	0.108	24.671	100.000	080603-08 2-2
13	0.270	55.971	3.643	0.299	1.018	14.358	3.192	0.086	21.164	100.000	080603-08 2-3
14	0.245	23.537	2.347	0.049	0.530	8.399	2.888	0.178	61.828	100.000	080603-08 3-1
15	0.221	63.449	3.349	0.048	0.945	15.656	4.410	0.126	11.797	100.000	080603-08 3-2
16	0.432	0.451	3.857	0.018	1.244	0.077	3.710	-0.005	90.217	100.000	080603-08 3-3
17	0.162	63.469	3.700	0.304	1.016	15.799	3.790	-0.073	11.833	100.000	080603-08 4-1
18	0.135	67.020	4.033	0.329	1.075	17.633	3.943	0.054	5.779	100.000	080603-08 4-2
19	0.192	68.066	4.016	0.297	1.058	17.889	3.452	-0.086	5.116	100.000	080603-08 4-3
20	0.167	63.204	3.827	0.043	0.940	16.226	2.694	0.131	12.769	100.000	080603-08 4-4
21	0.127	58.837	3.268	0.191	1.461	14.696	3.095	0.027	18.299	100.000	080603-07 1-1
22	0.201	64.797	3.921	1.000	1.777	16.792	2.939	0.017	8.556	100.000	080603-07 1-2
23	0.102	47.821	2.294	0.165	1.329	11.373	1.969	0.075	34.872	100.000	080603-07 2-1
24	0.087	48.304	2.973	0.141	1.367	12.678	2.288	0.074	32.088	100.000	080603-07 2-2
25	0.627	23.977	1.123	6.116	2.941	9.913	3.247	0.190	51.867	100.000	080603-07 3-1
26	0.504	5.931	1.788	7.279	5.816	1.646	4.674	0.021	72.342	100.000	080603-07 3-2
27	0.143	54.696	1.676	5.877	4.730	14.312	2.507	-0.015	16.075	100.000	080603-07 3-3
28	0.174	47.349	3.243	0.201	0.958	12.624	2.737	-0.066	32.780	100.000	080603-07 4-1
29	0.159	54.582	3.862	0.479	1.390	13.716	2.915	0.092	22.806	100.000	080603-07 4-2
30	0.166	44.236	3.875	0.161	0.901	12.560	2.477	0.026	35.599	100.000	080603-07 4-3
31	1.117	34.882	1.357	4.023	3.372	9.050	3.089	0.072	43.039	100.000	080604-09 1-1
32	1.541	36.044	1.185	3.302	2.563	9.022	3.251	0.103	42.990	100.000	080604-09 1-2
33	1.181	26.543	1.470	4.674	3.776	7.098	3.291	0.113	51.855	100.000	080604-09 1-3
34	1.309	28.742	0.990	3.236	1.889	8.823	3.413	-0.075	51.673	100.000	080604-09 1-4
35	0.166	29.365	4.619	0.852	0.681	11.149	2.327	-0.101	50.942	100.000	080604-09 2-1
36	0.047	30.686	4.559	0.634	0.464	11.604	2.667	-0.051	49.390	100.000	080604-09 2-2
37	0.069	66.571	5.168	0.049	0.411	17.088	2.391	0.085	8.169	100.000	080604-09 2-3
38	0.028	64.868	5.998	0.106	0.375	16.362	2.347	-0.092	10.009	100.000	080604-09 3-1
39	0.021	66.861	5.055	0.066	0.439	17.226	1.864	0.040	8.428	100.000	080604-09 3-2
40	0.032	67.517	5.948	0.287	0.771	17.271	2.326	0.089	5.758	100.000	080604-08 1-1
41	0.015	67.064	5.484	0.056	0.564	17.520	2.510	0.007	6.780	100.000	080604-08 1-2
42	0.034	67.717	5.564	0.047	0.505	16.830	2.382	0.110	6.812	100.000	080604-08 1-3
43	0.039	70.858	5.709	0.216	0.490	18.971	1.898	0.105	1.716	100.000	080604-08 2-1
44	0.060	71.805	4.859	0.100	0.490	17.936	2.025	0.001	2.724	100.000	080604-08 2-2
45	0.044	71.969	5.383	0.104	0.372	19.028	2.058	0.016	1.026	100.000	080604-08 2-3
46	0.037	74.037	5.327	0.043	0.327	18.842	1.811	0.135	0.000	100.557	080604-07 1-1
47	0.071	72.717	5.518	0.073	0.294	18.824	2.287	0.173	0.043	100.000	080604-07 1-2
48	0.048	62.455	4.569	0.509	0.691	15.140	3.204	0.020	13.365	100.000	080604-07 2-1
49	0.057	70.520	4.573	0.181	0.586	18.329	1.860	-0.081	3.976	100.000	080604-07 2-2
50	0.119	72.882	5.054	0.233	0.501	19.244	2.085	0.058	0.000	100.174	080604-07 3-1
51	0.107	68.640	5.311	0.143	0.399	17.691	1.992	0.085	5.633	100.000	080604-07 3-2
52	0.260	21.744	4.179	0.525	0.626	7.501	1.892	0.265	63.006	100.000	080604-07 4-1
53	0.093	61.604	4.293	0.105	0.920	15.437	1.801	-0.066	15.814	100.000	080603-06 1-1
54	0.060	68.311	5.592	0.031	0.903	17.703	1.498	0.045	5.856	100.000	080603-06 1-2
55	0.077	67.693	4.880	0.064	1.187	16.916	2.053	-0.095	7.225	100.000	080603-06 1-3
56	0.382	73.041	1.746	0.081	1.017	18.335	3.215	-0.100	2.283	100.000	080603-06 2-1
57	0.521	70.978	1.975	0.102	1.211	18.292	3.536	0.152	3.233	100.000	080603-06 2-2
58	0.240	58.326	1.070	0.063	0.656	12.994	2.991	-0.068	23.728	100.000	080603-06 2-3

Table 8 continued.

No.	Na_2O	SiO_2	CaO	FeO	MgO	Al_2O_3	K_2O	BaO	H_2O	Total	Comment
1	0.085	59.228	3.269	0.051	1.375	11.867	1.923	0.034	22.169	100.000	080603-01 1-1
2	0.068	64.339	3.018	0.081	1.837	15.126	1.595	0.122	13.814	100.000	080603-01 1-2
3	0.175	53.091	3.125	0.082	0.672	11.700	4.342	0.042	26.772	100.000	080603-01 1-3
4	0.287	48.197	2.731	0.189	2.348	10.983	1.282	0.045	33.940	100.000	080603-01 2-1
5	0.085	66.803	3.246	0.164	0.835	14.524	1.613	-0.055	12.784	100.000	080603-01 2-2
6	0.053	66.853	3.290	0.178	0.897	15.480	1.613	0.041	11.594	100.000	080603-01 2-3
7	0.035	66.253	3.186	0.095	0.903	15.284	1.778	0.068	12.397	100.000	080603-01 2-4
8	0.067	66.701	3.199	0.163	0.989	14.853	1.498	0.057	12.473	100.000	080603-01 2-5
9	0.068	65.246	3.178	0.148	0.909	16.648	1.924	0.013	11.867	100.000	080603-01 2-6
10	0.218	69.500	3.222	0.196	1.704	17.773	2.308	0.011	5.069	100.000	080602-03 1-1
11	0.150	68.440	3.273	0.156	1.707	17.648	2.111	-0.029	6.543	100.000	080602-03 1-2
12	0.278	68.747	3.258	0.053	1.619	17.520	2.498	0.032	5.996	100.000	080602-03 1-3
13	0.024	61.455	3.078	0.216	2.524	14.930	1.574	0.034	16.165	100.000	080602-03 1-4
14	0.084	60.091	3.514	0.196	2.682	14.414	1.158	-0.014	17.875	100.000	080602-03 2-1
15	0.022	58.959	3.181	0.334	2.541	14.251	1.447	0.047	19.218	100.000	080602-03 2-2
16	0.083	57.405	4.219	0.259	3.057	14.316	1.392	0.160	19.110	100.000	080602-03 3-1
17	0.053	56.138	2.814	0.046	1.363	17.752	2.347	-0.058	19.546	100.000	080604-01 1-1
18	0.078	45.104	2.922	0.151	1.954	14.436	2.352	0.011	32.994	100.000	080604-01 1-2
19	0.113	63.304	3.411	0.116	1.741	15.957	2.206	-0.004	13.157	100.000	080604-01 2-1
20	0.069	65.948	3.569	0.062	1.006	16.139	2.372	-0.033	10.868	100.000	080604-01 2-2
21	0.032	68.380	3.505	0.072	0.989	17.700	2.170	0.129	7.024	100.000	080604-01 2-3
22	0.055	66.128	3.349	0.069	1.921	16.592	2.744	0.072	9.070	100.000	080604-01 3-1
23	0.045	64.506	3.416	0.027	1.989	16.235	2.788	0.073	10.921	100.000	080604-01 3-2
24	0.207	69.835	2.899	0.059	2.264	17.432	1.145	0.085	6.075	100.000	080604-01 4-1
25	0.154	71.434	2.997	0.077	1.883	18.175	2.105	0.147	3.029	100.000	080604-01 4-2
26	0.115	70.841	3.509	0.018	1.667	18.472	2.545	0.050	2.782	100.000	080604-01 4-3
27	0.047	70.297	3.190	0.203	1.400	18.218	2.523	0.027	4.096	100.000	080604-01 4-4

APPENDIX SAMPLE STUB BINOCULAR MICROSCOPE IMAGES

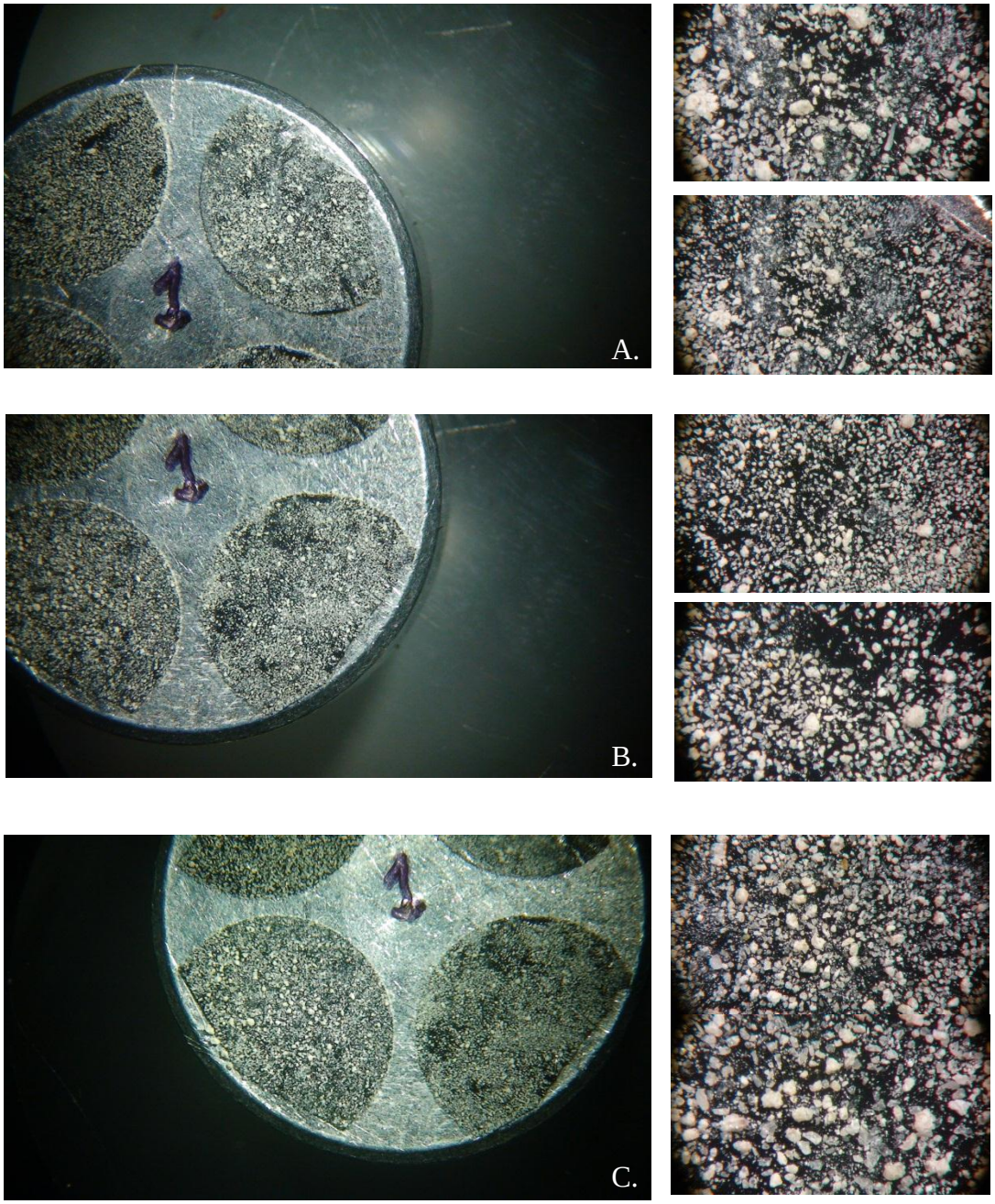

Figure 1. A) jwt080602-01, B) jwt080602-02, C) jwt080602-03

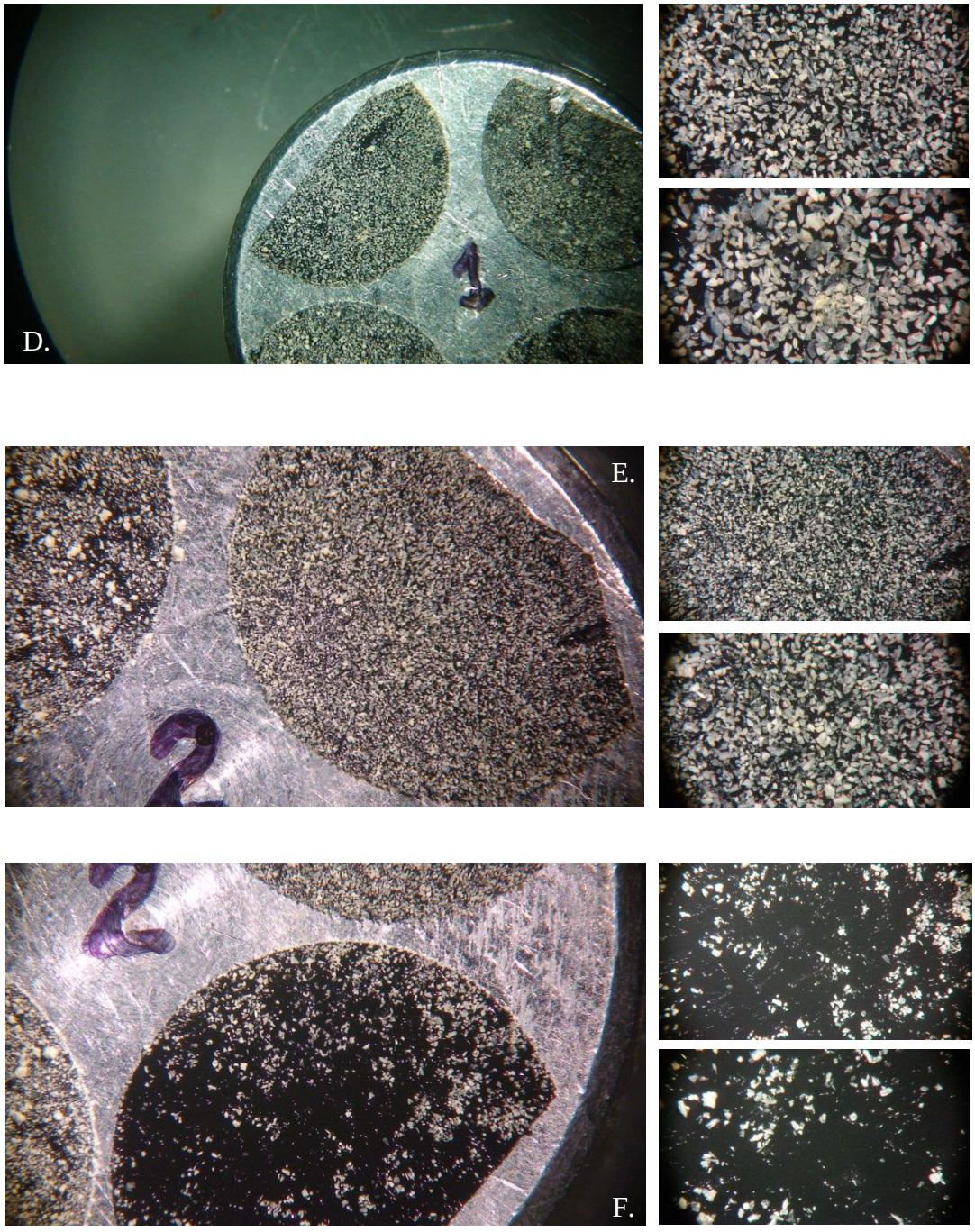

Figure 1 continued. D) jwt080603-01, E) jwt080603-02, F) jwt080603-03

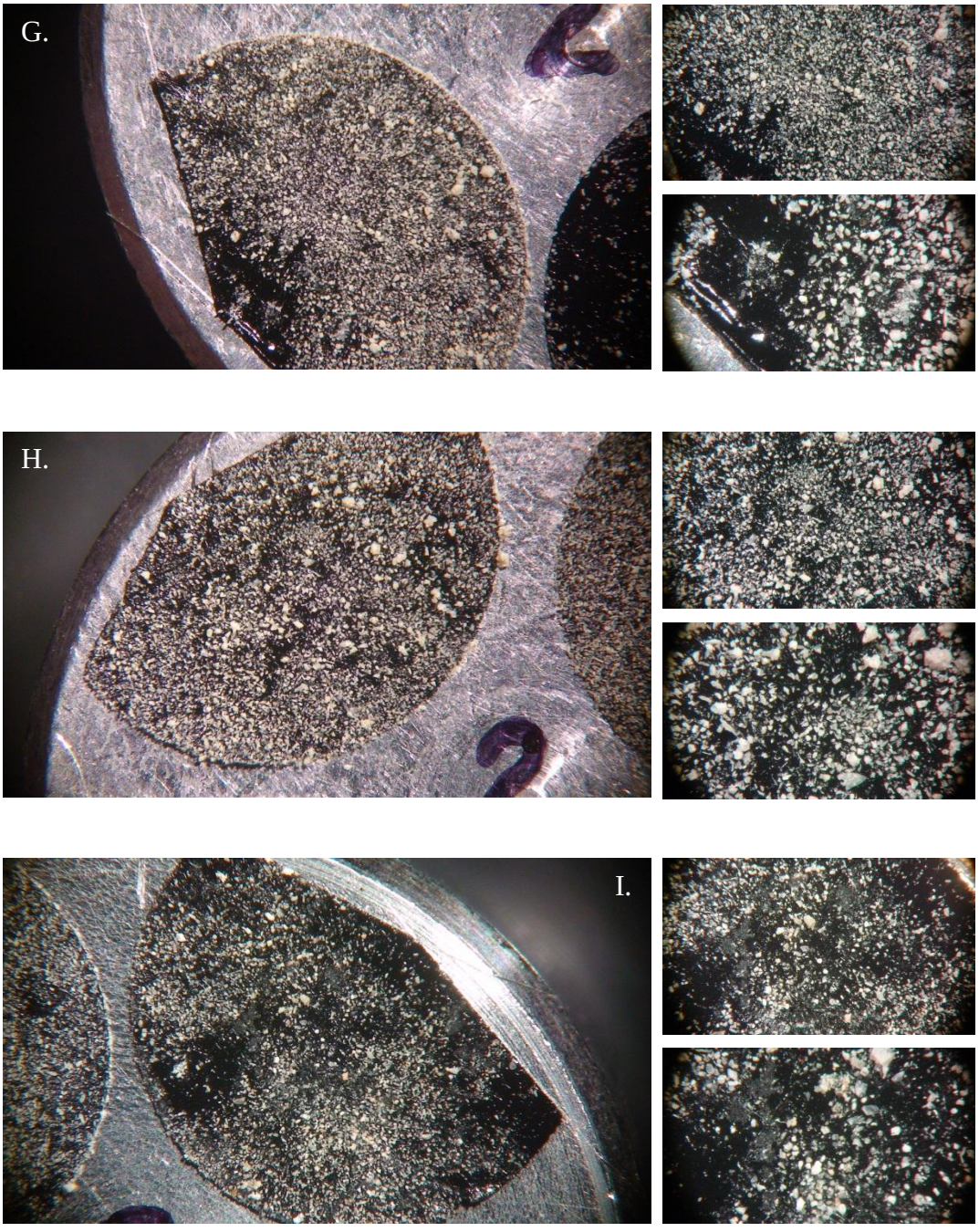

Figure 1 continued. G) jwt080603-04, H) jwt080603-05, I) jwt080603-06

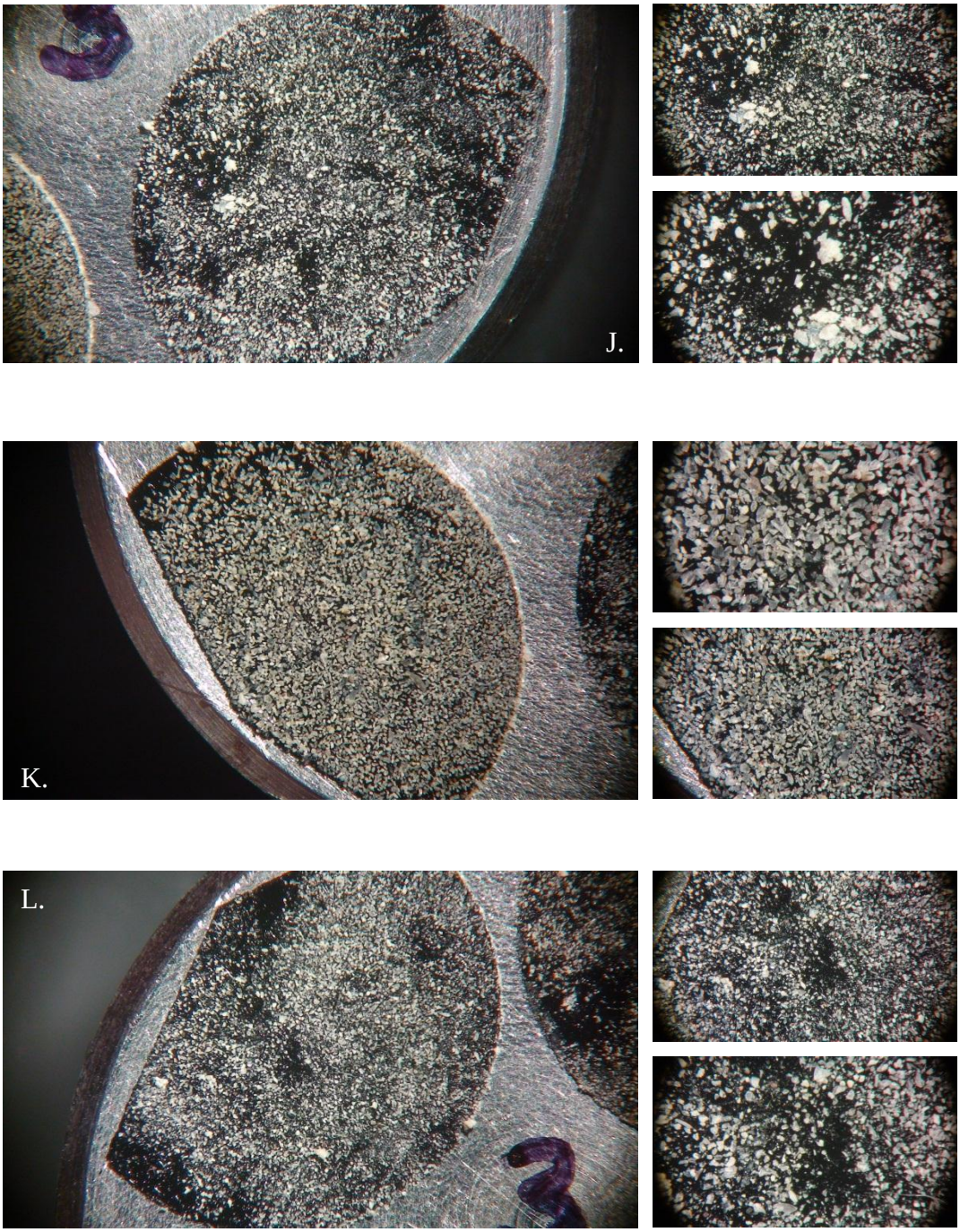

Figure 1 continued. J) jwt080603-07, K) jwt080603-08, L) jwt080604-01

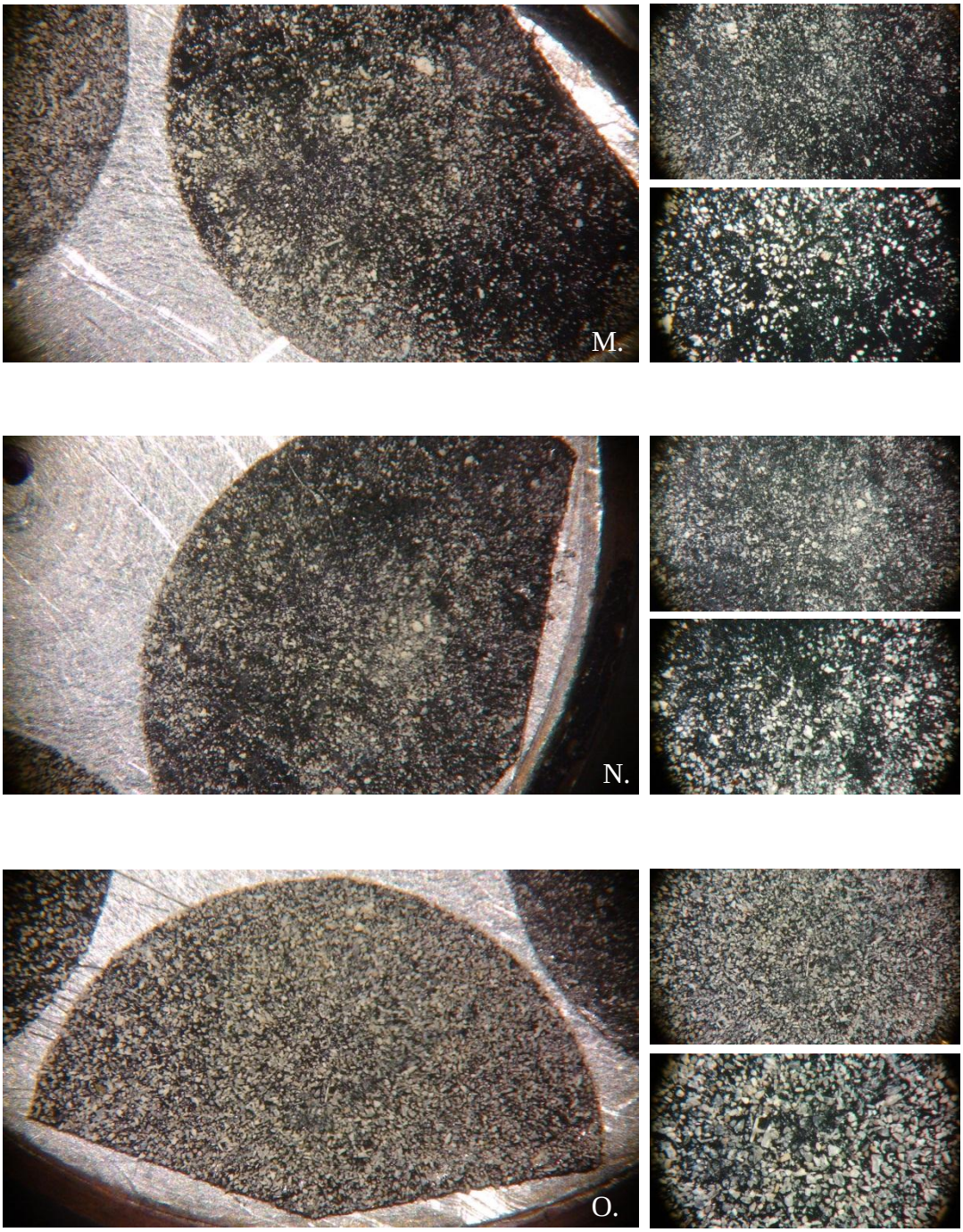

Figure 1 continued. M) jwt080604-03, N) jwt080604-06, O) jwt080604-07

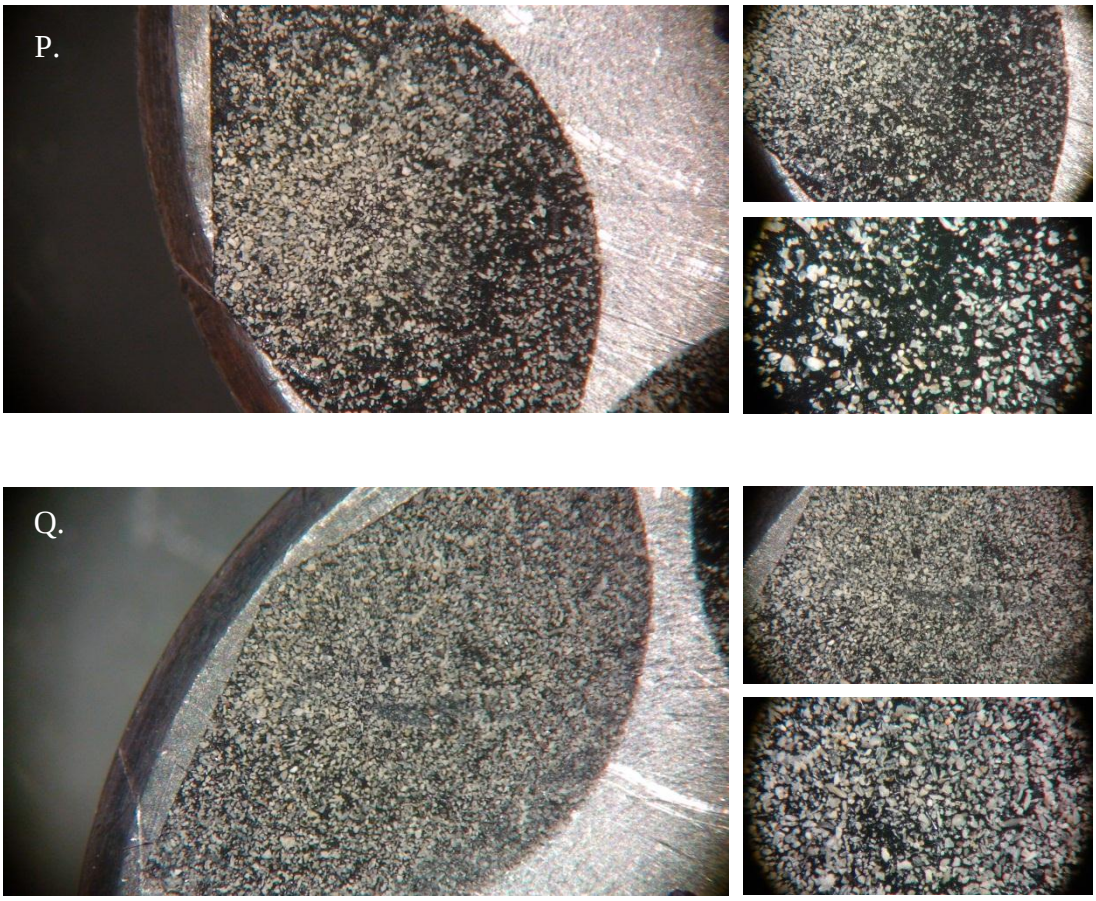

Figure 1 continued. P) jwt080604-08 & Q) jwt080604-09

APPENDIX EMPA FIBER SCANS

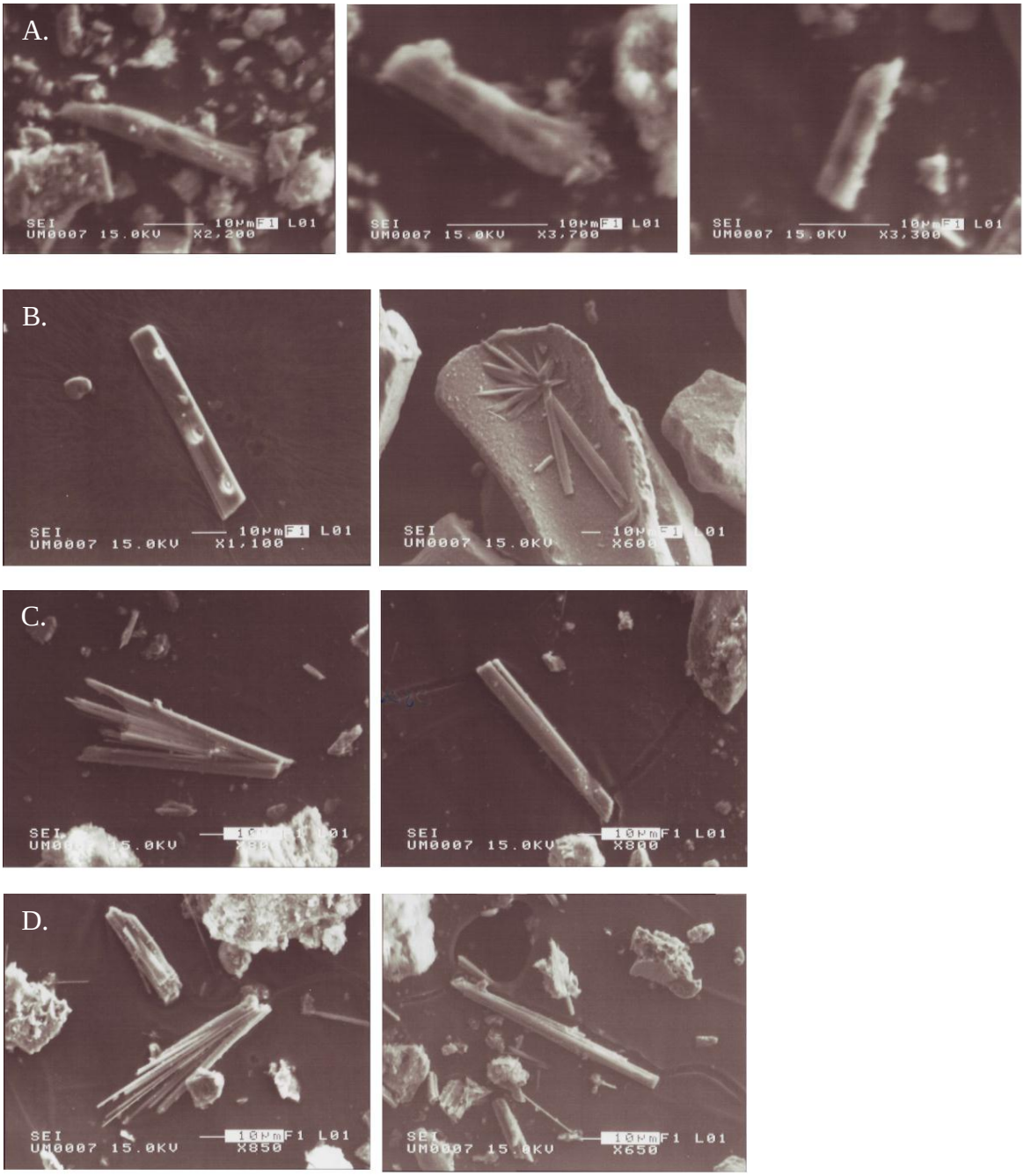

Figure 2. A) jwt080602-03, Fibers 1-3, B) jwt080603-01 (Second fiber not scanned), C) jwt080603-06, fibers 1 & 2, D)jwt080603-07, fibers 1-3

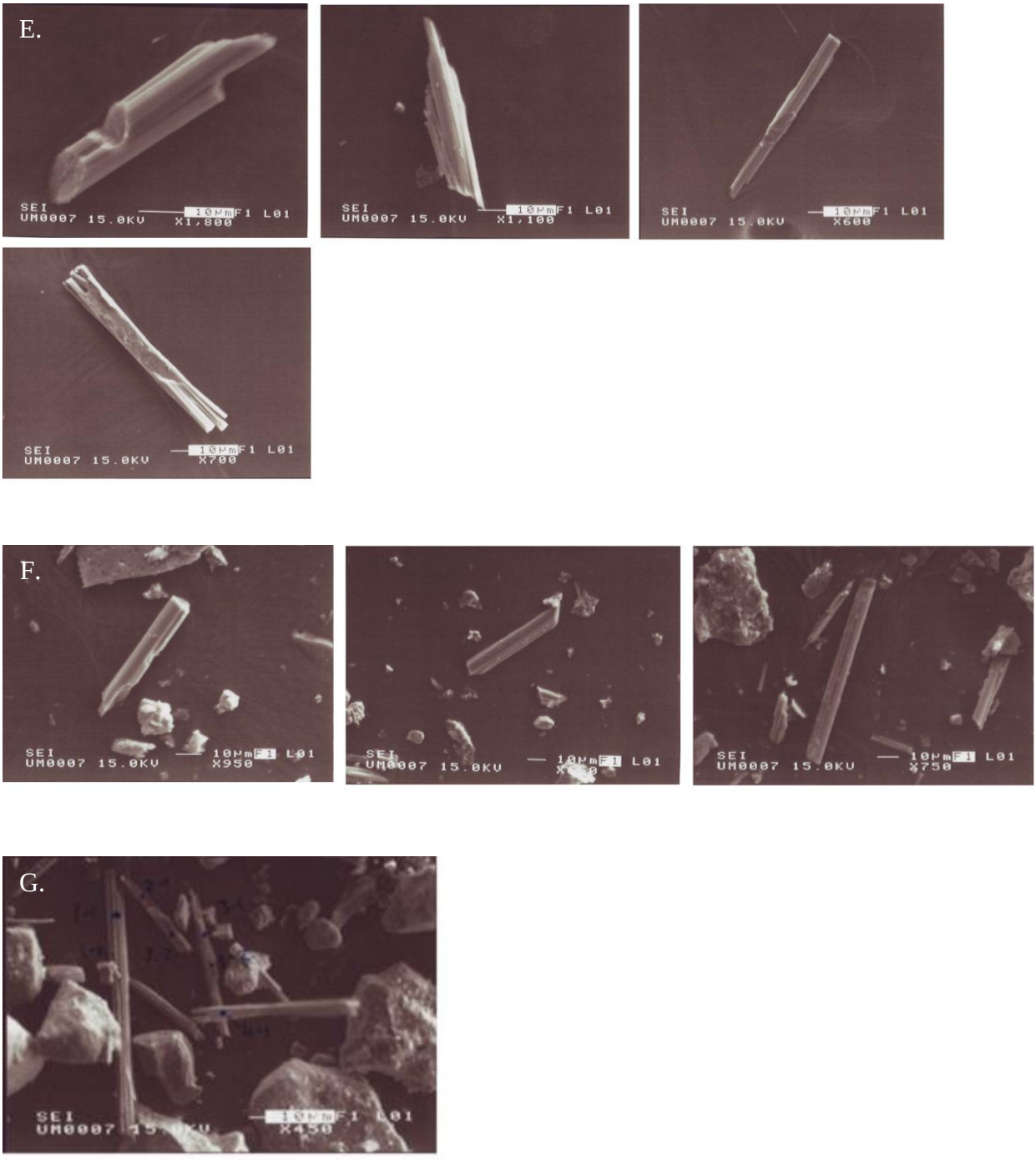

Figure 2 continued. E) jwt080603-08, fibers 1-4, F) jwt080604-01, fibers 2-4, G) jwt080604-07, fibers 1-4

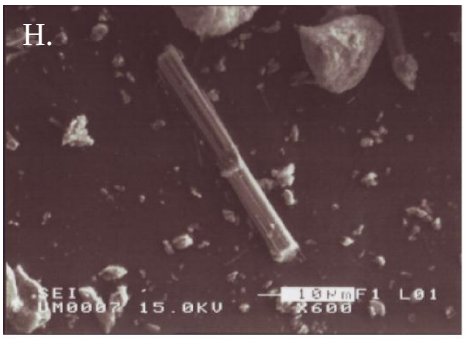

Figure 2 continued. H) jwt080604-08 & I) jwt080604-09, fibers 1 & 2

APPENDIX SAMPLING AND FIELD PHOTOGRAPHS

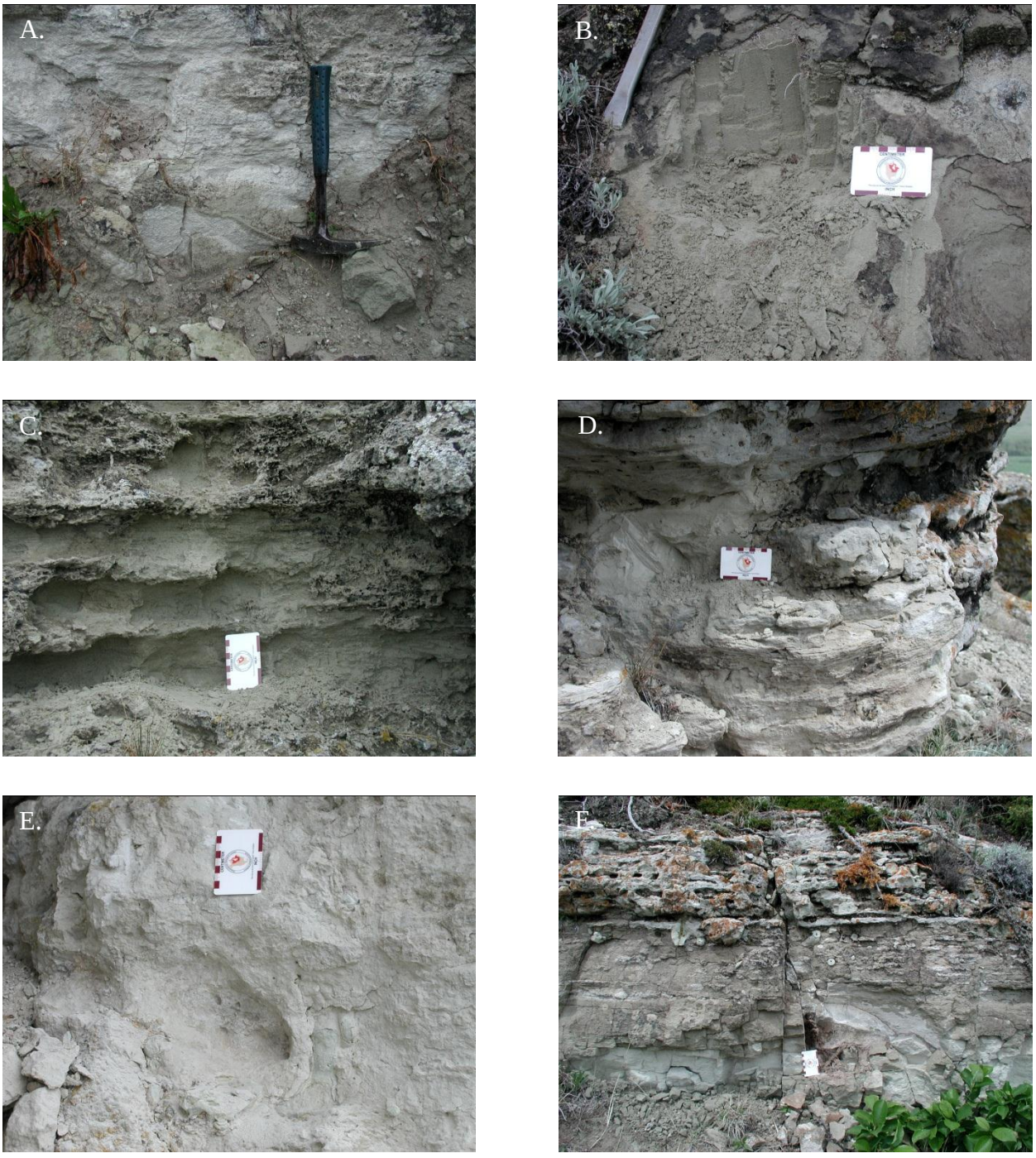

Figure 3. A) jwt080602-01, B) jwt080603-01, C) jwt080603-02, D) jwt080603-03, E) jwt080603-05, F) jwt080603-06

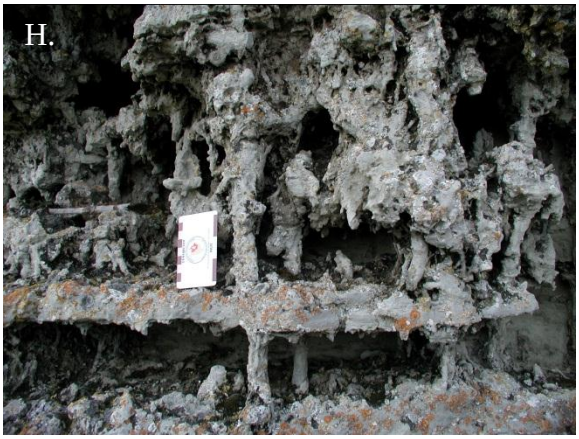

Figure 3 continued. G) jwt080603-08, H) jwt080603-09, I) jwt080604-01, J) jwt080604-02, K) jwt080604-05, lithic fragment, L) jwt080604-07

APPENDIX SEM IMAGES OF FIBROUS MINERALS (NDSU SEM)

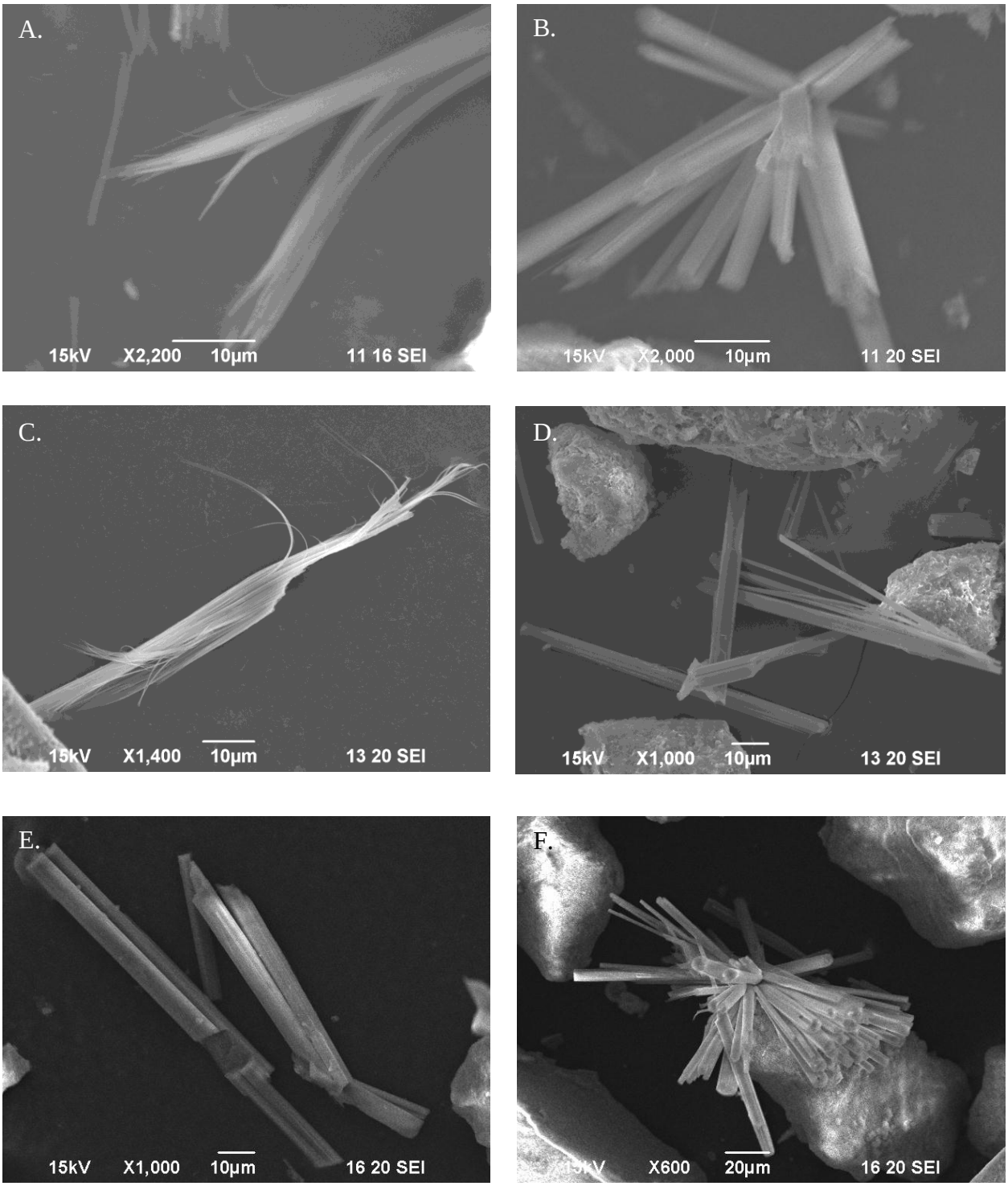

Figure 4. A) SEM1191, B) SEM1192, C) SEM1193, D) SEM1194, E) SEM1468, F) SEM1469

APPENDIX XRD JWT MICROGRAPHS

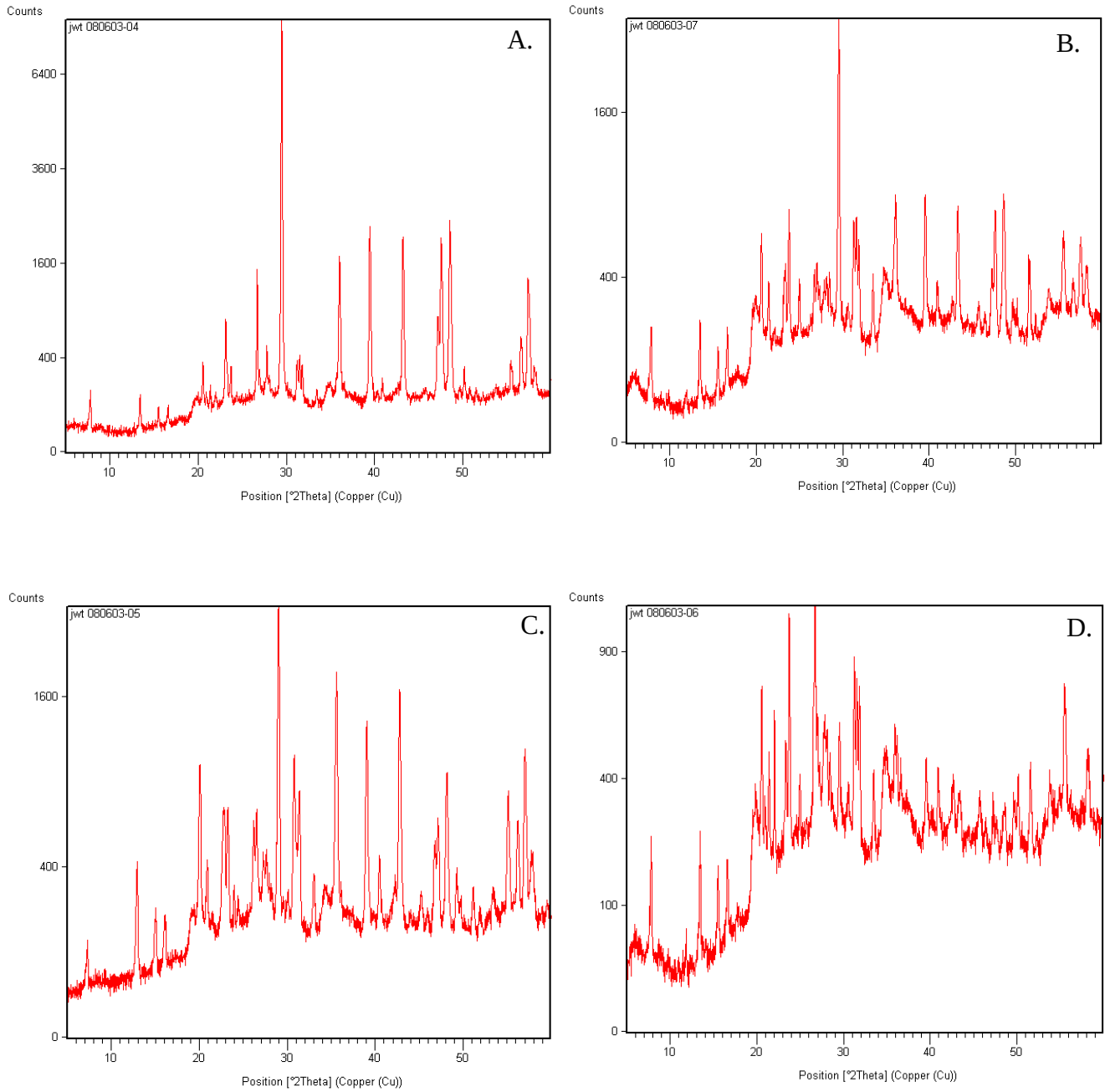

Figure 5. A) jwt080603-04, B) jwt080603-07, C) jwt080603-05, D) jwt080603-06

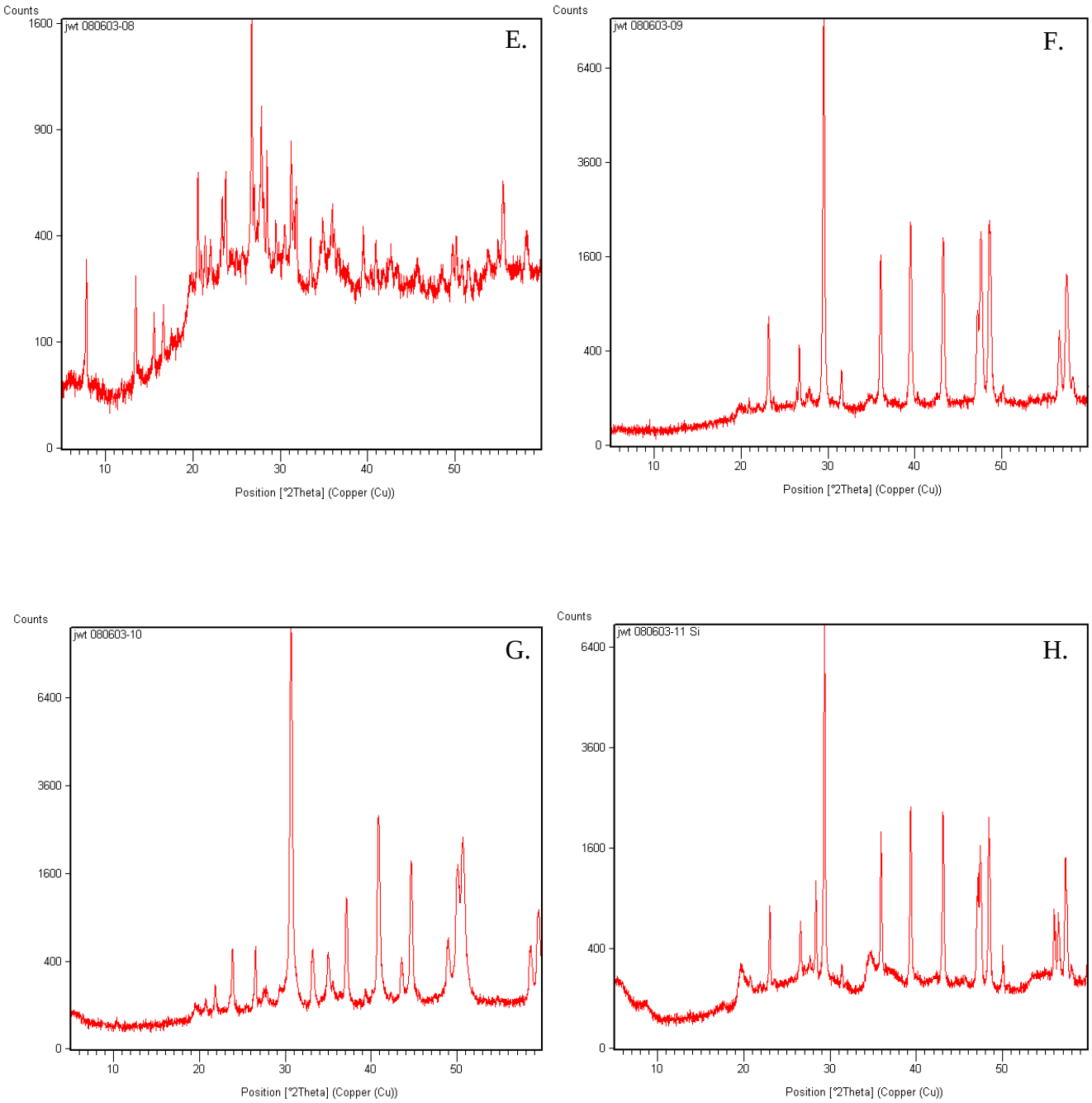

Figure 5 continued. E) jwt080603-08, F) jwt080603-09, G) jwt080603-10, H) jwt080603-11 Si

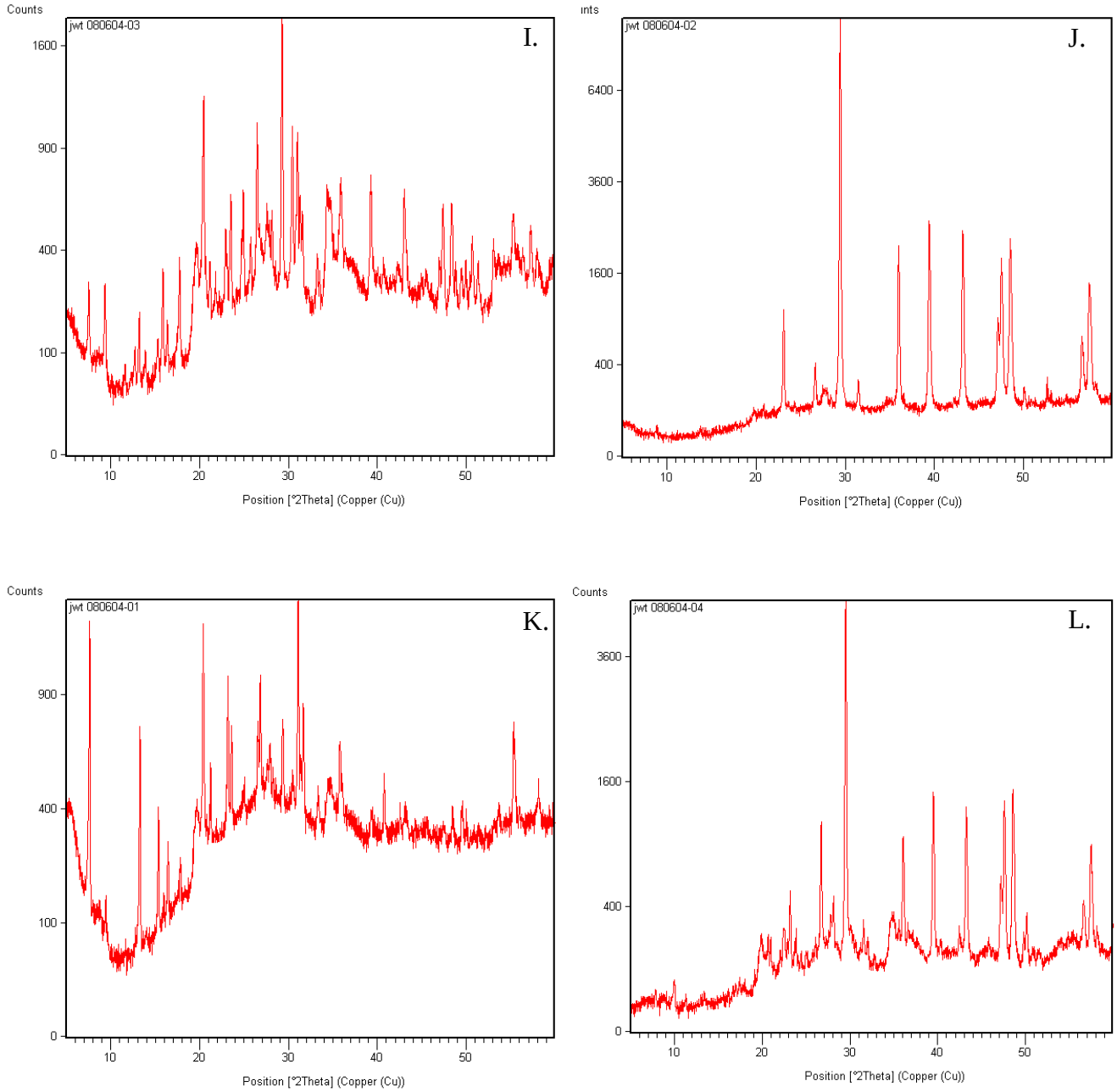

Figure 5 continued. I) jwt080604-03, J) jwt080604-02, K) jwt080604-01, L) jwt080604-04

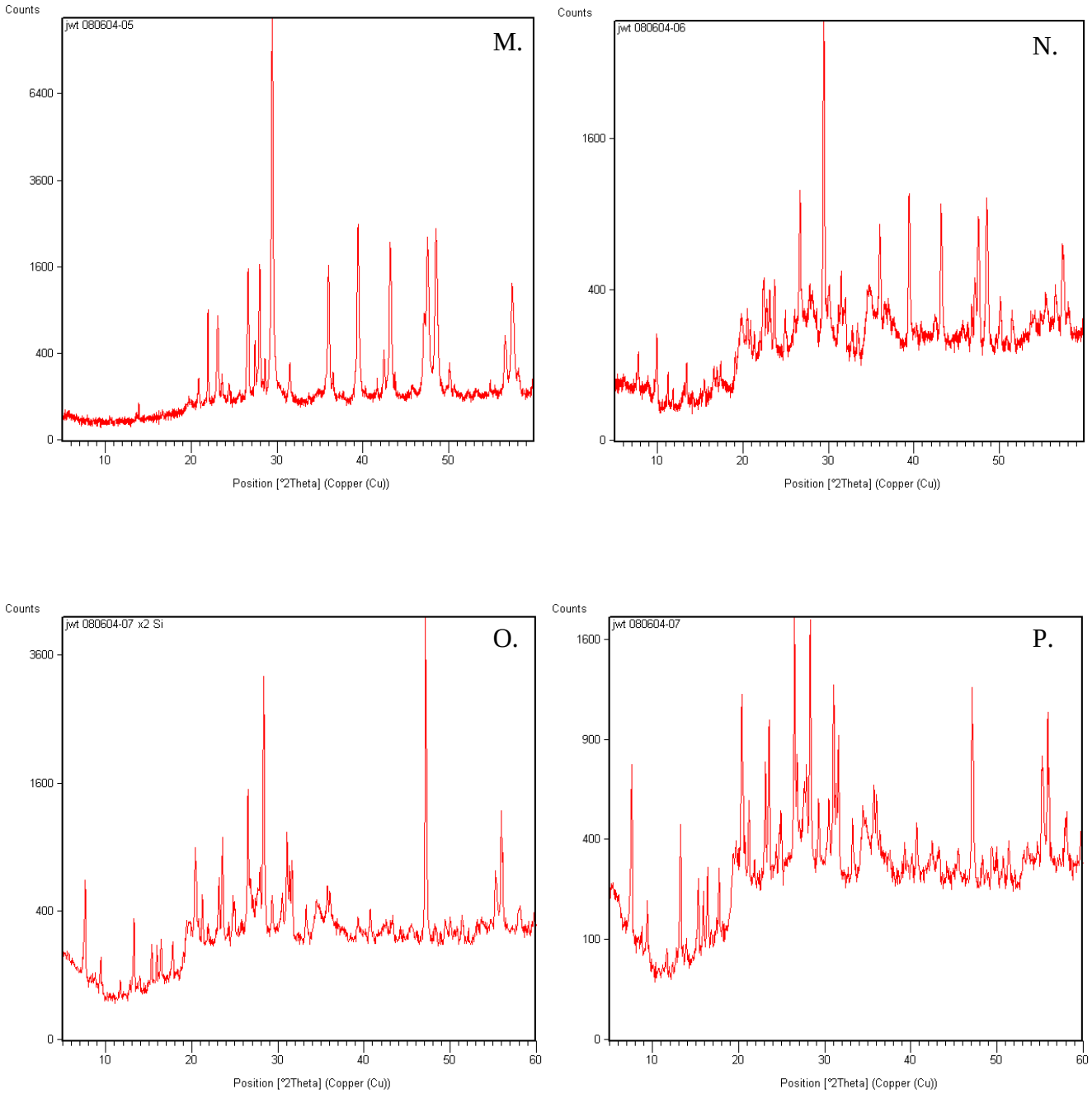

Figure 5 continued. M) jwt080604-05, N) jwt080604-06, O) jwt080604-07 Si, P) jwt080604-07

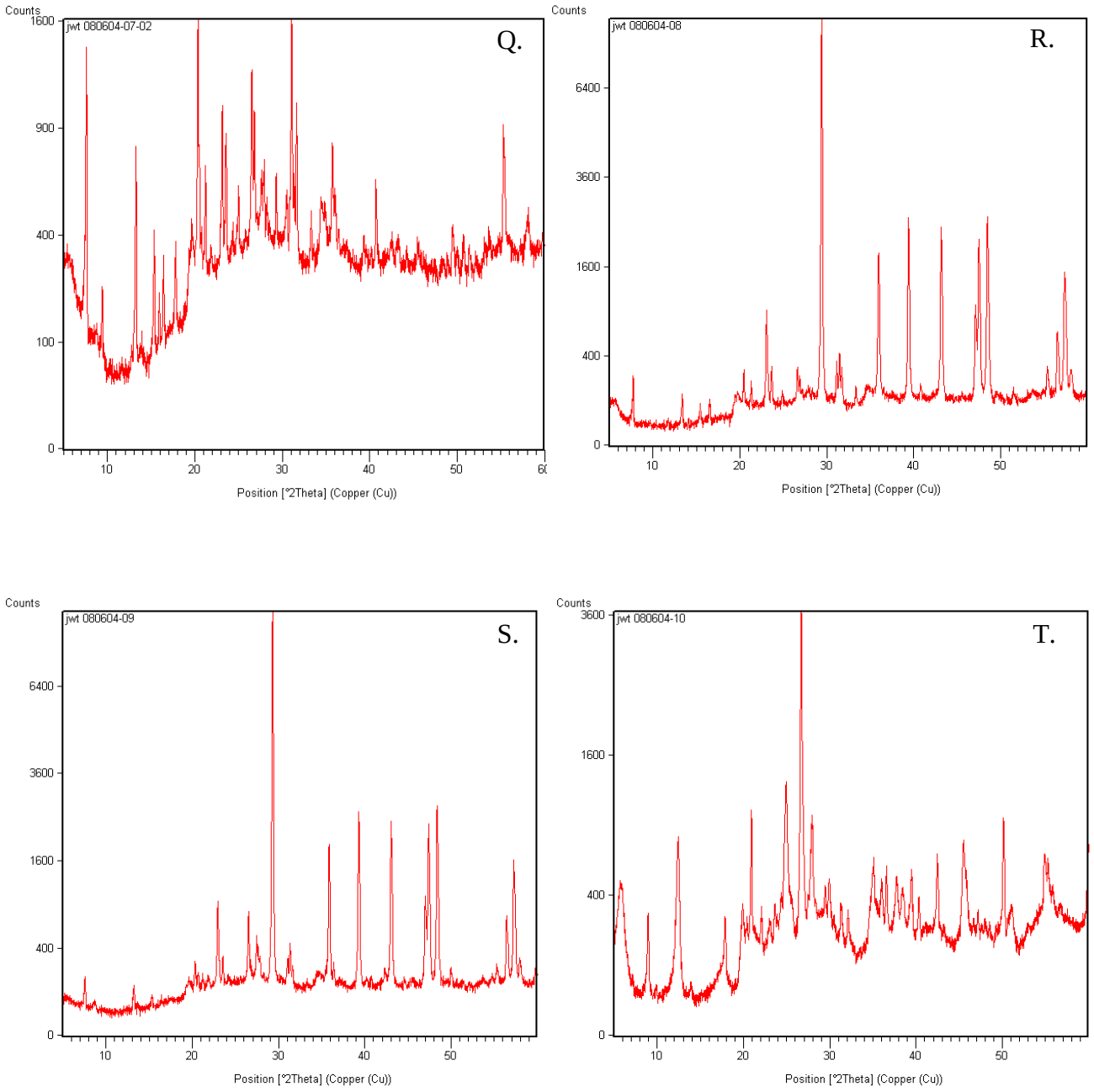

Figure 5 continued. Q) jwt080604-07-02, R) jwt080604-08, S) jwt080604-09, T) jwt080604-10

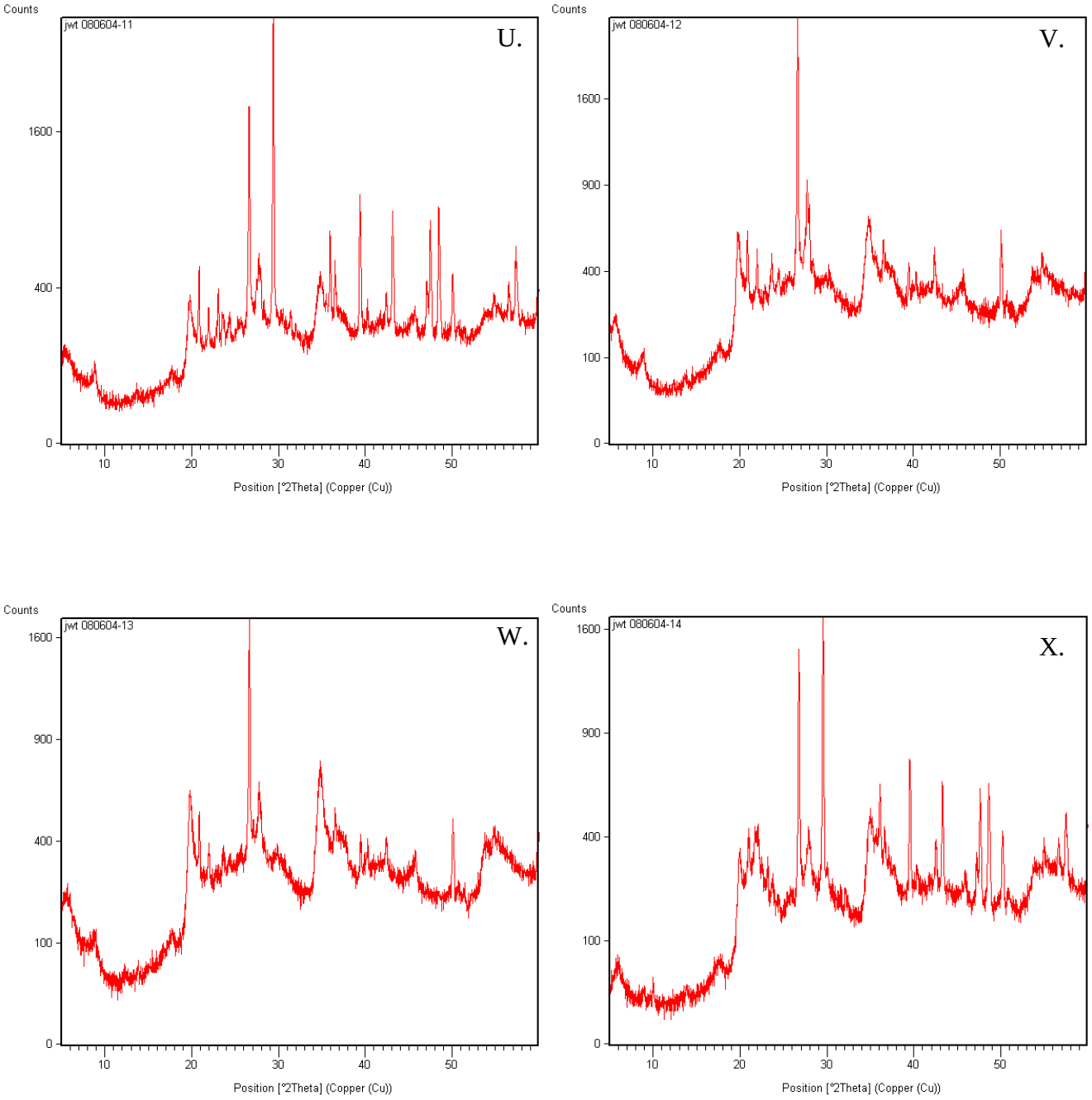

Figure 5 continued. I) jwt080604-03, J) jwt080604-02, K) jwt080604-01, L) jwt080604-04

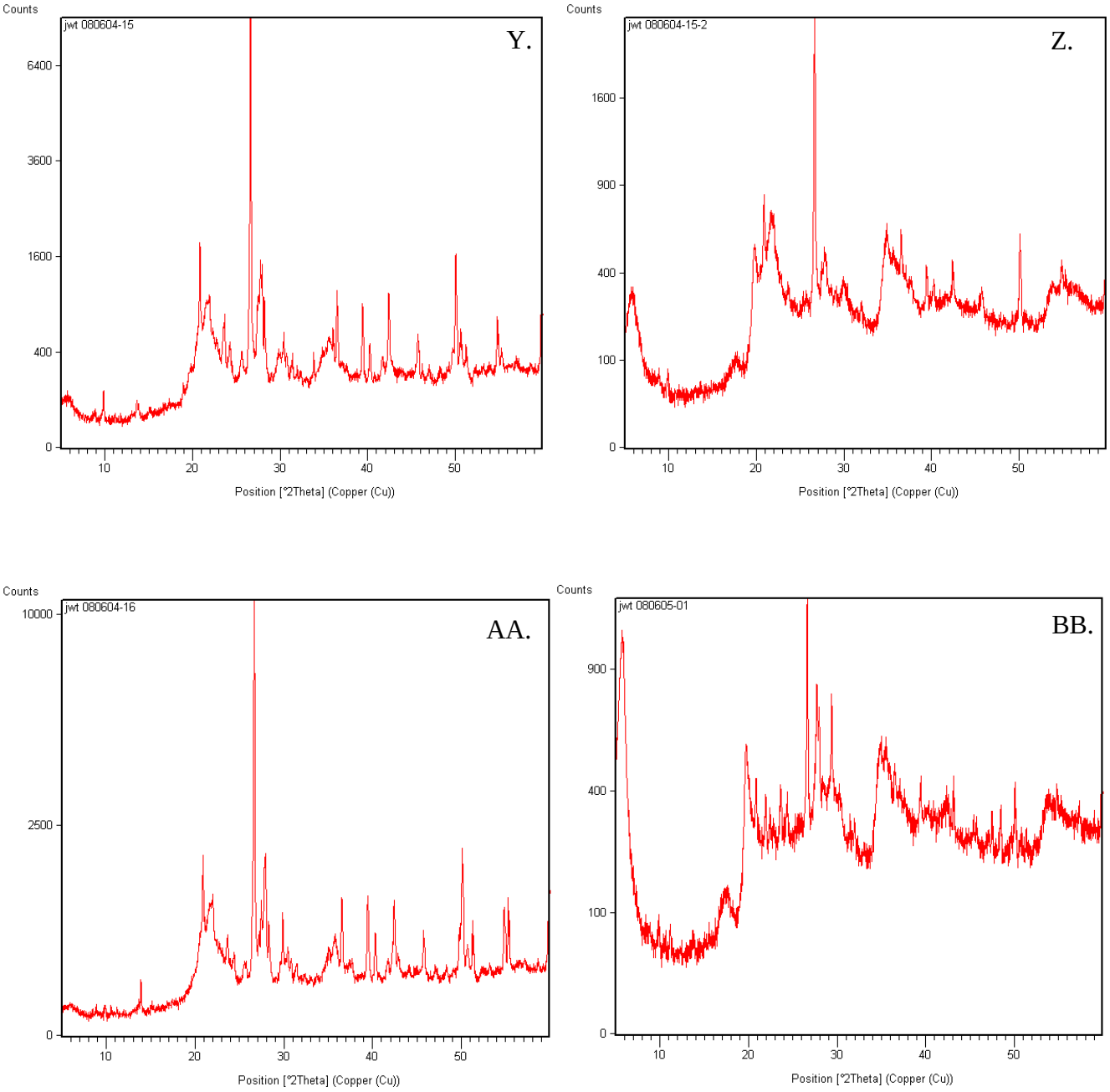

Figure 5 continued. Y) jwt080604-15, Z) jwt080604-15-02, AA) jwt080604-16, BB) jwt080605-01

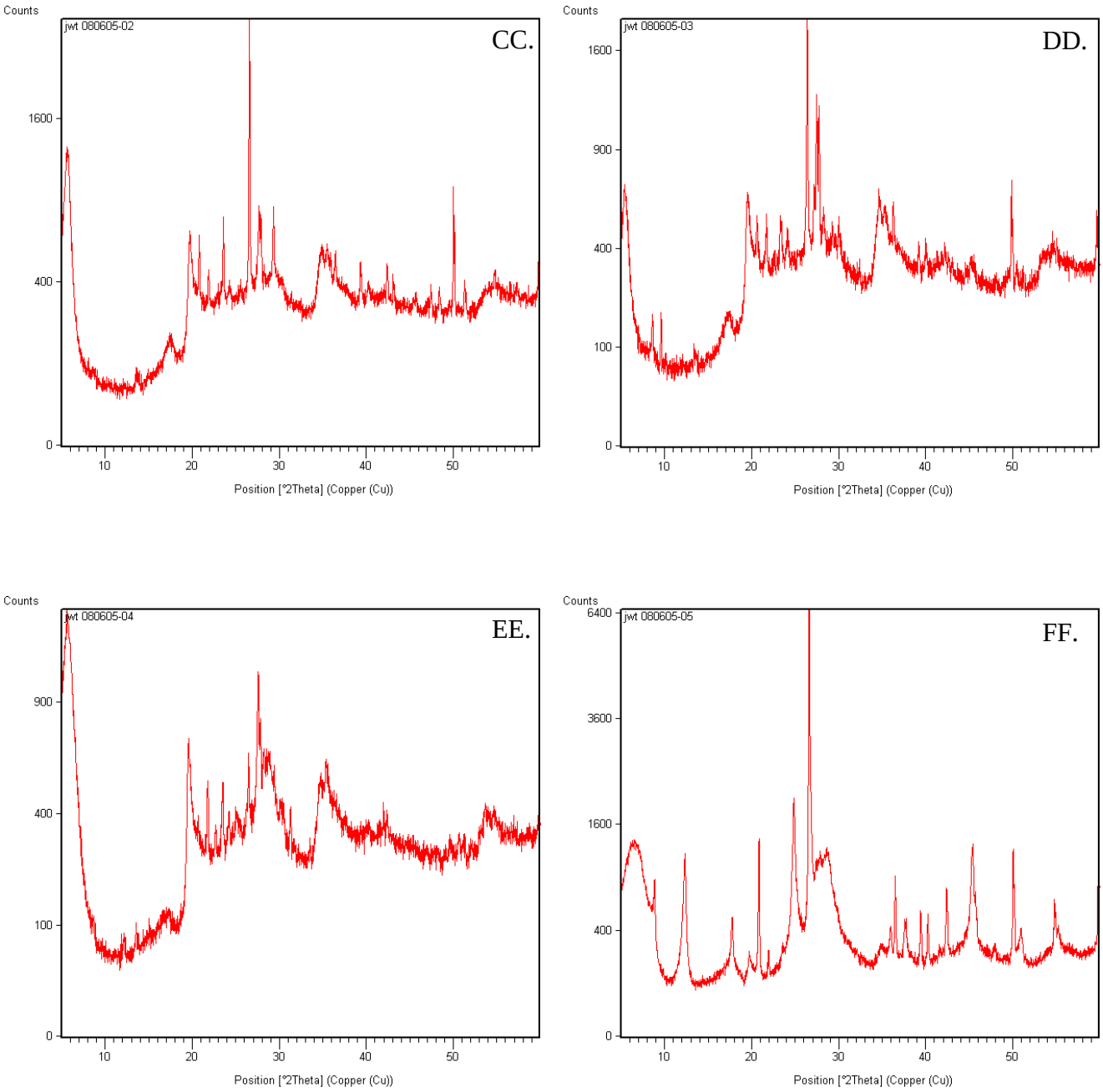

Figure 5 continued. CC) jwt080605-02, DD) jwt080605-03, EE) jwt080605-04, FF) jwt080605-05

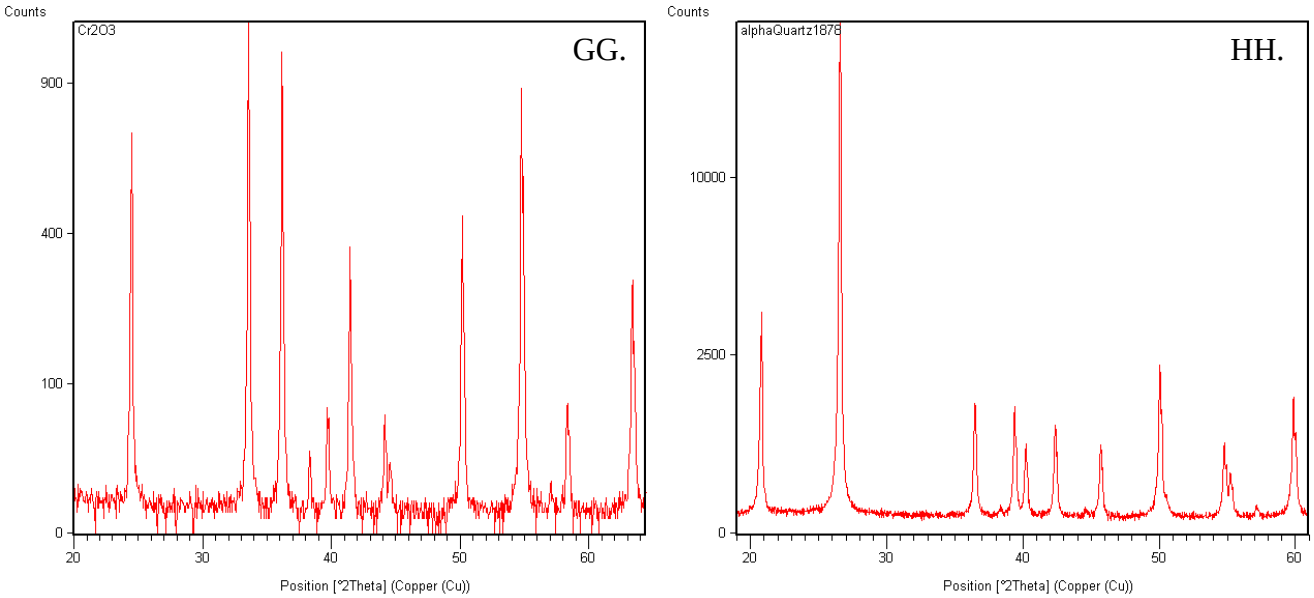

Figure 5 continued. GG) Cr_2O_3 & HH) Alpha Quartz